AFRICA CENTER OF EXCELLENCE FOR WATER MANAGEMENT ADDIS ABABA UNIVERSITY

GROUNDWATER RECHARGE ESTIMATION AND AQUIFER CHARACTERIZATION.

A CASE STUDY OF WALGA CATCHMENT UPPER GIBE BASIN, CENTRAL ETHIOPIA

BY

TEKALIGN WAKJIRA

ADVISOR : TILAHUN AZAGEGN (PHD)

A THESIS SUBMITTED TO:

AFRICA CENTER OF EXCELLENCE FOR WATER MANAGEMENT,
ADDIS ABABA UNIVERSITY
IN PARTIAL FULFILLMENT OF THE REQUIREMENTS FOR THE DEGREE OF MASTERS OF SCIENCE IN WATER MANAGEMENT (**HYDROLOGY AND WATER RESOURCES**)

ADDIS ABABA, ETHIOPIA
Nov, 2020

AFRICA CENTER OF EXCELLENCE FOR WATER MANAGEMENT

ADDIS ABABA UNIVERSITY

GROUNDWATER RECHARGE ESTIMATION AND AQUIFER CHARACTERIZATION. A CASE STUDY OF WALGA CATCHMENT UPPER GIBE BASIN, CENTRAL ETHIOPIA

BY

TEKALIGN WAKJIRA

GSR/5584/11

A thesis submitted to:

Africa Center of Excellence for Water Management, Addis Ababa University
in partial fulfillment of the requirements for the degree of masters of science in water management (**Hydrology and Water** R**esources**)

Addis Ababa, Ethiopia

Nov, 2020

AFRICA CENTER OF EXCELLENCE FOR WATER MANAGEMENT

ADDIS ABABA UNIVERSITY

This is to certify that, thesis prepared by **TEKALIGN WAKJIRA YADETA**, entitled: "Groundwater recharge estimation and aquifer characterization". A case study of Walga catchment, central Ethiopia, upper Gibe basin and submitted in partial fulfillment of the requirements for the degree of Masters of Science in water management (**Hydrology and Water R**esources) complies with the regulations of the University and meets the accepted standards with respect to the originality and quality.

Signed by the Examining committee:

Examiner

Dessie Nedaw (PhD) Signature_____ Date _____

_____ Signature_____ Date _____

Advisor

Tilahun Azagegn (PhD) Signature_____ Date _____

Co-Advisor

_____ Signature_____ Date _____

Chairperson

_____ Signature_____ Date _____

DECLARATION

I, the undersigned, declare that this thesis is my original work, has not been presented for a degree in any other university and that all sources of material used in this thesis have been duly acknowledged.

Name	Signature	Date
Tekalign Wakjira	_____	**23/11/2020**

(Africa Center of Excellence
For Water Management)

Abstract

Groundwater is mainly used for irrigation and water supply in Walga catchment as other parts of the country. The main objective of this study is to quantify the amount of groundwater recharge using WetSpass model and characterization of aquifers using Aquifer test in the upper Omo-Ghibe basin of Walga catchment. Meteorological data like rainfall, wind speed, temperature, relative humidity, sunshine hours were collected from meteorological stations located within the catchment and nearby area. Potential evapotranspiration was calculated using Penman-Montieth based FAO CROPWAT software. Slope and topography map were generated from Shuttle Radar Topographic Mission elevation data while Land use land cover were prepared from Landsat OLI8 satellite images downloaded from United States Geological Earth Explorer. Parameter table (dbf data) and grid maps were prepared for WetSpass model input with the help of ArcMap 10.4. Using the model the mean annual recharge of the catchment was found to be 7.5% of the precipitation whereas surface runoff was 38.25% of the annual precipitation. The aquifer hydraulic properties were estimated from the pumping test by fitting mathematical models (type curves) to response data (water level changes) through computer software known as AQUIFER TEST. Yield or discharge of bore holes values range from 0.15 l/sec. to 61 l/sec, whereas Transmissivity ranges from 3.5 $x10^{-4}$ m^2/day to 290 m^2/day with an average of 50.94 m^2/day. Hydraulic conductivity values ranges from 0 to 16.04 m/se with mean values of 1.2 m/s. The sum of the yield from 72 boreholes is 430 l/s (119.4 m^3/hr), this gives a total of 37152000 liters per day. 65.8% of Walga catchment coverage is under Satisfactory ground water potential while 0.72% is classified under very good groundwater potential. The mean descriptive statics value of groundwater quality of Walga catchment is below WHO limit and also good for irrigation water quality. The study area is characterized by lowest groundwater recharge relative to surface runoff and actual evapotranspiration due to effect of impermeable soils, morphology of the land and land use land cover of the area. The lowest transmissivity value is indicative of the poor permeability in the pyroclastic lithologic formations and low discharge to wells. It also implies that it will take a considerable time for the aquifers to replace water into wells removed during pumping.

Key Words: Walga catchment; WetSpass; Groundwater recharge, Aquifer characterization,

Acknowledgement

My deepest gratitude tends to my advisor Tilahun Azagegn (PhD), for his unreserved advice, support and guidance to the completion of this research.

I would like to thanks South West Shoa Zone Irrigation Development Authority for their kindness of facilitating and sponsoring me in following my education. Although I express my warmest gratitude to Mr Biniam Yosef (ECDSWC) for his generosity in acquiring me necessary data and Ashebir Gebre (ECDSWC) and Tsegaye (WVE) helping me with fundamental idea during the development of WetSpass model.

Staff of ACEWM, friends and other people who helped me a lot in one way or the other for the completion of this research work are never forgotten.

I am grateful to Hard Rock Drilling and Engineering P.L.C, South West Shoa Zone Water Resource Development and Energy office, National Meteorological agency, Ethiopian Construction Design and Supervision Works Corporation and other private firms and individuals, for their great contribution in providing me valuable data.

I have no words to express my feelings which I have for my family; especially my wife Kumeshi Degefa for her prayer, encouragement and support which gave me strength to carry out the present research study and my deepest love also goes to my sons Firisa and Wasingitan.

TABLE OF CONTENTS

FIGURES

TABLES

List of Annexes

List of Abreactions

A.S.L Above Sea Level

ATA Agricultural Transformation Agency

AHP Analytical Hierarchy Process

CMB Chloride Mass Balance

Dbf Database file

DEM Digital Elevation Model

ECDSWC Ethiopian Construction Design and Supervision Works Corporation

GPR Ground Penetrating Radar

GWR Groundwater Recharge

HDW Hand Dug Well

MCDA Multi criteria decision analysis

MWIE Ministry of Water Irrigation and Energy

OLI/TIRS Operational Land Imager and Thermal Infrared Sensor

SMBM Soil Moisture Balance Method

SNNP Southern Nation, Nationalities and Peoples Representative

SRTM Shuttle Radar Topographic Mission

SWSZWREO South west shoa zone water resource and energy office

WetSpass Water and Energy Transfer between Soil, Plants and Atmosphere under quasi-Steady State

WTWSSE Woliso Town Water Supply and Sewerage Enterprise

CHAPTER ONE

1. INTRODUCTION

1.1.Background

Much of the world's population lives in places where demand for water exceeds supply, or poor quality limits its use. Scarcity of water and inequities in access, use, and decision-making can threaten life itself, diminish the quality of life, and impede integral human development. Water scarcity and inequities are also risk factors for violent conflict. Water-related violence is already common in many parts of the world and is generally expected to increase in the years ahead (Hamerlynck, 2013).

Groundwater is a main source for industries, communities and agricultural consumptions in the world and due to its freshness, chemical compounds, constant temperature, lower pollution coefficient and higher reliability level, it is considered as a basic source of supplying reliable fresh water in urban and rural areas (Zeinolabedini & Esmaeily, 2015).

The recharge boundary of a groundwater circulation system is a permeable boundary with a specified hydraulic head, with water flowing into the system under natural conditions or ones affected by its exploitation (Hoque & Burgess, 2012). The conceptual model of the groundwater recharge process accounts for identifying the scale of the hydrological process, the inlets and outlets of the water circulation system as well as its temporal and spatial limitations, such as an area's infiltration predisposition and the type or character of a hydrological active zone (Yair & Kossovsky, 2002).

Quantification of the rate of natural ground water recharge (Eilers et el., 2017) is a basic pre-requisite for efficient ground water resource management (Goulburn-Murray, 2010). It is particularly important in regions with large demands for ground water supplies, where such resources are the key to economic development. However, the rate of aquifer recharge is one of the most difficult factors to measure in the evaluation of groundwater resources. The advent of Geographic Information Systems (GIS), physical-based hydrologic modeling, enabled to address some of the problems (Dereje & Nedaw, 2019).

Walga catchment is the area of increasing competitive demand of water for agriculture and water supply. Groundwater recharge study of the area has not been based on physically varying methodology of estimating long tem average. WetSpass, a GIS based model, was built as a physically based methodology for estimation of the long-term average, spatially varying, water balance components: surface runoff, actual evapotranspiration and groundwater recharge (Batelaan & De Smedt, 2007). By using long-term average standard hydro-metrological parameters as input, the model simulates the temporal average and spatial differences of surface runoff, actual evapotranspiration, and groundwater recharge of Walga catchment.

Pumping test was used to determine the performance and efficiency of a well and also to characterize and parameterize the hydraulic properties of an aquifer in Walga catchment. The Cooper Jacob's Straight-line Equation was used to analyze the pumping test results of drawdown with respect to time. The aquifer hydraulic properties was estimated from the pumping test by fitting mathematical models (type curves) to response data (water level changes) through computer software known as AQUIFER TEST (Ita et al., 2018).

Thus, estimation of groundwater recharge and Hydrogeological characterization of aquifer in Walga watershed has its own role in solving the problems related to the management and planning of water resources for sustainable development using WetSpass model.

1.2. Statement of the Problem

Groundwater is one of the major resource of water for various purposes in urban and rural areas of Walga catchment as other parts of Ethiopia. It is the largest area where groundwater is abstracted for Woliso, Wolkite, Wonchi, Goro, Gindo town and surrounding rural community. The demand of groundwater for water supply, and agriculture is increasing from time to time in this study area.

Water resource management faces specific challenges in the area due to; intense competition among upstream and downstream users, among different types of use, communities interest of using water exceeding supply and absence of groundwater potential area identification. Walga River is shared among eight woredas of Oromia Regional State (Ameyya Woliso, Wanchi, Goro , Ambo, Dawo, Tiku Inchini and Dendi) and partly two woreda of SNNP (Abeshege and Kebena).

Due to over use of this River and its tributaries, scarcity of water and inequities in access, use, and decision-making can threaten and diminish the quality of life, and impede integral human development.

There increasing competitive demand of water resources for domestic, agricultural & other purposes in the area is due to rapid population growth along with increasing living standard, intensified irrigation agriculture & other developmental activities like Ecotourism. This indicate the need for efficient utilization through further investigation of the water resources potential, particularly the groundwater.

Hydrological models, WetSpass with the help of GIS and remote-sensing techniques was used in Walga catchment to quantify amount of groundwater recharge based on qualitative and quantitative hydrogeological parameters. Characterizing the aquifer type and properties, identifying groundwater quality variations and mapping groundwater potential of the area has its own role in solving the problems related to the management and planning of water resources for sustainable development.

1.3. Objectives

1.3.1. General Objectives

The objective of this study was to estimate spatial distribution and long term average groundwater recharge, characterization of the aquifer system, determining groundwater potential and groundwater quality variations of Walga Watershed.

1.3.2. Specific Objectives

The primary objectives were achieved through the following sub-objectives;

- To estimate groundwater recharge using physically based methodology
- Characterizing aquifers using Hydrogeological parameters
- To determine groundwater potential using weighted overlay analysis.
- To determine Physio-chemical parameters and groundwater quality variations using result of laboratory analysis.

1.4. Significance of the Study

The findings of this study has identified the water budget of Walga catchment. The long term spatially and temporally distributed groundwater recharge, actual evapotranspiration and surface runoff of this catchment was estimated. The groundwater potential of Walga catchment, the hydrogeological parameters of aquifers, hydro-geochemistry of water were the outputs of this research. In general, the research is helpful for the planners and administrator to manage the resource properly and for their future plans of using groundwater and surface water wisely. The new data gathered will also enable the researchers interested to do on contaminant transport modeling, steady and unsteady groundwater flow modeling and related topics in the area and surrounding.

1.5. Scope and Limitation of the Study

The study has focused on Walga catchment Upper Omo-Gibe Basin, located in central Ethiopia 115km from Addis Abba having an area of 2228 km^2 bounded with Beda kero, Dase Jabo, Wonchi-Dendi and Roge mountains from the NE, N,NW and Guraghe mountain from the Southern direction respectively. WetSpass, ArcGIS, Global mapper, Surfer, Aquifer test 9.0 and Grapher 14 are software's that was applied for the success of this research. The study also included geology, hydrogeology, Hydro-geochemistry, meteorology and Hydrology. Missing data of meteoroidal data, budget for water sample, soil sample laboratory analysis, absence of groundwater monitoring data and spread of COVID-19 were the main problems in this research.

1.6.Structure of the thesis

The thesis is organized into six chapters. In the first chapter, the introduction part of the thesis that includes research issues related to groundwater recharge and aquifer characterization, statement of the problem and the objectives are presented.

In the second Chapter, the literature review related to the principle of groundwater modeling and recharge estimation techniques, aquifer characterization techniques, groundwater potential mapping, surface and groundwater chemistry and groundwater management are discussed.

Third chapter contains description of the study area. It also includes detail study area location, climate, geology, hydrogeology and drainage system of the area.

The fourth chapter is more about materials and methods. Hydro-meteorological data needed for WetSpass modeling, hydrogeological data for aquifer characterization, GIS and RS raster map for groundwater potential mapping and hydrochemical data for groundwater chemistry variation are described.

Fifth chapter is result and discussion of WetSpass out puts, aquifer characteristics, groundwater potential and groundwater quality variations.

Finally, the last chapter is conclusion and recommendation

CHAPTER TWO

2. LITERATURE REVIEW

2.1. Concepts of Groundwater Recharge

Groundwater recharge is the amount of water that flows by gravity, through the soil beyond the reach of the surface vegetation ultimately reaching the saturated zone, i.e. an aquifer, through the processes of vertical percolation or seepage. This water is then discharged to a stream as base flow, unless it feeds natural springs or is withdrawn by wells for human use. Unlike precipitation and direct runoff, groundwater recharge is nearly impossible to measure directly. It is difficult because groundwater recharge depends not only on precipitation but also on meteorological conditions, as well as on soil type, land surface slope, soil-moisture status, vegetation cover and condition, cultivation practices, and most of all, on evapotranspiration, which is a function of the previously noted factors (Erickson & Stefan, 2008).

A lot of researchers has given different definition for groundwater recharge. It can be defined as an addition of water to a groundwater reservoir (Dhar et al., 2014). The four main modes of recharge distinguished are; downward flow of water through the unsaturated zone reaching the water table, lateral and/or vertical inter-aquifer flow, induced recharge from nearby surface water bodies resulting from groundwater abstraction and artificial recharge such as from borehole injection or man-made infiltration ponds (Lorentz, & Hughes, 2003).
Naranjo et al., (2015), also defined; recharge is a complex natural phenomenon and one of the most difficult hydrological variables to measure and/or estimate considering the unavoidable simplifications to calculate it; wide temporal and spatial variability; paucity of observations; gaps in data series; and lack of measurements of the hydraulic parameters needed to apply recharge calculation codes and models.

Groundwater recharge can be either a natural or an artificial process. The natural recharge occurs when it stems from the direct infiltration of rainfall or from the water percolation of adjacent water bodies, and the artificial recharge when it is induced by human activity such as irrigation, urbanization, construction of injection boreholes or river spreading. Depending on the route followed by percolating water towards the water table, recharge can be classified as direct recharge

when talking about diffuse infiltration of recharge water towards groundwater, or as indirect recharge when along river and other main channels (Pollution & Recharge, 2015).

2.1.1. Groundwater Recharge estimation techniques

There are many techniques available for quantifying groundwater recharge as there are different sources and processes of recharge. Each of the methods has its own limitations in terms of applicability and reliability. The objective of the recharge study should be known prior to selection of the appropriate method for quantifying groundwater recharge as this may dictate the required space and time scales of the recharge estimates (Scanlon et al., 2002). According to them, techniques for estimating recharge are subdivided into various types, on the basis of the three hydrologic sources, or zones, from which the data are obtained, namely surface water, unsaturated zone, and saturated zone.

Chloride Mass Balance, Stable Isotopes (Rushton, 1991), Soil Moisture Balance Method (SMBM), Water table fluctuation method (Eilers et al., 2017) and WetSpass modeling method ((Batelaan & De Smedt, 2001; Hasanuzzaman et al., 2017; Teklebirhan et al., 2012) are among techniques widely utilized for recharge estimation.

2.1.2. Factors that Affect Groundwater Recharge

Rukundo & Doğan,(2019) has identified, groundwater recharge is affected by many parameters and complex processes which themselves are influenced by many factors. Precipitation is affected by climatic factors such as wind and temperature, resulting in complex and dynamic distributions while the intensity and spatial distribution of precipitation influences the amount of recharge. According to them, large scale vegetation determines the amount of net rainfall, infiltration rate, deep drainage and the available storage capacity of the groundwater system. Any change in vegetation, say from forest to grassland can have a large effect on recharge. The nature of land cover has a big influence on recharge and hence groundwater recharge modelling should not assume that vegetation is a constant factor. For example, the removal of the indegenious vegetation in large parts of south eastern australia more than 100 years ago caused a significant increase in groundwater recharge.

Vegetation influences recharge through interception and transpiration. The amount of stored water that can be removed by vegetation depends mainly on the rooting depth. Shallow rooted grasses

will remove less water than deepen rooted shrubs and trees (Jyrkama, 2007). It is well known that the degree of water saturation of the root zone determines the distribution of hydraulic conductivity and as a result the percolation to the groundwater table. It also influences the water uptake by roots and thus the actual evapotranspiration (Brendchet, 2004).

2.2. WetSpass Modeling Method

A number of studies have been conducted on groundwater recharge using WetSpass model in Ethiopia. Meresa & Taye, (2018) has estimated long tem average annual and seasonal groundwater recharge for Birki watershed in Northern Ethiopia and identified as there is high groundwater recharge value and Evapotranspiration with low runoff in the watershed. Another study by Teklebirhan et al., (2012) estimated the distributed groundwater recharge, surface runoff and evapotranspiration amount of Ilala sub basin, Northern Ethiopia using WetSpass modeling method. They have characterized the watershed by low groundwater recharge due to the presence of high evapotranspiration rate associated with high temperature, dry wind, low rainfall and relative humidity. Yenehun et al., (2017) have used WetSpa to study the spatial and temporal variation of recharge in the Geba basin, Northern Ethiopia. They have identified, groundwater recharge spatially varies and mainly controlled by the distribution of rainfall amount, followed by soil and land-use, and to a certain extent, slope.

According to Tilahun & Merkel, (2009), the amount of recharge they have investigated using WetSpass model is less than what was previously thought and informed the future groundwater development and management in the area to take this into account. Recharge was estimated using physically based distributed recharge model called WetSpass in Upper Bilate. The study revealed that the groundwater recharge estimation using WetSpass model is reasonable and useful for quantification of annual groundwater recharge with spatial and seasonal variation and also capable in the identification of groundwater recharge zones in the area under study (Dereje & Nedaw, 2019).

One of the main challenges in groundwater recharge estimation is accurately estimating its distributed values in a hydrologically and geographically variable catchment. According to Dereje & Nedaw, (2019); Teklebirhan et al., (2012), the advent of Geographic Information Systems (GIS), physical-based hydrologic modeling, enabled to address some of the problems. WetSpass was built as a physically based methodology for estimation of the long-term average, spatially

varying, water balance components: surface runoff, actual evapotranspiration and groundwater recharge (Batelaan & De Smedt, 2007). It is an acronym for water and energy transfer between soil, plants and atmosphere under quasi-steady state that was built upon the foundations of the time dependent spatially distributed water balance model (Batelaan & De Smedt, 2001).

Regional groundwater models used for analyzing groundwater systems (infiltration–discharge relations) are often quasi-steady state and therefore need long-term average recharge input. On the other hand, the spatial variation in the recharge due to distributed land-use, soil type, slope, depth to groundwater , meteorological conditions, etc. can be significant and should be accounted. Hence, WetSpass was built as a physically based methodology for estimation of the long-term average spatial patterns of surface runoff, actual evapotranspiration and groundwater recharge. The model is especially suitable for studying long-term effects of land-use changes on the water regime in a basin. The total water balance, per raster cell and season, can now be calculated using the previously described water balance components for vegetated, bare-soil, open-water and impervious parts of a raster cell.

$$ET_{raster} = a_v ET_V + a_s E_S + a_o E_O + a_i E_i$$

$$S_{raster} = a_v S_v + a_S S_S + a_o S_O + a_i S_i$$

$$R_{raster} = a_v R_v + a_S R_S + a_o R_O + a_i R_i$$

Where ET_{raster}, S_{raster} and R_{raster} are respectively, the total evapotranspiration, surface runoff and recharge in a raster cell. a_v , a_S , a_o and a_i are respectively the vegetated, bare-soil, open-water and impervious area fractions of a raster cell (Batelaan & De Smedt, 2001).

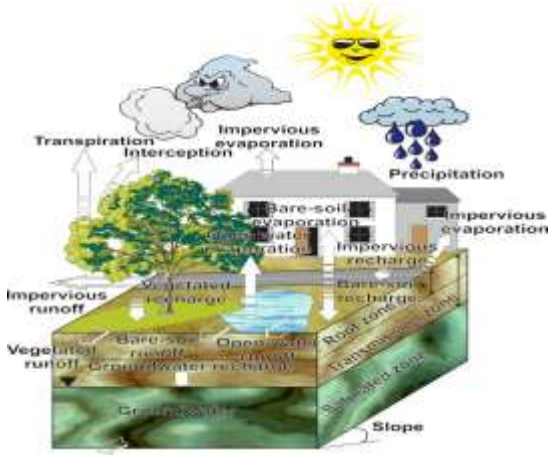

Figure 1. Schematic WB of an hypothetical raster cell (after O.Betelaan and D.Smelt 2007)

2.3.Aquifer Characterization

Bodies of saturated rocks or geological formations through which volumes of water find their way (permeability) into wells and springs is studied by (Yu et al., 2012). Shekhar (2017) has identified aquifer: it is geological formation, which can store and transmit groundwater in sufficient quantity so that the water can be economically utilized from the aquifer. Aquifer characterization is a processes by which the three-dimensional structure, hydraulic and transport properties and chemistry of groundwater are evaluated (Robert.G et al.,2016). It provides the foundation for groundwater modeling, which is ubiquitously used to evaluate aquifers. Detailed aquifer characterization is particularly important where solute transport as a concern, as aquifer heterogeneity has a much greater impact on groundwater flow direction and rates than it does on aquifer heads.

According to Yu et al., (2012), aquifer characterized in-terms of hydraulically important parameters such as hydraulic conductivity (K), porosity (n), or any other applicable quantity. Such parameters are frequently assumed for individual lithofacies since real data are often unavailable.

Aquifers are unconfined if they occur at the surface, this means they can receive recharge directly from rainfall. If they are buried under sediments they receive recharge by slow leakage from overlying aquifers. Rainfall percolates through the surface sediments until it reaches the water table. It then flows under gravity through local, intermediate and regional flow systems within the aquifers (Harold F. et al., 2015). Local flow systems have flow paths of less than 5 km. They mostly occur in upper aquifers or the unconfined fractured rock of the lower aquifers or basement. These aquifers respond quickly to changes in rainfall, extraction or land use. Groundwater in a local system has a relatively short residence time before it discharges to local streams (Shekhar, 2017).

Aquifer properties that affect ground-water availability include aquifer thickness and the size, number, and degree of interconnection of pore spaces within the aquifer material. These properties affect the ability of an aquifer to store and transmit ground water. Porosity, the ratio of void space to unit volume of rock or soil, is an index of how much ground water the aquifer can store. Permeability, a property largely controlled by size and interconnection of pore spaces within the material, affects the fluid-transmitting capacity of materials (Khadri & Moharir, 2016).

The water-transmitting characteristics of an aquifer are expressed as hydraulic conductivity and transmissivity. Hydraulic conductivity is a measure of the rate that water will move through an aquifer; it is usually expressed in gallons per day through a cross section of one square foot under a unit hydraulic gradient(Okon et al., 2018). Transmissivity is equal to the hydraulic conductivity multiplied by the saturated thickness of the aquifer. The storage characteristic of an aquifer is expressed as the storage coefficient (Tse & Amadi, 2010).

Single well test is more common than aquifer test with having observation well, since the advantage of single well test is that the pumping test can be conducted on the production well with the absence of observation well. A kind of single well test, which is step-drawdown test used to determine the efficiency and specific capacity of the well, however in case of single well test it is possible to estimate Transmissivity, but the other parameter which is Storativity is overestimated (Dinu et.al , 2017).

Comprehensive hydrogeological field survey, compilation of relevant data from different sources (Ayenew et al., 2008), pumping test, well lithological logs, and indirect information from hydro-chemical data enable to classify/characterize the aquifers and their hydraulic characteristics including groundwater recharge and discharge conditions (Tamilnadu, 2010).

Among groundwater hydrologists, the most familiar curve matching procedure for estimating aquifer properties from pumping tests is due to Theis (1935). The Theis method allows one to estimate the transmissivity and storativity of a non-leaky confined aquifer having infinite extent by means of matching the Theis type curve to water-level changes (drawdowns) measured in wells during a constant-rate pumping test.

Constant rate pumping tests are most often interpreted using the Theis [1935] method or Jacob's semilogarithmic approximation (Meier et.al, 1998). Both of these techniques use the temporal evolution of pumping-induced drawdown to obtain estimates of transmissivity and storativity under the assumptions of homogeneity, a two-dimensional domain, and confined conditions. Jacob's method is based on the fact that the Theis well function plots as a straight line on semilogarithmic paper at large dimensionless times. The analytical solution underlying the Theis and Jacob techniques is based on the assumption of aquifer homogeneity.

2.3.1. Aquifer Hydrogeological Characterization Techniques

Development of proper groundwater management strategy requires characterization of aquifer and ambient spatiotemporal monitoring of groundwater (Ewusi & Kuma, 2014). In the present work, hydrological characterization of an aquifer has been performed. The characterization of aquifers could be done using certain geophysical techniques like Electrical Resistivity, Electromagnetic Induction, Ground Penetrating Radar (GPR),Seismic Techniques, Statistical spatiotemporal modeling and Pumping test data. Aquifer Characterization is dependent on the petro-physical properties (porosity, permeability, seismic velocities etc.) of the subsurface. Results of this Aquifer Characterization could be observed and analyzed using varying geophysical software (WinRESIST, RADpro etc.) and Aquifer test to better image the subsurface (Okan et al., 2018; Yu et al., 2012; Dhar et al., 2014).

Okan et al., (2018) has identified as pumping tests are important and most effective tools that provide information on the hydraulic characterization of a borehole and aquifer parameters, Constant Rate Test also give information about the drawdown and aquifer properties resulting from specific pumping rate.

2.4. GIS and RS Techniques and AHP analysis

The occurrence, origin, movement and chemical constituents of groundwater are dependent on geology/lithology, geomorphology, drainage density, rain fall, geological structures/lineaments, slope, land use/land cover and soil of groundwater regime (Gintamo 2015; Yeh, et al. 2016).

Since groundwater occurs out of our sight deep in the subsurface; there is no direct method to facilitate observation of water below the surface. Its presence or absence can only be inferred indirectly by studying the groundwater occurrence and distribution controlling parameters. Thus, in order to ensure wise use of groundwater, a systematic evaluation of groundwater potential area is required (Murthy etal., 2003). Groundwater potential zones are demarked with the help of, among others, remote sensing and Geographic Information System (GIS) techniques (Jhariya et al, 2016; Sener et al.2005; Waikar & Nilawar 2014).

Nowadays, both Geographical Information System (GIS) and Remote Sensing (RS) are regarded as essential tools for groundwater studies especially for extended and complex systems (Nag, 2008).The information on the input parameters in the above can be acquired and integrated through

remote sensing and Geographical Information System (GIS) techniques. The concept of integrated remote sensing and GIS has proved to be an efficient tool in groundwater studies, in facilitating better data analysis and their interpretations (Murthy et al., 2003).

The main advantages of using remote sensing and GIS techniques for groundwater exploration are the reduction of cost and time needed, the fast extraction of information on the occurrence of groundwater and the selection of promising areas for further groundwater exploration (Hammouri, 2012; Barakat, 2012), its ability to generate information in spatial and temporal domain, which is very crucial for successful analysis, prediction and validation (Hammouri et al., 2012; Bashe, 2017).

Gintamo, (2015) has focused on the evaluation of groundwater potential zone in south Ethiopian rift escarpment, the Bilate River catchment in SNNPR, based on integrated Geographical information system (GIS) and remote sensing techniques. In his study, an attempt had been made to delineate and classify possible groundwater potential zones in the Bilate River. The thematic layers considered were lithology, geomorphology, drainage density, lineament density, rainfall, soil, slope and land use/ land cover were prepared using the Landsat ETM+ imagery and ArcGIS software. Remotely sensed data and geographic information systems were applied for groundwater potential map of Weito watershed, the southernmost sub-basin of the rift valley lakes basin in Ethiopia. Thematic maps were developed using Landsat 8 OLI/TIRS images, shuttle radar topographic mission (SRTM) digital elevation model (DEM) and other data sources using overlay analysis (Bashe, 2017).

According to Hussein et al. (2017) eight major biophysical and environmental factors like geomorphology, lithology, slope, rainfall, land use land cover (LULC), soil, lineament density and drainage density were considered to delineate the groundwater potential areas using geospatial and MCDA tools in Northern Ethiopia, Wollo Zone, in Gerardo River Catchment district. The sources of these data were satellite image, digital elevation model (DEM), existing thematic maps and metrological station data.

Solomon & Quiel, (2006) has conducted Groundwater study using remote sensing and geographic information systems (GIS) in the central highlands of Eritrea. They have identified as Lithology, lineament, landform, slope, vegetation, groundwater recharge and discharge are common features used for many groundwater resource assessments in hard rock areas. GIS techniques facilitate

integration and analysis of large volumes of data, whereas field studies help to further validate results. Integrating all these approaches offers a better understanding of features controlling groundwater occurrence in hard rock aquifers. Yeh et al., (2016) have used a GIS approach to integrate five contributing factors: lithology, land cover/land use, lineaments, drainage, and slope Mapping groundwater recharge potential zone using a GIS approach in Hualian River, Taiwan. They have also identified Many factors affect the occurrence and movement of groundwater in a region, including topography, lithology, geological structures, depth of weathering, extent of fractures, primary porosity, secondary porosity, slope, drainage patterns, landform, land use/land cover, and climate.

2.5. Groundwater and Surface Water Quality

Results from the 2016 Ethiopia Socioeconomic Survey found that 66% of the Ethiopian population uses drinking water from improved sources, with distribution varying by place of residence. In rural areas, 59% of the population reported using an improved source, usually protected springs, tube wells, and dug wells. Source type also differs by region; almost all households in Addis Ababa and 72% in Tigray reported using improved sources (CSA et al., 2017).

Analysis of Physico-chemical Characteristics of Water Collected from Different Sampling Sites of Lake Hawassa, Ethiopia suggested that both point and non-point pollution sources such as human sewage, industrial waste from ceramics, textile, plastics and food processing industries, urban storm water, agricultural runoff and land development were impacting the lake (Haile & Mohammed, 2019).

Groundwater is a major source of water for drinking and irrigation in Ethiopia. Further, mapping spatial variation of groundwater parameters are important for proper developing of new groundwater schemes and management of groundwater resources. Kawo & Karuppannan, (2018) were collected and analyzed groundwater samples to determine suitability of groundwater for drinking and irrigation uses in Modjo river basin. They have used WQI and SAR to identify drinking and irrigation water quality respectively and obtained majority of samples shows that groundwater is suitable for drinking and irrigation.

The major water quality problems in main Ethiopian rift valley is associated with high fluoride concentration in groundwater (Tekle-Haimanot et al., 2006). They have analyzed on 1438 water

samples and obtained 24.2% had fluoride concentrations above the 1.5 mg/l recommended optimum concentration by WHO.

The composition of surface and underground waters is dependent on natural factors (geological, topographical, meteorological, hydrological and biological) in the drainage basin and varies with seasonal differences in runoff volumes, weather conditions and water levels. Human intervention such as the building of dams, draining of wetlands and diversion of flow has significant effects on water quality (Meybeck et al.,1996; Ayenew, 2006).

The geochemistry of ground water may influence the utility of aquifer systems as sources of water. The types and concentrations of dissolved constituents in the water of an aquifer system determine whether the resource, without prior treatment, is suitable for drinking-water supplies, industrial purposes, irrigation, livestock watering, or other uses(Canora etal., 2019).

Quality can vary greatly across an aquifer, through its profile and over time. This is caused by physical and chemical processes occurring in aquifers that can affect salinity, temperature, pH levels, heavy metals and organic substances such as: Dissolved rocks and minerals being transported and re deposited as groundwater moves along the flow path; Evaporation from high water tables causing minerals and salts to concentrate in groundwater; Changes in groundwater levels resulting in saline water being drawn into an aquifer; Chemical reactions that change the chemistry of groundwater or thermal sources such as volcanoes, hot rocks or the sun heating the groundwater (Lapworth et al.,2017).

Groundwater quality varies greatly across an aquifer, through its profile and over time as a result of physical and chemical processes that change the temperature, salts and minerals it conveys (Baxter, 2016).

2.6. Estimation of Missing Data

One of the first steps in any hydrological and meteorological study is accessing reliable data. However, precipitation data is frequently incomplete. The incompleteness of precipitation data may be due to damaged measuring instruments, measurement errors and geographical paucity of data (data gaps) or changes to instrumentation over time, a change in the measurement site, a change in data collectors, the irregularity of measurement, or severe topical changes in the climate of a zone (Sattari et al., 2016). He also explained that, the accurate planning and management of

water resources depends on the presence of consistent and exact precipitation data in meteorology stations.

Estimation of missing climatological data is an important task for meteorologists, hydrologists and environment protection workers all over the world. It is particularly important in mountain and forest regions where meteorological stations are scarce, and the observed climatological data are strongly influenced by topography and the forest microclimate (Xia et al,1999, Aslan et al., 2013). Xia et al, (1999) estimated the missing data of daily maximum temperature, minimum temperature, mean air temperature, water vapor pressure, wind speed, and precipitation with six methods. They determined that the multiple regression analysis method was most effective in estimating missing data. According to them, the multiple regression analysis method was most effective in estimating missing data. The multiple regression model employs step-wise regression to determine the coefficients for all the significant neighbor stations (Edmond Moeletsi, Phumlani Shabalala, De Nysschen, & Walker, 2016).

Rainfall data is important for hydrological modeling, agricultural and water budget estimation. Therefore, for performing the effective rainfall analysis, it is essential to estimate the missing value in rainfall series. For that purpose, different methods are used for estimating the missing rainfall data for specific regions (Romman et al., 2019). From the literature review and his previous experience, Aslan et al., (2013) has chosen six techniques: simple arithmetic averaging, inverse distance method, normal ratio method , single best estimator, multiple regression analysis, the traditional method of the UK meteorological office (constant ratio or constant difference and closest station method.

Measuring and archiving of different weather elements like rainfall, temperature or humidity is an important exercise. Long-term meteorological data can be used to influence decisions in different sectors including agriculture, aviation, hydrology and engineering. Accurate and complete climatological data is important for the successful design and operation of natural resource management systems(Edmond et al., 2016).

Edmond et al.,(2016), missing or faulty climate data have to be estimated in order to provide a complete dataset, especially for modelling purposes. The accuracy of the estimations is dependent on a number of factors including the closeness of the stations used and the location of the patching stations in relation to barriers like mountains.

CHAPTER THREE

3. DESCRIPTION OF THE STUDY AREA

3.1. Location

Walga watershed is located in the Central Ethiopia, Oromia Regional state in South West Shoa zone about 115 km South Western part of Addis Ababa along Jimma main asphalt road in the upper Omo-Gibe basin. This catchment covers about eight woredas of Oromia regional state and two woredas of SNNPR.

The river catchment starts from the highlands of Wonchi-Dandi mountain, Beda kero, Roge and Dase jabo and flows towards south western part to Omo Ghibe basin. Geographically, the area extends $8.26^{0}00$' to $8.818^{0}00$' North and 37.535^{0} to 38.13^{0} East having an area of 2228.12 km^2 and a perimeter of 237. 54 km (figure 3).

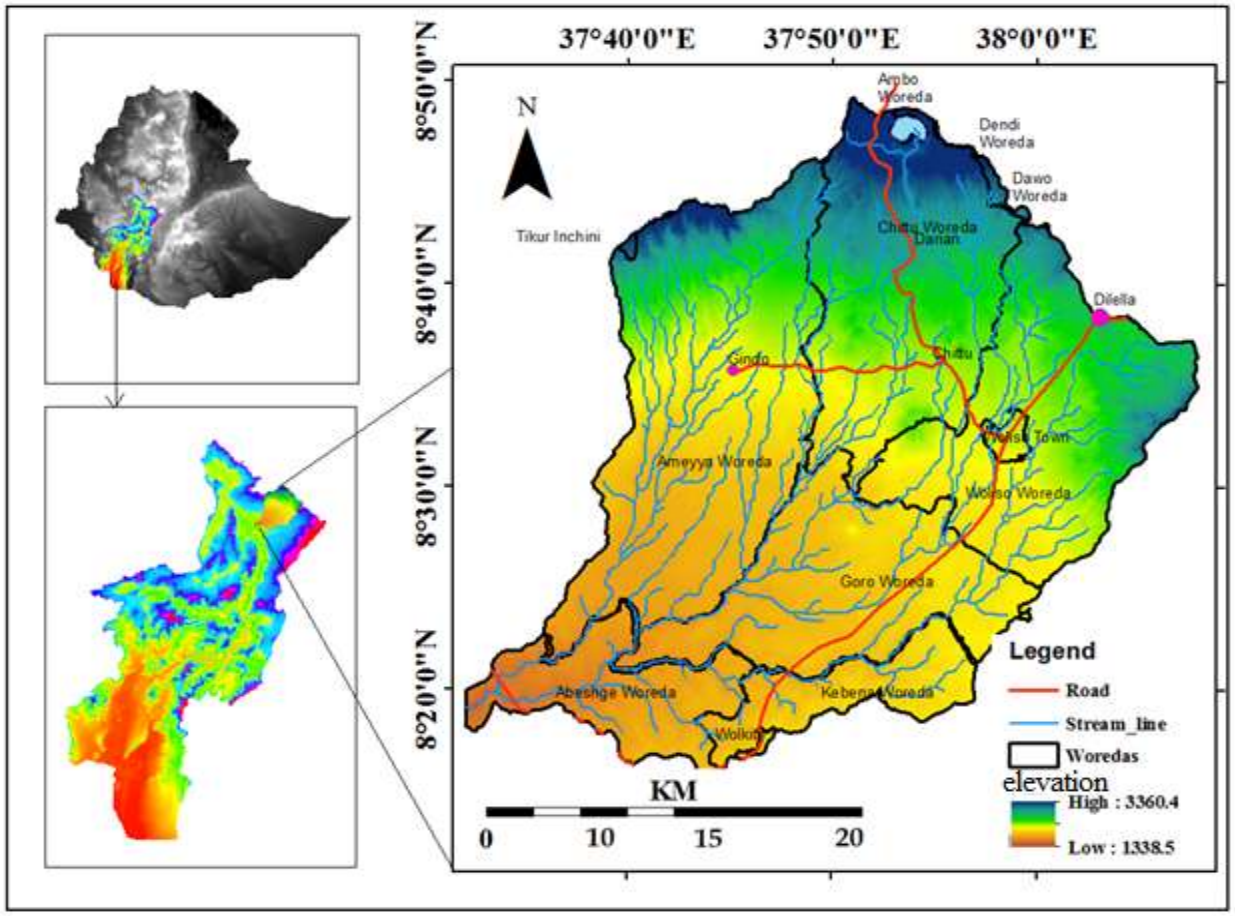

Figure 2. Location map of the Study Area

3.2.Physiography

Walga watershed is characterized by different type of topography with its elevation in the catchment ranges from 1338m to 3300 m a.s.l. The upstream part of the watershed is characterized by mountainous and highly separated terrain with steep slopes while the central and downstream part is characterized by an undulating topography and gentle.

The physiographic set up of the study area is the result of volcano- tectonic, rifting, erosion and deposition processes. The catchment is divided into three physiographic regions: highlands, intermediate and flat lands. Soils in the area are: Clay, clay loam, sandy clay loam and sandy loam.

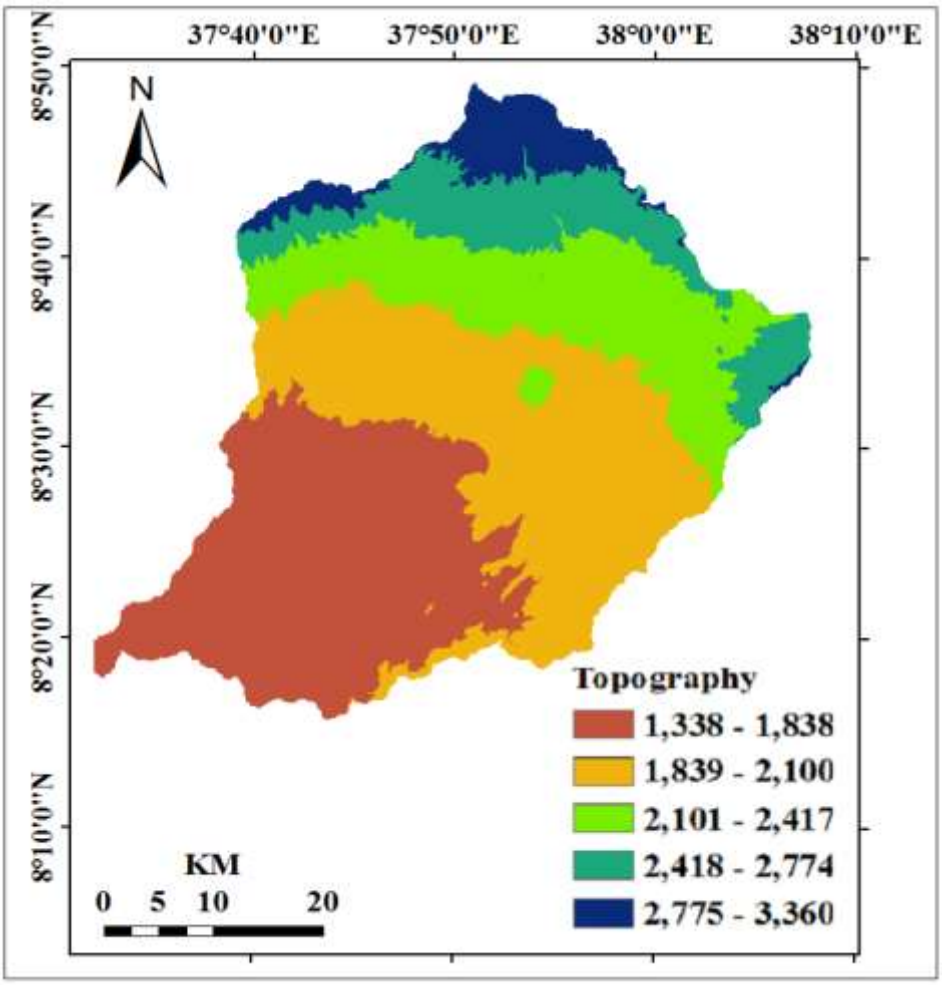

Figure 3. a) Elevation

3.3.Climate

The study area has unimodal (single peak) rainfall pattern with the main rainy season is June to September. Annual rainfall of eight meteorological station (table 1) was analyzed and 344.1 mm is maximum average monthly rainfall recorded at Haro meteorological station (figure 5) since 2018 and minimum and mixiumum average annual rainfall is 1014.48 mm and 1828mm at Ambo and Ameyya respectively. The maximum and Minimum temperature of the catchment is 20.5 ^{0}c and 18.8 ^{0}c respectively (figure 11). The average annual rainfall of the area is 1357.43mm/year.

Figure 4. Spatial distribution of rainfall

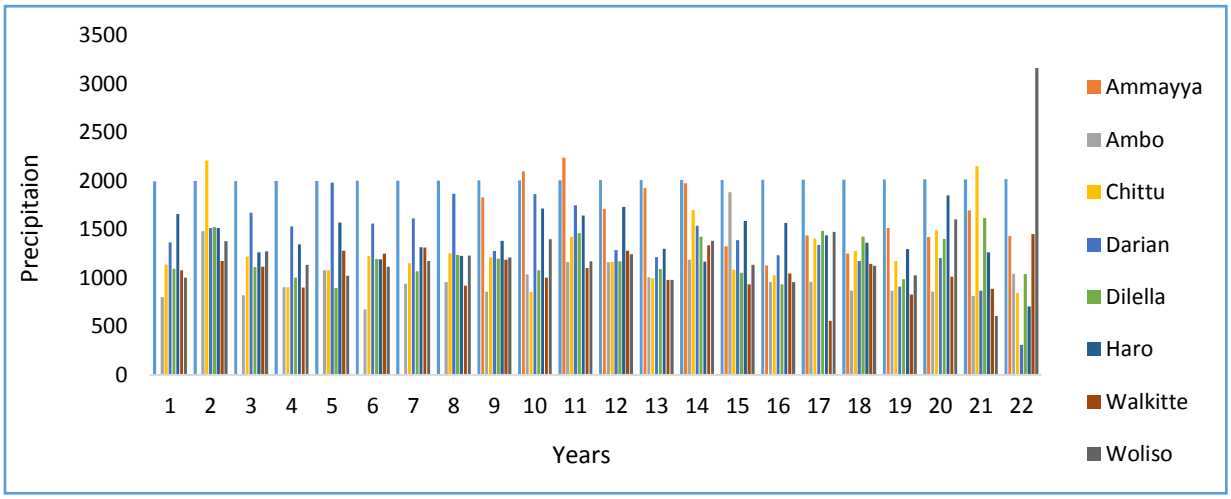

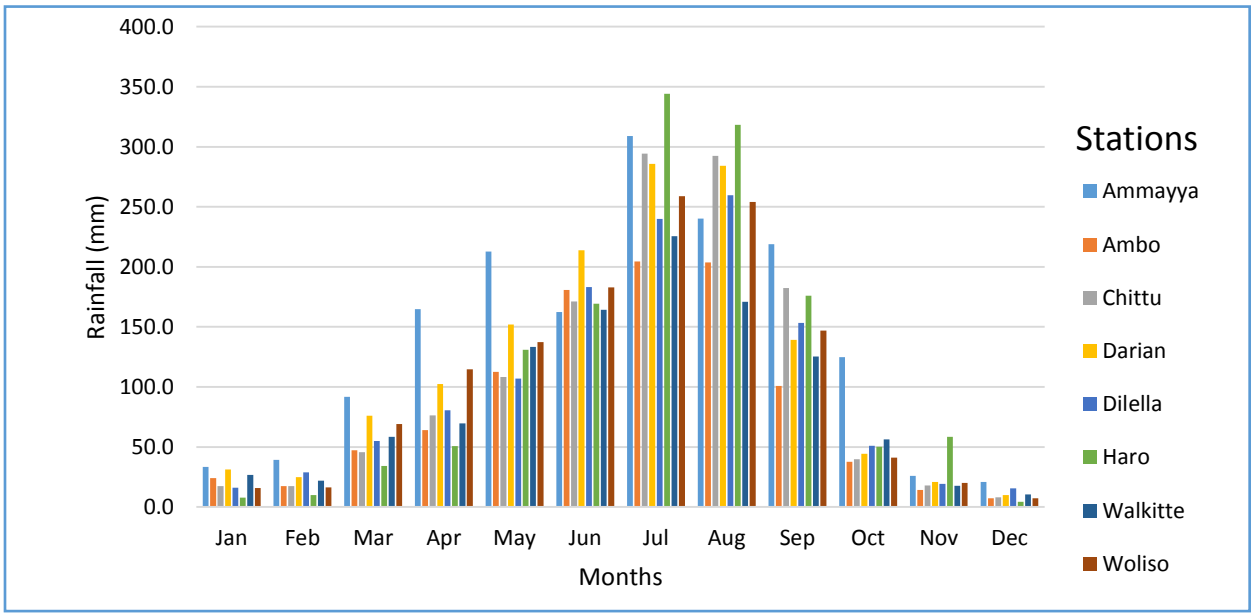

Figure 5-. Mean monthly Rainfall (1997-2018)

Table 1. Mean monthly Rainfall of Walga meteorological stations (1997-2018)

Station	UTM X	UTM Y	Z	Jan	Feb	Mar	Apr	May	Jun	Jul	Aug	Sep	Oct	Nov	Dec
Ammayya	362400	947000	2277	33.4	39.2	91.9	164.7	212.6	162.4	308.9	240.1	218.8	124.8	25.9	20.9
Ambo	371879.6	993784.3	2068	24.2	17.4	47.3	64.1	112.5	180.8	204.4	203.6	100.9	37.7	14.3	7.2
Chittu	380556.7	940168.3	2150	17.5	17.5	45.7	76.3	108.3	171.3	294.4	292.5	182.4	39.9	17.9	8.2
Darian	377536	961369.8	2604	31.4	24.9	76.1	102.3	152.1	213.9	285.7	284.2	139.1	44.4	20.8	9.9
Dilella	393893.9	955151.2	2429	16.0	28.7	55.0	80.7	107.0	183.2	239.9	259.7	153.3	51.0	19.2	15.7
Haro	374048.3	972252.7	3119	7.9	10.0	34.1	50.7	130.9	169.3	344.1	318.4	175.9	50.2	58.4	4.2
Walkitte	369000	917905	2000	26.7	22.0	58.6	69.6	133.3	164.3	225.4	170.8	125.4	56.4	17.7	10.5
Woliso	387542.4	945677.7	2058	15.9	16.2	69.2	114.6	137.3	182.9	258.8	254.0	146.8	41.0	20.1	7.3

3.4.Geology and Hydrogeology

3.4.1. Regional Geology

Walga catchment lies at the South Western margin of main Ethiopian rift. The rift floor and escarpments are highly faulted due to volcanic eruption. All geological Eras and Periods are manifested in the country through their relics as basement (metamorphic), sediments and sedimentary rocks, and volcanic . The plateau and the rift part encompasses the major parts of the country (Ethiopia) including the central land mass of the country where volcanism and volcanic have played a remarkable role in the geological set-up of the area.

Pliocene volcanics:- Dendi-Wonchi Pyroclastic deposits, Wachacha trachyte and Nazret group (middle), welded to partially welded pyroclastic deposits;

Miocene volcanics:- Entoto formation (lower), trachyte lava flows with pyroclastic deposits intercalated with sediments and upper trachyte flows and pyroclastic, upper trachyte flows with plagioclase phyric basalt, ignimbrite, pyroclastic falls and flows and agglomerate are majorly found in the catchment.

Oligocene volcanic:- Jimma upper volcanic of rhyolite and trachyte flows with minor basalts

The pre rift volcanic was result of central or fissure type eruption. Similarly, the post rift volcanic of Quaternary age was not the result of a single eruption but the results of a series eruption.

Volcanic mainly comprised by basalts in Woliso area is part of the Quaternary volcanic and referred to as Woliso-Ambo basalts.

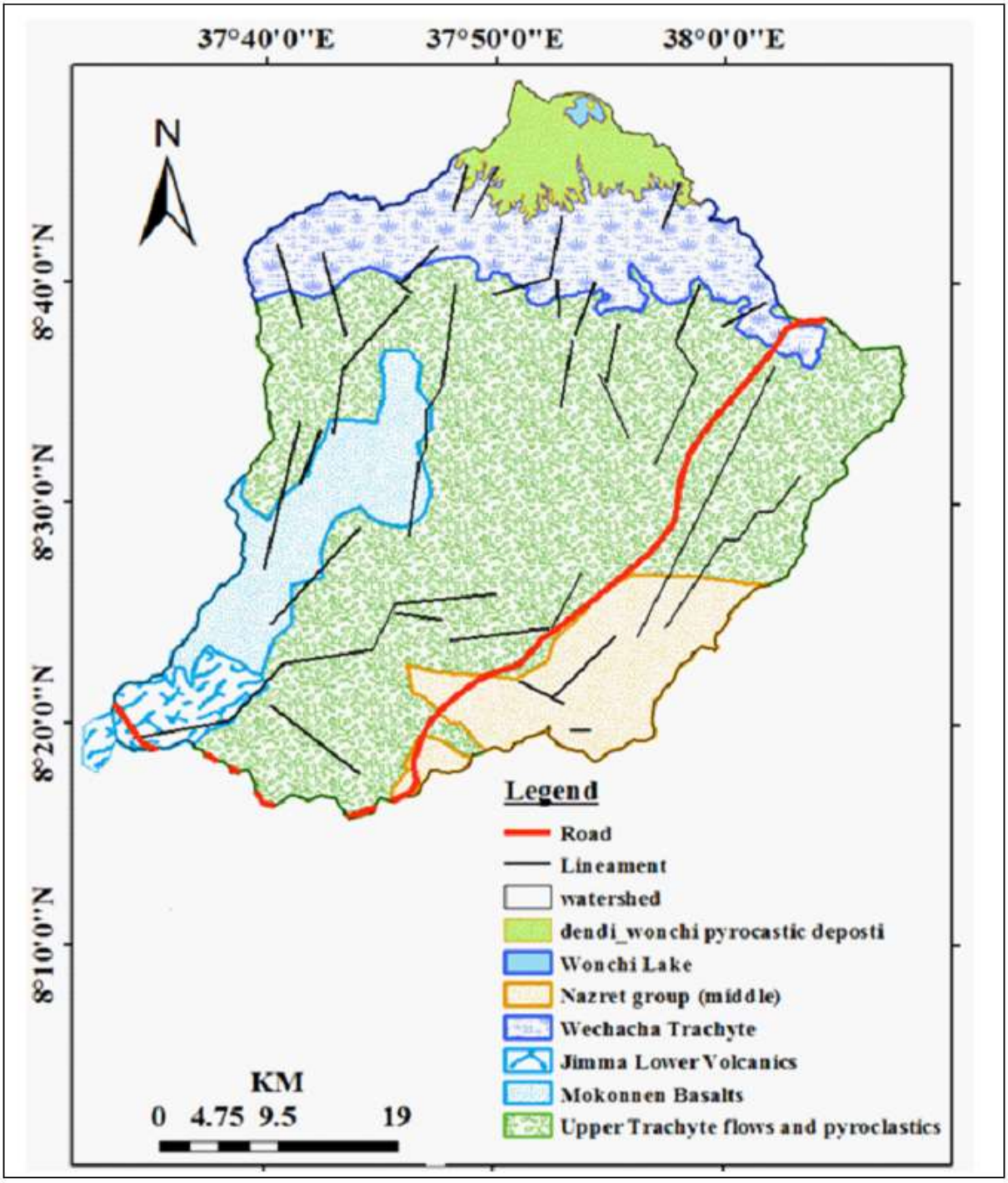

Figure 6. Geological formation of the study area (modified from ATA map, 2013)

3.4.2. Local Geology and Structure

Walga Catchment is part of the South western margin of main Ethiopian rift that comprises mainly Quaternary and partly Tertiary volcanic including basalt, scoria, trachyte and rhyolite. Though not prominent, there are also other pyroclastic. The present landscape of the area is the manifestation of the long-term geological and tectonic activities adhered to both regional and local dynamics and superimposed by erosion and deposition. Woliso town is lying on a caldera floor surrounded on east, southeast with ridges that also acts as water divide.

The geological structures, mainly faults, are oriented northeast- southwest and north-south (north-west and southeast). Faults have played a leading role for groundwater movement and storage as well as in displacing different rocks in the area. Sometimes an abruption of different lithology or the presence of volcanic plagues such as in the center of the town is observed mainly due to different geological structures.

3.5. Hydrogeology of the Area

The hydrogeological set-up of Walga catchment is controlled by both lithology and geological structures, which is common in many cases, as manifested in the geomorphology of the area. The weathered basalt (fractured, scoraceous, etc.) and pyroclastic along with faults have the leading role in the occurrence, movement and geo-chemical properties of groundwater in the area.

Based on the feasibility study documents and the field visit as well as lithological logging of existing wells, the major aquifer in Woliso area is fractured and scoraceous basalts; this forms multilayer aquifer system (source: SWSZWREO). Some existing boreholes in the area are artesian confirming the multilayer aquifer nature of the area. Pyroclastic, mainly pumice and tuff are also another aquifer in the area, commonly intercepted at depth. This aquifer is perceived to be the sources of high fluoride content of groundwater. A lot of bore holes were closed due to their high fluoride content.

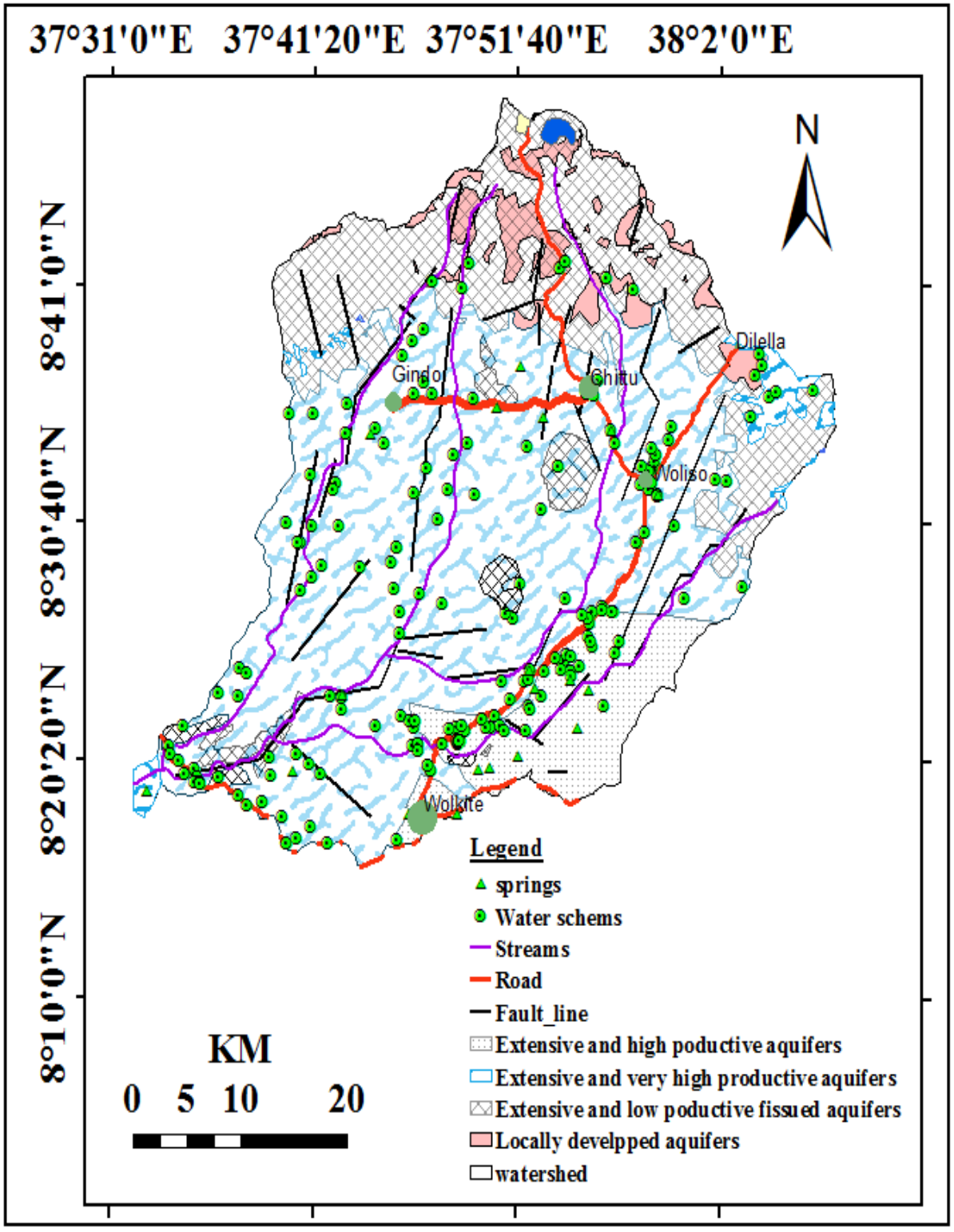

Figure 7. Hydrogeological map of the area (Source ATA map)

3.6. Drainage system

The area is located at a water divide of three basins namely; Abbay, Awash and Omo-Ghibe basins. The drainage pattern of the area is controlled by the rift shoulder uplifted topography and the predominant fracture systems and the central volcanoes. Most of the major rivers follow the NE–SW lineament trend. The main water bodies that characterized the drainage system of the Walga catchment are Lake, rivers and streams. Wenchi crater Lake is located at the upper northern flank of the basin. Many perennial and intermittent rivers are found in Walga watershed

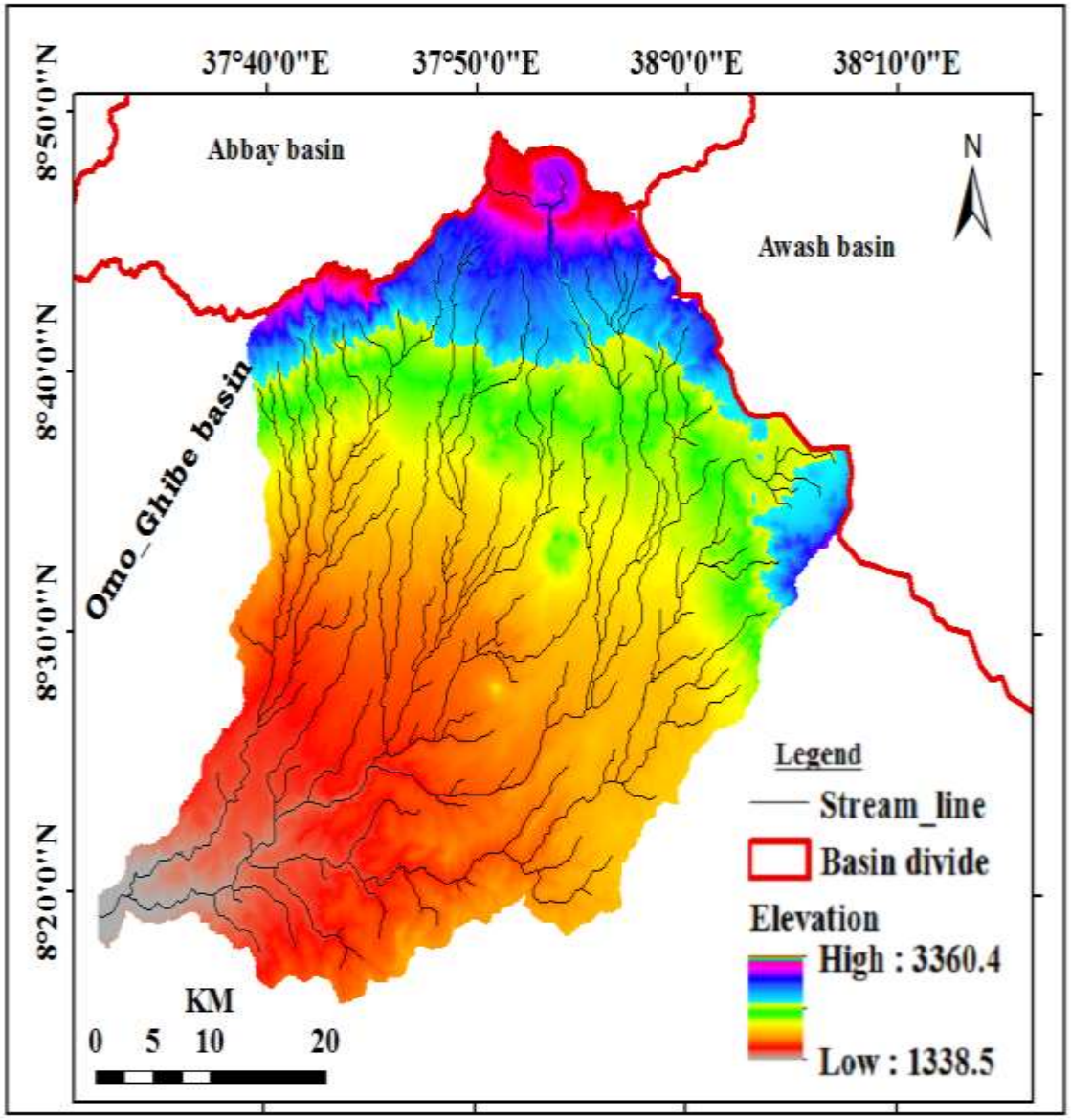

Figure 8. Drainage System of Walga watershed.

Major perennial rivers crossing the watershed is Walga, while Ejersa, Rebu, deddebia, amegna, kulit and others are small rivers that are joining Walga and draining to Omo Ghibe basin. They are characterized by dendritic drainage pattern; however major rivers in the area are parallel to each other indicating that they are structurally controlled. Walga and Rebu are gauged at the location of 0345831m Easting and 0921338 m Northing and 0366029 m Easting and 0923114 m Northing respectively.

CHAPTER FOUR

4. MATERIALS AND METHODS

4.1. Methodology and Techniques

In order to achieve the objectives of the research project, the following methodology and techniques containing different steps were employed. The first step is data containing topographical data, hydrogeological data, geological data, hydro-chemical data, meteorological data, soil data were collected and satellite images for land use land cover were downloaded and processed. GIS and Remote sensing played great role in manipulating, storing and analyzing digital data. These data were needed to be adjusted and prepared to raster grid cell.

The watershed delineation has been done by using Digital elevation model (DEM) which is obtained from the SRTM. ArcMap 10.4 and its spatial extension was used for further processing of the DEM and delineation of the basin. Land use land cover map of the study area was prepared using ArcMap 10.4 from Landsat OLI8 satellite image taken on 27 Feb, 2020 and correlated with field data collected using GPS. Raster map of meteorological data, groundwater level, LULC, reclassified soil map, elevation map and slope map were prepared using ArcGIS.

Then, a physically based quasi-steady state time independent model, WetSpass, has been used to estimate the long-term average spatially varying water balance components. The model uses this raster data to calculate annual and seasonal recharge maps, actual evapotranspiration and surface runoff for the study area (figure 9).

In order to estimate the value of a variable over a continuous spatial field, kriging interpolation was used. The values for other points were estimated from known values and surface data was created from point data using ArcGIS 10.4. Data collected from different bore holes and shallow wells were used to calculate hydraulic properties using aquifer test 9 software and their hydraulic properties were characterized.

Thirdly, hydro-geochemical data was analyzed using piper plot to identify water quality variation of Walga catchment. Finally, groundwater potential of the study area was mapped using multi criteria overlay analysis using raster data prepared for WetSpass input data.

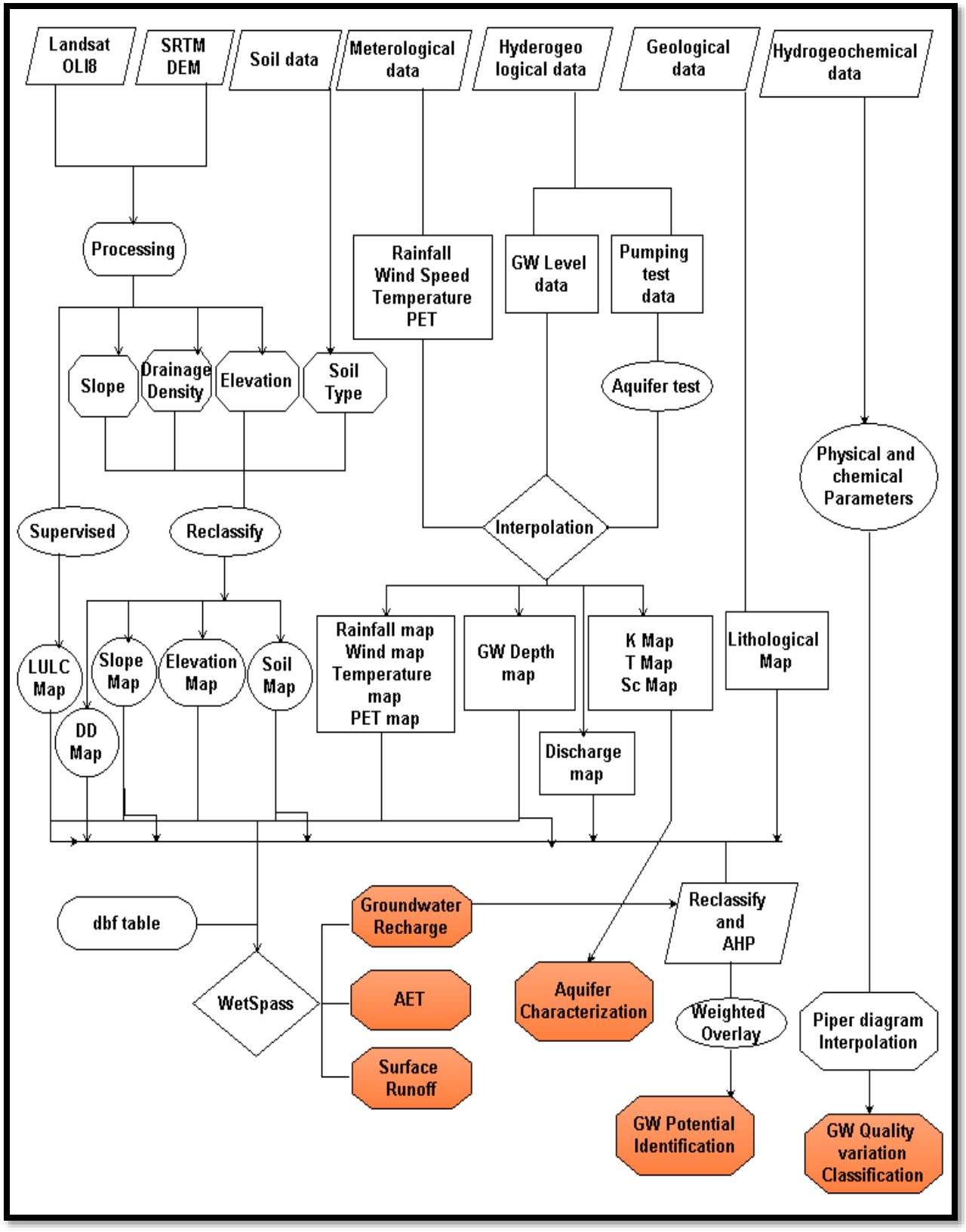

Figure 9. Methodological Flow Chart

4.2. WetSpass Modeling

WetSpass was applied to estimate long-term seasonal/annual average recharge as a function of land-cover, soil type, topography and hydro-meteorological factors (Batelaan & De Smedt, 2001) in Walga catchment. As WetSpass modeling was developed for temperate regions by Batelaan and DeSmedt (2001,2007) which has different climatic and land conditions compared to the tropics, some input parameters modification was used to apply it in tropical region. In temperate region, summer and winter have six month each while in Ethiopia summer contains four months and winter covers eight months (Dereje & Nedaw, 2019; Teklebirhan et al., 2012,). In addition to this, the seasons of rainfall period and land-use/land-cover are not the same. According to them, to apply the WetSpass for Walga catchment, input of the meteorological grid map was done using eight months of winter and four months of summer. Also, summer and winter land-use parameter tables were modified for use (Annex 4 and 5).

By using long-term average standard hydro-metrological parameters as input, the model simulates the temporal average and spatial differences of surface runoff, actual evapotranspiration, and groundwater recharge. Since evapotranspiration from shallow groundwater can be significant, especially in groundwater dependent wetlands, the position of the water table is taken into account, through the use of a coupled groundwater model, in the estimation of recharge. WetSpass is integrated in GIS ArcView as a raster model. Parameters such as land-use and related soil type, are connected to the model using attribute tables of the land-use and soil raster maps (Tilahun & Merkel, 2009).

The seasonal water balance for a vegetated fraction of a raster cell (Fig. 1) is

$$P = I + S_V + T_V + R_V \quad \ldots\ldots 1$$

where P is the precipitation [L], I the interception [L], S_V the surface runoff [L], T_V the actual transpiration [L] and R_V the groundwater recharge [L] in the vegetated fraction of the raster cell. The actual evapotranspiration, ET_v [L], is the sum of T_V and the evaporation from the bare soil, E_s [L]. The total actual evapotranspiration, ET_{tot} [L], is the sum of I, T_v and the evaporation from the bare soil, Es [L]. The surface runoff, S_v, is simulated in two stages. First, the potential surface runoff, Sv–pot, is calculated as:

$$S_{V-pot} = f_1(V,ST,S,D)(P-I) \quad \ldots\ldots 2$$

Where f_1 is a runoff factor from look up table whose value is dependent on vegetation type (V), soil texture (ST), slope (S), and groundwater saturated areas (D), and is based on characteristic values derived.

In the second stage, the potential surface runoff is adjusted for recharge areas by taking into account the seasonal precipitation intensity distribution (P_i) in relation to the soil infiltration capacity as:

$$S_V = f_2(P_i, I_c, D)\ S_{V-pot} \quad \text{.....3}$$

Where f_2 is a factor from a soil texture lookup table that partitions the precipitation for a hydrological season, in an effective and non-effective part for contribution to the surface runoff. It can be derived by estimating the fraction of seasonal precipitation with intensity higher than the infiltration capacity of a particular soil type.

Monthly Reference evapotranspiration was estimated using penman-Monteith equation from FAO CROPWAT 8.0.

For bare soil surface recharge was estimated using the equation:

$$P = S_S + E_S + R_S \quad \text{.....4}$$

Where the index s refers to bare soil surfaces. The surface runoff S_S was simulated in a similar way to the vegetated area fraction in two stages—Eqs. (2) and (3).

The water recharge for open water area fraction of a cell is defined as:

$$P = S_o + E_o + R_o \quad \text{.....5}$$

Where the index *o* refers to open water surfaces.

The water balance for impervious surfaces is given as:

$$P = S_i + E_i + R_i \quad \text{.....6}$$

where the index i refers to impervious surfaces.

The total water balance, per raster cell and hydrological season is stated as:

$$ET_C = a_v ET_v + a_s E_s + a_o E_o + a_i E_i \quad \text{.....7a}$$

$$S_C = a_v S_v + a_s S_s + a_O S_O + a_i S_i \quad \text{.....7b}$$

$$R_C = a_v R_v + a_s R_s + a_i R_i \quad \text{.....7c}$$

where the index c refers to raster cell, with ET_C, S_C , R_C [L] respectively, the total evapotranspiration, surface runoff and recharge in a raster cell and a_v, a_s, a_o *and* a_i respectively the vegetated, bare soil, open water and impervious area fraction of a raster cell. In a vegetated or

cropped area, there is evaporation from the soil in between the plants and transpiration from vegetation, resulting in evapotranspiration (ET_V) in Eq. (7a). From the portion of the catchment on which there is no vegetation (i.e. practically bare land), only evaporation from the bare soil E_s occurs, in Eq. (7a).

In the equation (7c) above there is no recharge Ro, because it is assumed that the recharge, Ro, derived from the precipitation on the open water fraction, is negligible compared to the possible recharge from the surface water body itself. If the Penman open water evaporation, E_o, is smaller than the precipitation, the remaining water will contribute to the surface runoff, So (Batelaan & De Smedt, 2007).

4.2.1. WetSpass Input Data

The WetSpass model requires a set of basic input data, including meteorological data (precipitation, air temperature, wind speed, and potential evapotranspiration), distributed groundwater depth, soil types, topography (DEM and slope), and land use/land cover of the investigated area. Such input data were prepared as grid maps using Geographical Information Systems collected for the period of 1997 to 2018. The climate data for eight stations around the Walga catchment was obtained from Ethiopian Meteorological Services Agency. Seven of the stations (Ameyya, Chittu, Darian, Haro, Woliso, Wolkitte and Dilella) are located in the catchment area while the other one (Ambo) is located outside of the catchment. Woliso and Ambo provides complete data of more than thirty years while the others contains only precipitation data. Among these stations Ameyya has only 12 years rainfall record with two years missing data.

The WetSpass model was applied for the study area using grid cells of 100 x 100 m with 677 columns and 639 rows. The model functions on two seasonal data sets. For this purpose the year was divided into two seasons with summer (June to September) and winter (October to May) with respective input data (land-use, precipitation, potential evapotranspiration, temperature, wind speed, and groundwater depth). The major rainy season of Walga catchment is from June to September.

Two types of inputs were required so as to run the WetSpass model: Parameter tables (dbf data) such as inputs of land use, soil and runoff characteristics parameter tables are required. Then, this table was added to map as attribute. The runoff characteristics parameter tables contain runoff

coefficient, slope and soil type for each corresponding land use and grid map is also prepared using ArcMap 10.4. ArcMap (version 10.4) together with its spatial analyst extensions was used in order to prepare these input parameters. This raster grid maps were converted to asci format using ArcMap conversion tools. The input map preparation is as follows:

Precipitation

Annual rainfall map of the study area was prepared using the historical rainfall data of long years measured at the meteorology stations located in the catchment and surrounding study area (Annex 1). Incompleteness of precipitation data at all stations was filled using linear regression and GIS with its spatial analyst tool (interpolation) used to analyze data of eight meteorological stations in the Walga river catchment and nearby station. Kriging spatial interpolation was applied to know the areal distribution of precipitation over the catchment.

Accordingly, the area receives an average annual rain fall of 1357.43mm per year. The summer annual average rainfall is 794 mm while winter average rainfall is 541mm.

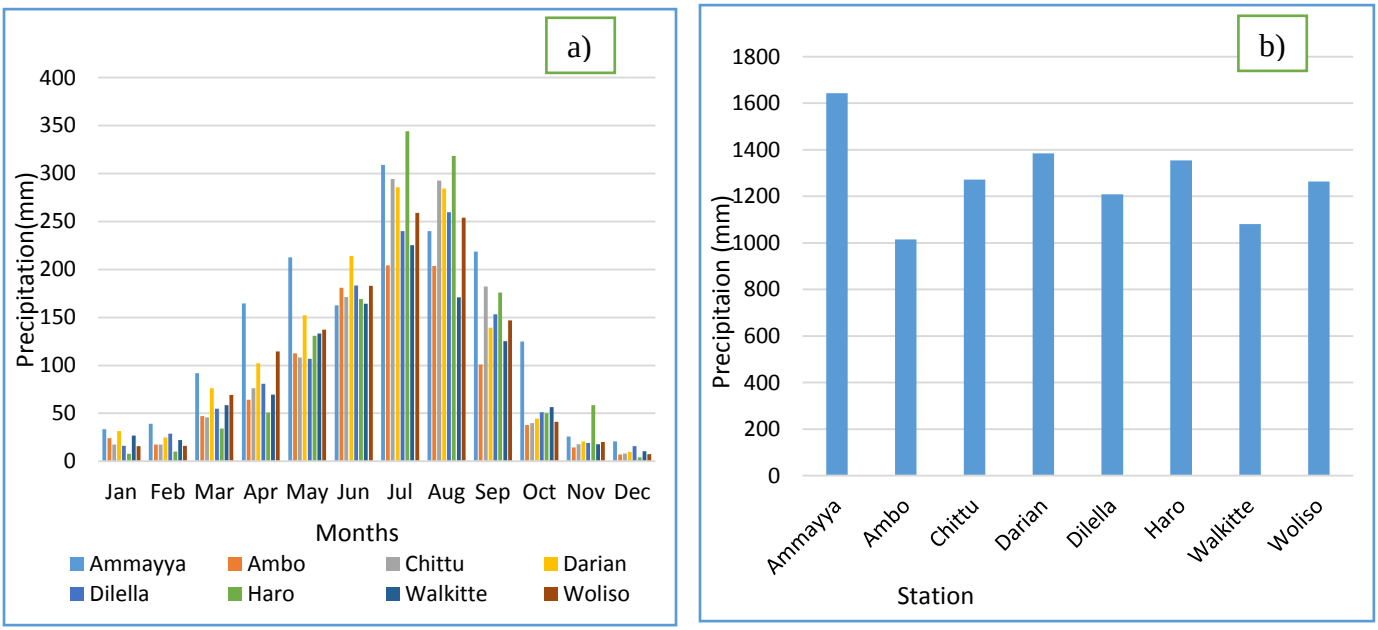

Figure 10. a) Mean monthly precipitation b) Mean Annual precipitation

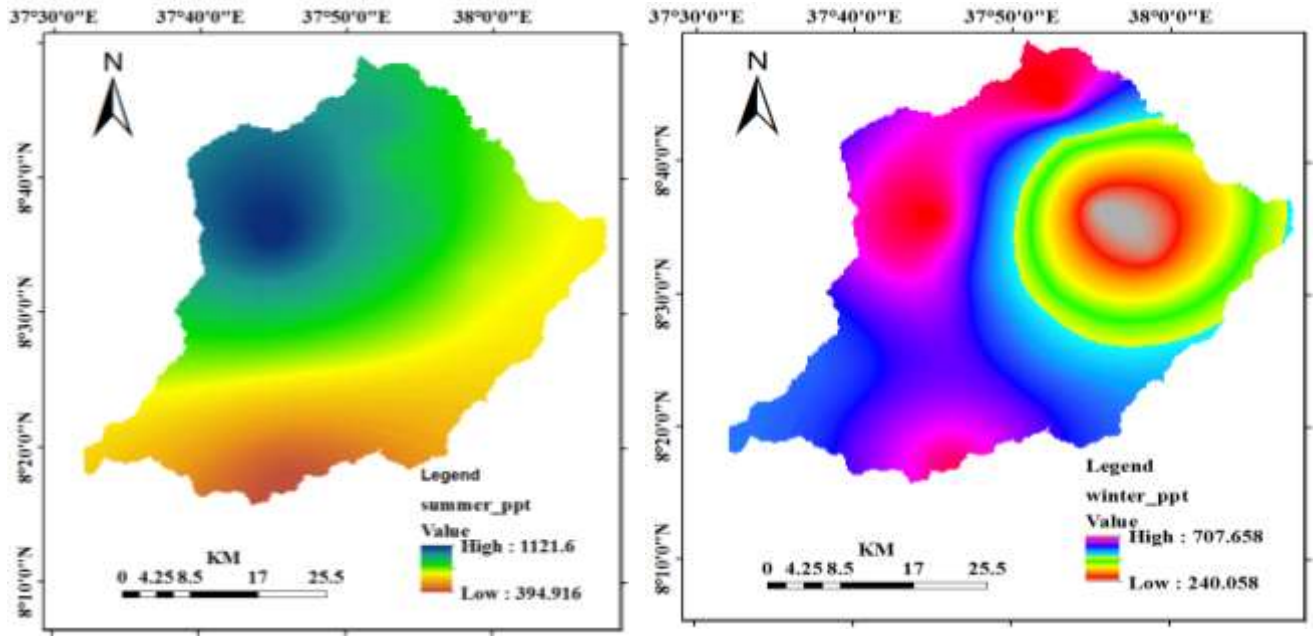

Figure 11. Summer and Winter precipitation map of Walga watershed

Temperature

Temperature data is available for only four weather stations. Ameyya has 15 years recorded data while the others, Ambo, Woliso and Wolkite have more than 30 years recorded data. The summer season average temperature is 17 ^{0}c while the winter is 19.98^{0}c. The annual minimum and maximum average temperature is 17.4^{0}c and 20.4^{0}c respectively. Minimum monthly temperature was recorded at Walkite station since December 2013 while maximum monthly temperature is recorded at the same station since November 2015.

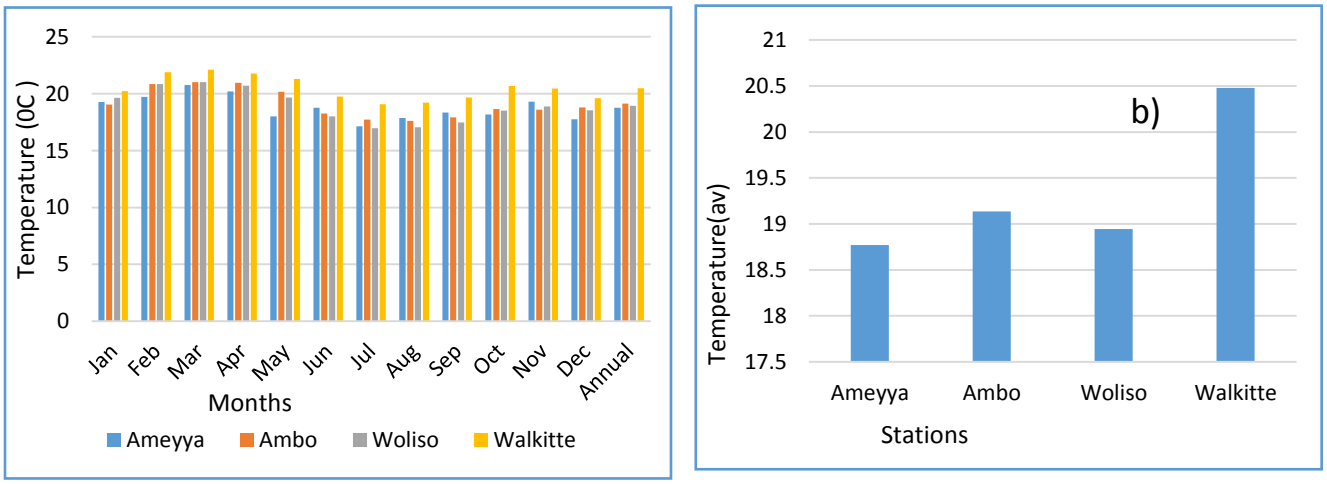

Figure 12. a)Long term mean monthly temperature b)Annual mean temperature of each station

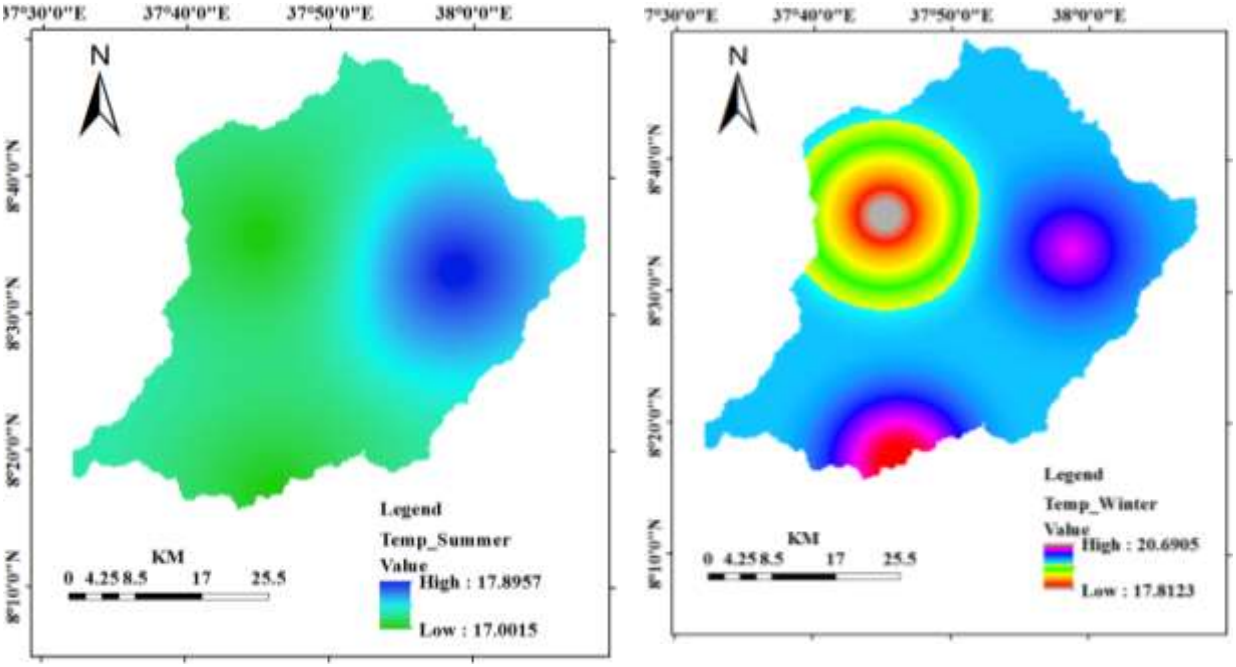

Figure 13. Summer and Winter average Temperature of Walga catchment

Wind Speed

Wind speed data are available only for Ambo and Woliso station. These data were used uniformly over the watershed. Average wind speed of summer and winter is 1.12 m/s and 5.37 m/s respectively. The maximum, minimum, average and stdev of annual wind speed is 3.84m/s, 2.13m/s, 3.24m/s and 0.26 respectively.

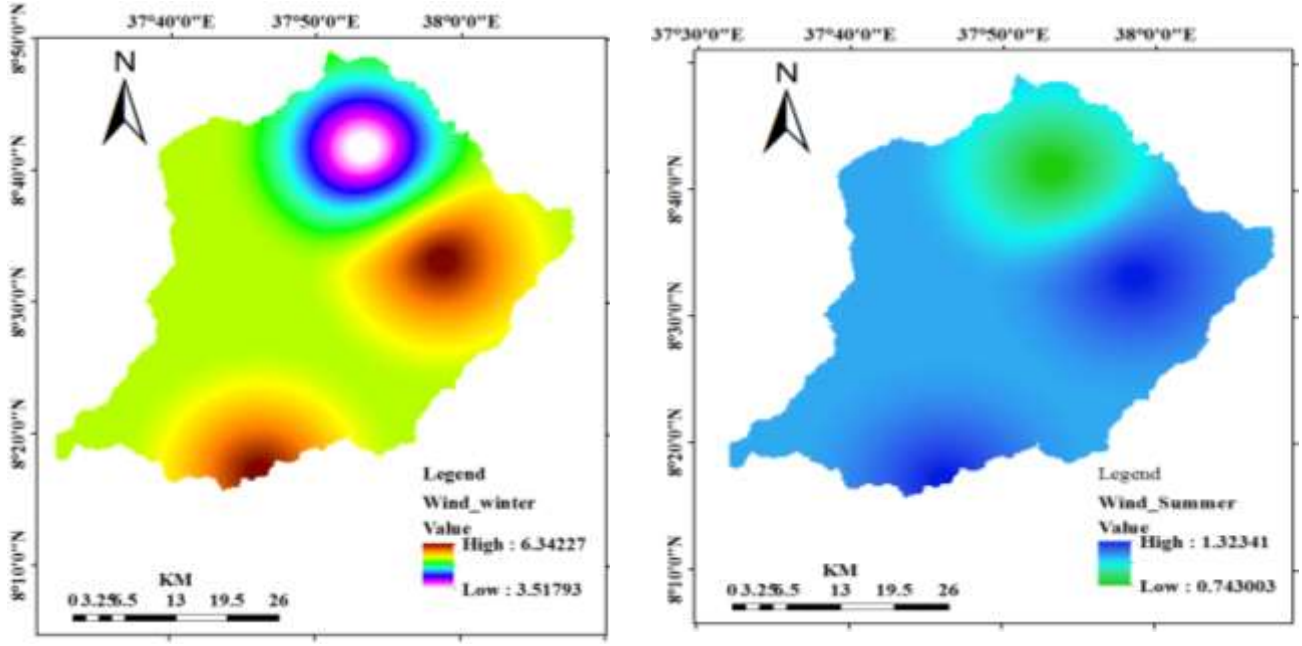

Figure 14. Summer and Winter average wind speed map of Walga catchment

Potential Evapotranspiration

Potential evapotranspiration (PET) is the maximum amount of water that can be removed from a land surface through evapotranspiration (ET) as sum of both evaporation and transpiration given abundant supply of soil moisture (Amatya et.al, 2014). In last few decades several different methods varying from empirical to temperature-based to physically-based process models have been developed, tested, and applied to estimate PET for various types of land covers from soil surface to crop, water, and vegetation.

Potential evapotranspiration of Walga watershed was calculated using Penman-Montieth based FAO CROPWAT software for two meteorological stations having recorded minimum and maximum temperature, wind speed, sunshine hours and relative humidity. As other meteorological data, PET Calculated monthly results were subdivided into two main seasons i.e. 4 months of summer (rainy season) and 8 months of winter (Dray season). Finally, those PET values of each season, were converted to spatially distributed grid maps by means of interpolation.

The grid maps of PET for both seasons were used with other input parameters in WetSpass model to estimate the recharge as well as actual evapotranspiration (AET). The average potential evapotranspiration of summer is 354 mm, where the winter is 982 mm, and the average annual potential evapotranspiration is 1336. 5 mm with 1311.07 mm and 1386.6 mm as the minimum and maximum annual PET respectively.

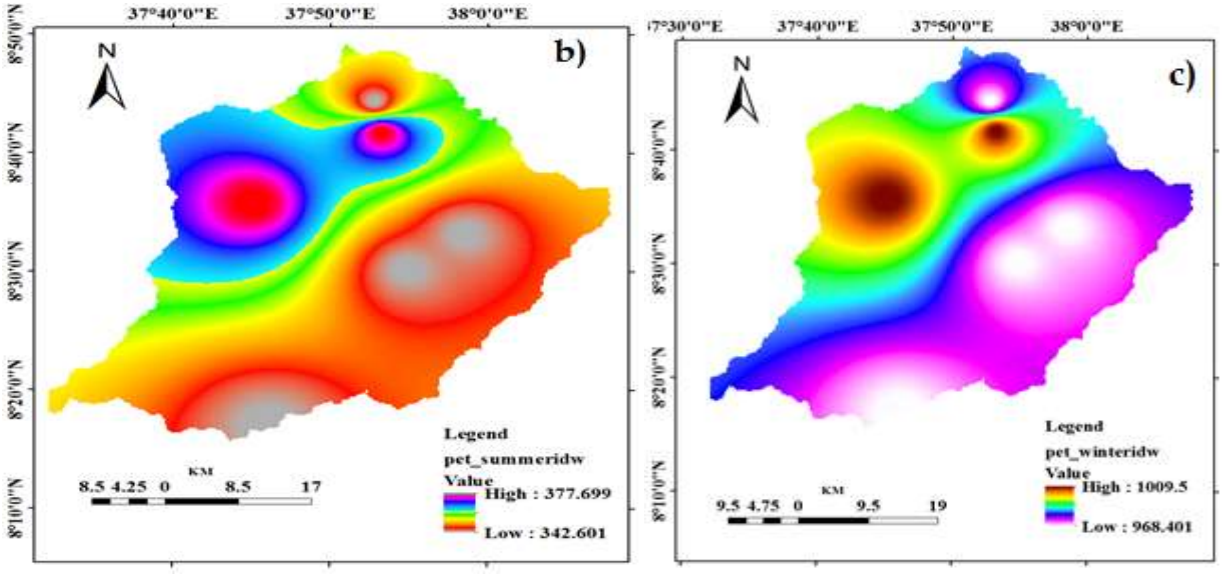

Figure 15. a) Annual PET b) Summer PET and c) Winter PET of walga catchment

Land Use Land Cover

The important characteristics of the runoff process that affects infiltration, erosion, and evapotranspiration is Land use. The main crops grown in the area are maize, wheat, teff, sorghum, barley, been, pea and different types of vegetables. Land cover units having different areal coverage are Vegetated area, grass and shrub lands, bare land, settlement, Agricultural area and open water body of Lake Wonchi. Climatic elements such as precipitation, temperature, humidity, sunshine, and wind are affected by geographic location and altitude. Seasonal classification over the study area is thus mainly based on the average rainfall distribution pattern over the year.

Classification process and analysis of the different LULC classes were done using one Landsat satellite images covering the Landsat 8 OLI/TIS acquired on 27 Feb, 2020. These images includes; L8 OLI/TIRS (path 169, rows 54). The Landsat images were down-loaded from United States Geological (USGS) Earth Explorer (https://earthexplorer.usgs.gov/). The selection of the Landsat satellite images dates was influenced by the quality of the image especially for those with limited or low cloud cover. Each Landsat was georeferenced to the WGS_1984 datum and Universal Transverse Mercator Zone (UTM) 37 Northern coordinate system.

For this study, only supervised classification was performed. Using the Image Classification toolbar and Training Sample Manager of ArcGIS 10.4, it was determined the training samples were representative for the area and statistically separate. Then a maximum likelihood classification was performed from the toolbar. The classified image was then cleaned to create the final land-use map as shown below (figure 16).

Table 2. Land use/Land cover of Walga catchment

No	Classes	Area (km^2)	Area (%)
1	Agriculture	1587.36	71.24
2	Mixed forest	78.43	3.52
3	Settlement	62.55	2.81
4	Bare Soil	0.35	0.02
5	Grass & shrub lands	495.73	22.25
6	Water body	3.75	0.17
	Total	**2228.17**	**100.00**

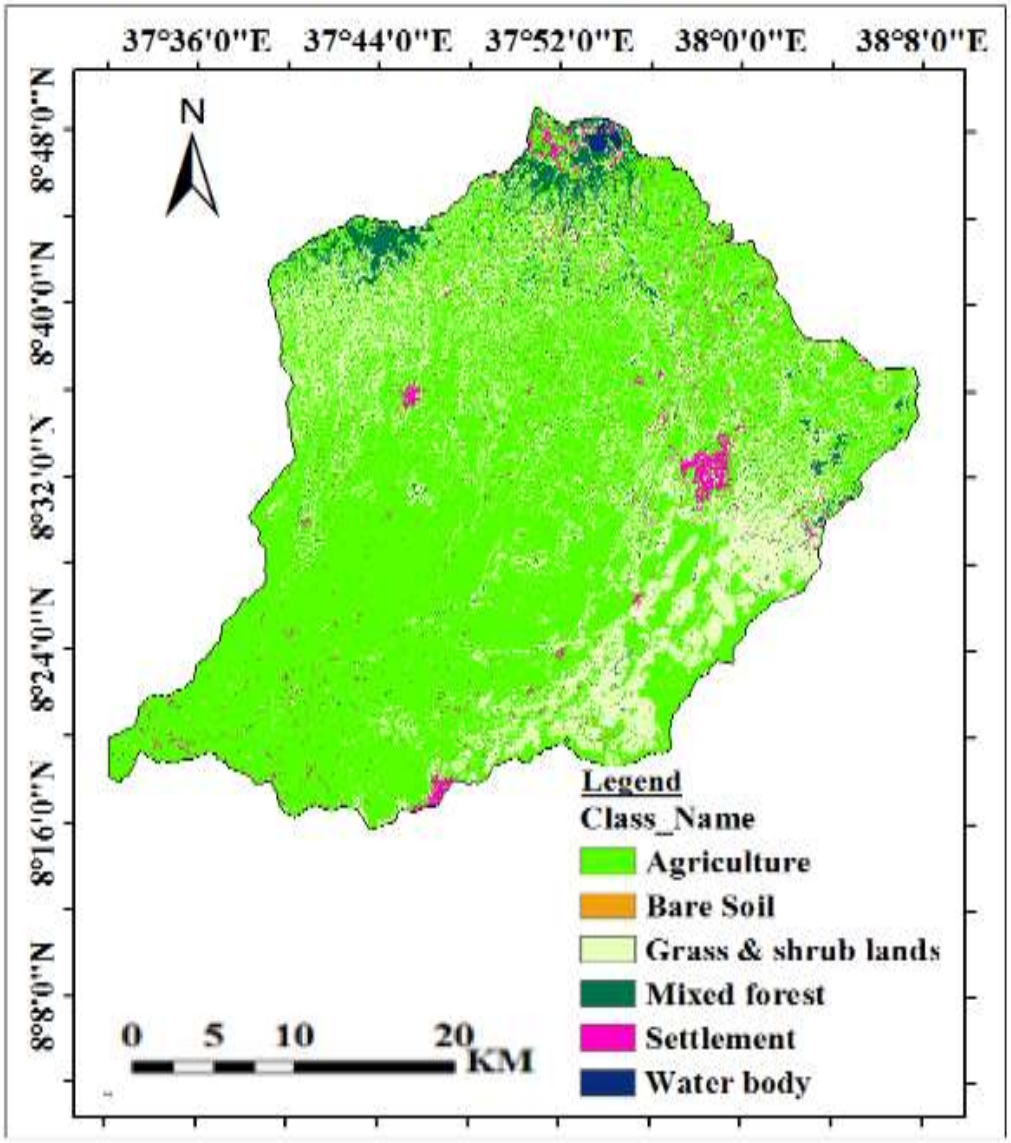

Figure 16. Land Use Land Cover of Walga watershed

Soil Map

The soil map of Walga catchment was extracted from the soil map of Ethiopia (scale 1:250,000) obtained from ministry of Water Irrigation and Energy.

The major textural system of the clay used in WetSpass is based on soil texture developed by FAO class based on the percentage of silt, clay and sand. Based on that the major soil classification of walga catchment is clay (11.78%), clay loam (70.5%), sandy clay loam (13.73%) and sandy loam (4%).

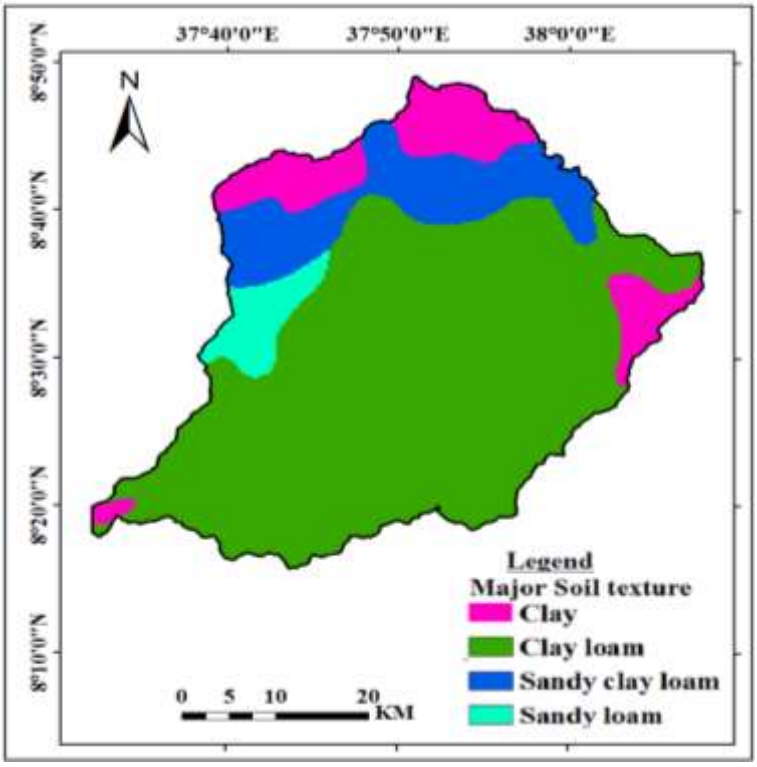

Figure 17. Soil map of Walga catchment (Source: MoWEI)

Table 3. Areal coverage of soil texture

S.N	Major soil texture	CODE	Area	Area %
1	clay loam	9	1571	70.4997
2	sandy clay loam	7	305.88	13.7264
3	sandy loam	3	89.06	3.99676
4	clay	12	262.44	11.7772
	Total		**2228.38**	**100**

Groundwater depth

Groundwater depth (Static water level) measurement was taken for accessible sites using deep meter through observation pipe installed during water well construction. Inaccessible bore hole sites groundwater depth and spring data were obtained from South West Shoa Water Resource Development and Energy office and Ethiopian Construction Design and Supervision Works Corporation (ECDSWC). The measured static water level was subtracted from surface elevation and its raster map prepared using kriging spatial interpolation.

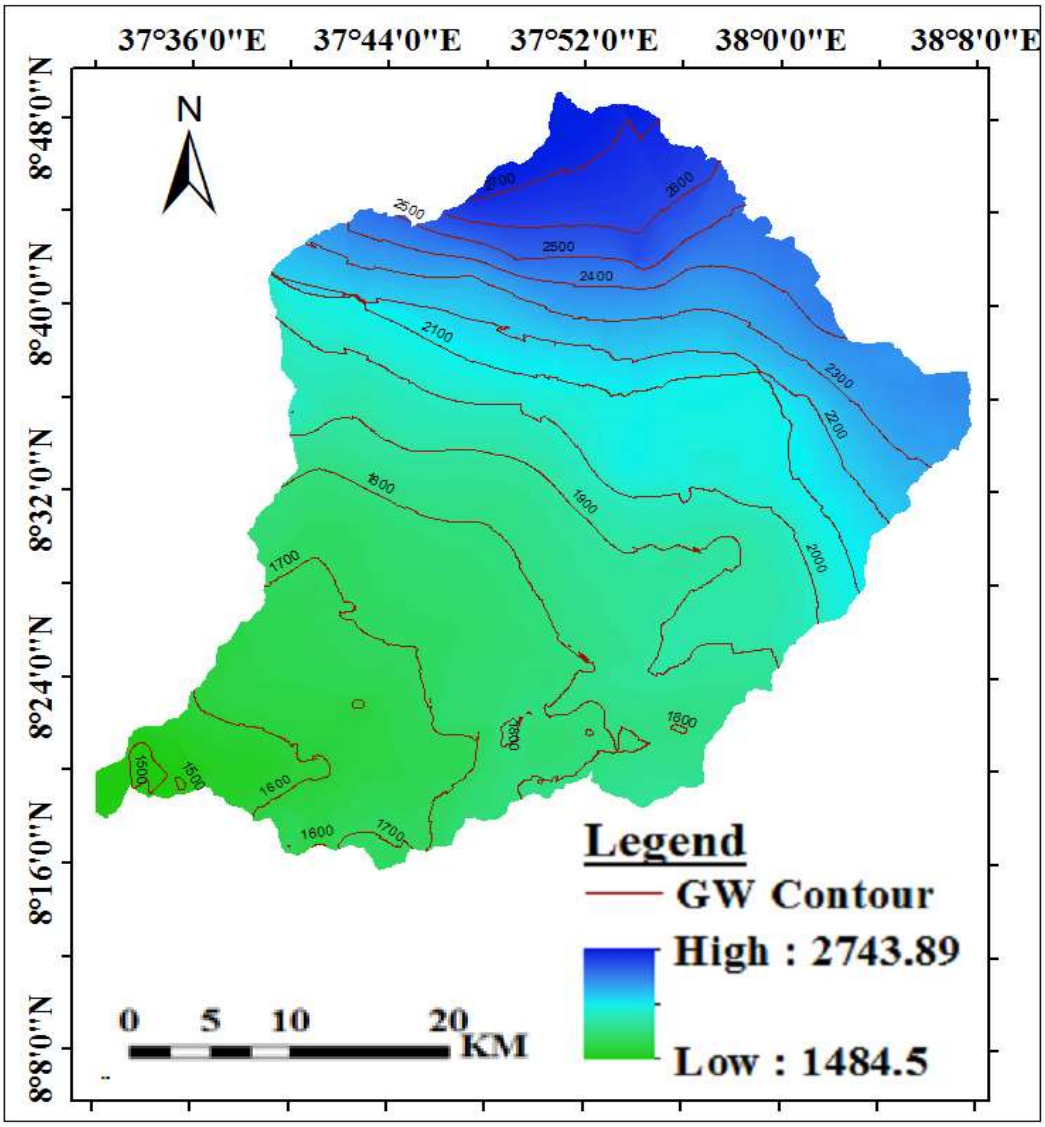

Figure 18. a) Groundwater depth and its contour map

Slope and Elevation

Digital elevation model (DEM) was downloaded from the Shuttle Radar Topography Mission (SRTM) data sets of the United States Geological Survey (USGS). The lowest (minimum) elevation point in the watershed is 1338.5 m in the downstream part and the highest is 3360.4 m in the upper stream part, while the mean elevation of the watershed is 2070.35m (Figure 3b) . The slope map of the watershed is derived from the digital elevation model using the spatial analyst tool of ArcGIS 10.4.1. The slope ranges from 0^0 to 46^0 with a mean of 4.11 and standard deviation of the slope is 4.25.

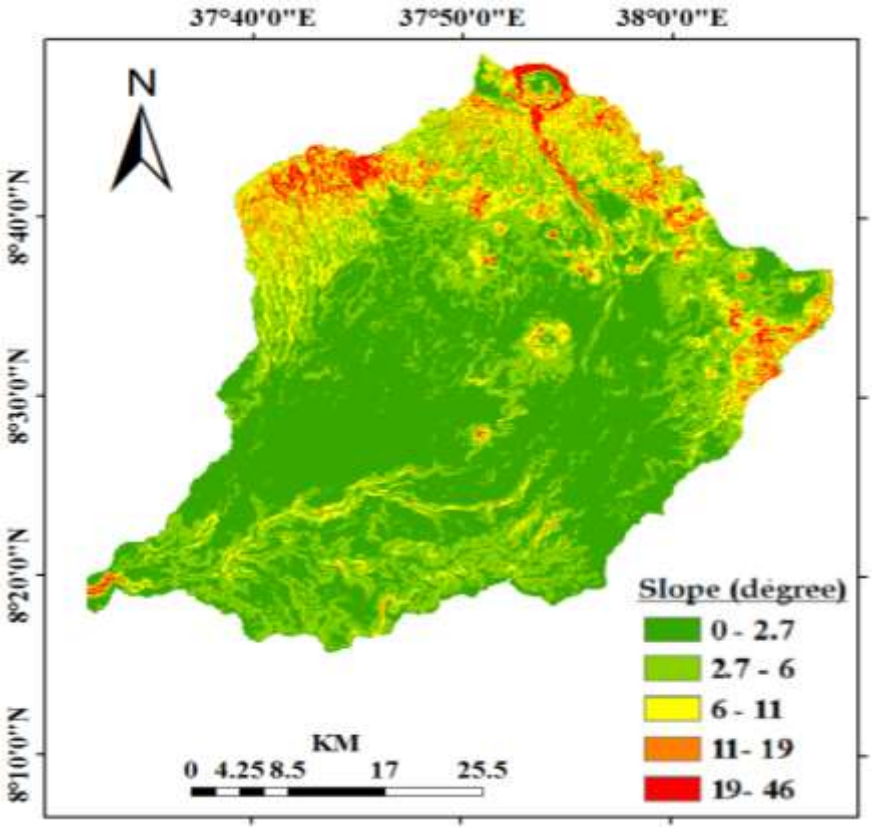

Figure 19. Slope and Elevation map of the study area

Table 4. Input data of WetSpass model and description

Input	Source	Resolution	Processing tool/method
Digital Elevation Model	Shuttle Radar Topography Mission (SRTM)	30 x 30	ArcGIS 10.4.1
LULC map	USGS OLI8 Satellite	30 x 30	ArcGIS 10.4.1
Soil map	MWEI	30 x 30	ArcGIS 10.4.1
Slope map	Calculate from DEM	30 x 30	ArcGIS 10.4.1
Groundwater depth	Direct measurement, SWSZWERO, ECDSWC	30 x 30	Ordinary Kriging Interpolation in ArcGIS10.4.1
Rainfall map	National Meteorological Agency	30 x 30	Ordinary Kriging Interpolation in ArcGIS10.4.1
PET	National Meteorological Agency	30 x 30	CROPWAT 8 and Ordinary Kriging Interpolation in ArcGIS10.4.1
Temperature	National Meteorological Agency	30 x 30	Ordinary Kriging Interpolation in ArcGIS10.4.1
Wind speed	National Meteorological Agency	30 x 30	Ordinary Kriging Interpolation in ArcGIS10.4.1

4.3. Aquifer characterization

The occurrence and distribution of groundwater is related to geomorphological and geological setting of the area. There is scarcity of hydrogeological data in the study area and scarce data obtained does not have systematic data base that can be easily used. In this study data is obtained from south west shoa zone water resource development and energy office, Woliso town water and sewerage authority and ECDSWC.

An aquifer test is a controlled field experiment used to estimate hydraulic properties of aquifer systems; such as transmissivity, hydraulic conductivity and specific capacity. Pumping test is among the fundamental aquifer testing methods of characterizing aquifer hydraulic properties (Okan et al., 2018) .

Single well test is more common than aquifer test with having observation well, since the advantage of single well test is that the pumping test can be conducted on the production well with the absence of observation well (Modelling et al., 2016). A kind of single well test, which is step-drawdown test used to determine the efficiency and specific capacity of the well, however in case of single well test it is possible to estimate Transmissivity, but Storativity is overestimated (Dinu et.al , 2017).

Among groundwater hydrologists, the most familiar curve matching procedure for estimating aquifer properties from pumping tests is due to Theis (1935). The Theis method allows one to estimate the transmissivity and storativity of a non-leaky confined aquifer having infinite extent by means of matching the Theis type curve to water-level changes (drawdowns) measured in wells during a constant-rate pumping test.

Hence the method consists of drawing a straight line through the late time data points and extending it backward to the point of zero drawdown (time axis intercept), which is designated t_o. The drawdown per log cycle is obtained from the slope m of the line. Values for transmissivity T and storativity S can then be found from

$$T=\frac{2.3Q}{4\Pi m} \quad \ldots\ldots 8$$

$$S=\frac{2.25Tt_0}{r^2} \quad \ldots\ldots 9$$

where Q is the constant pumping rate and r is the radial distance to the observation well; if drawdowns are measured at the pumping well, r is equal to the effective radius of the well (Tse & Amadi, 2010).

Discharge (l/s)

The topography of Walga catchment ranges from low land to very high elevated lands. Topographically high lands like, Wonchi, Beda Kero and Roge mountains are classified under area of recharge. Discharge areas are those area which are mostly at the foot of mountainous, manifested by the presence of springs at the contact of the elevated and the low land areas. Areas starting from Senkole down wards to Weliso & Walga, can be considered discharge zones by the presence of shallow ground water depth up to 6m & abundance of artesian type springs and bore holes. Presence of many springs at different elevations as a contact spring indicates that there is a shallow ground water circulation in addition to the regional flow of groundwater.

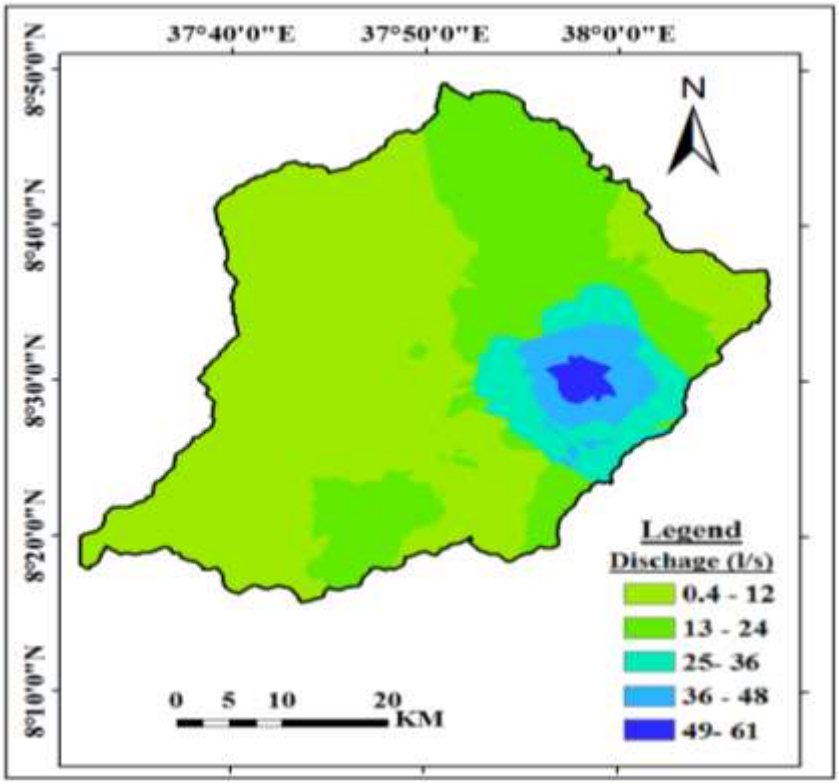

Figure 20. Spatial distribution of groundwater discharge using IDW of study area

Groundwater discharge data measured from bore hole during pumping test was obtained from government and non-governmental organization. The yield in the study area ranges from 0.4 l/s to 60.7 l/s. The average borehole yield in the area is 3.6 l/s. High discharge well producing 60.7l/s was obtained around Woliso in ignimbrite and basalt volcanic rocks while, poor discharge wells producing less than 1 l/s are also recorded in the area. Free flowing (artesian wells) are produced from fractured basalt at Meti walga 5km from woliso town and at Gurura town following Walga

catchment is a freely flowing without water tapping facilities. Cold and hot springs emanating at low topography are discharging up to 25 l/s.

Specific Capacity

The Specific Capacity of a well is the pumping rate (gpm) (Q) divided by the drawdown in feet (s). Specific Capacity can also be used to provide the design pumping rate or maximum yield for the well and to estimate the transmissivity of the surrounding formations penetrated by the well screens.

$$Sc = {}^{Q}/_{\Delta S} \quad \text{.....10}$$

Where Sc is specific capacity, Q well discharge and ΔS is change in draw dawn

The maximum pumping rate of a well can be estimated using the initial Specific Capacity. The maximum pumping rate is calculated as the Specific Capacity times the maximum available drawdown.

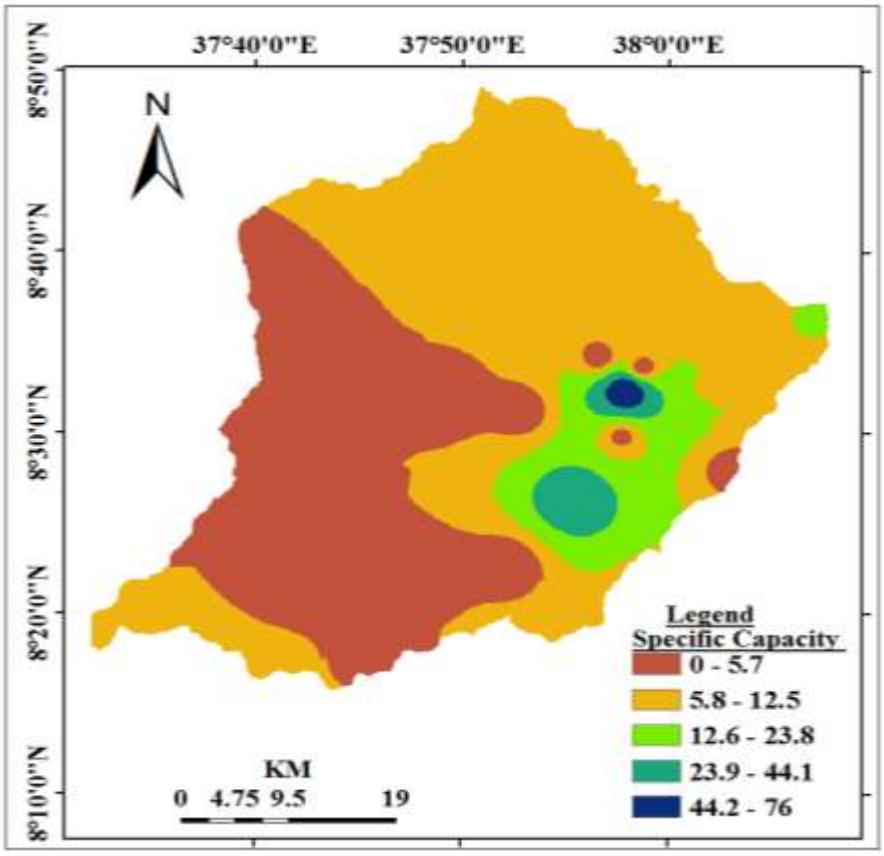

Figure 21. Spatial distribution of specific capacity using IDW

The initial Specific Capacity value can also be used to estimate the transmissivity (T) of the aquifer. Transmissivity is the rate water is transmitted through an aquifer under a unit width and a unit hydraulic gradient. It equals the aquifer's hydraulic conductivity (K) times the aquifer thickness (b). The higher the transmissivity, the greater the capability of the aquifer to move water and the lower the drawdown in the well.

Transmissivity (T)

A pumping test is the best available method to evaluate aquifer parameters. This test involves extracting water from a well at a controlled ate and observing the water level changes.The time gap between the onset of pumping and the beginning of an appreciable flow of water from the aquifer to the well depends mostly on the transmissivity of the aquifer(Khadri & Moharir, 2016).

Transmissivity (m^2/day) is the rate at which water of a prevailing density and viscosity is transmitted through a unit width of an aquifer or confining bed under a unit hydraulic gradient. It may also a measure of the amount of water that can be transmitted horizontally through a unit width by the full saturated thickness of the aquifer under a hydraulic gradient. It is a function of properties of the liquid, the porous media, and the thickness of the porous media.

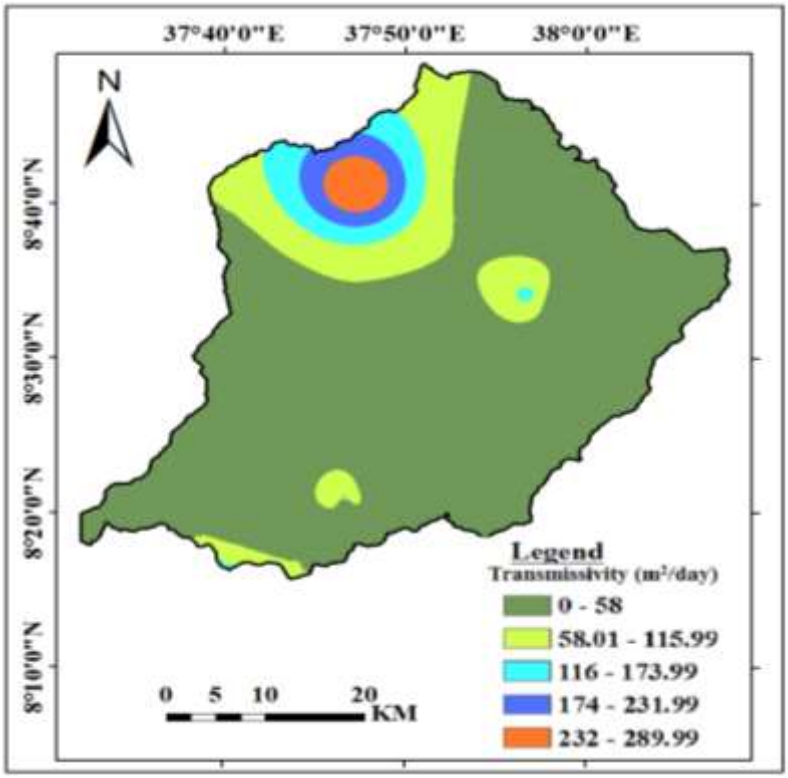

Figure 22. Spatial distribution of Transmissivity using in Walga

Single well aquifer testing can provide the value of Transmissivity, whereas preclude the cost and access of multi-well aquifer testing, so usually in this case the test data analyzed by Cooper-Jacob's (1946) straight line method due to its simplicity. Transmissivity was estimated by fitting a straight line between time versus drawdown on semi-logarithmic paper using the equation 8.

Hydraulic conductivity (K)

It is the quantitative measurement of permeability that is the ease in which water can pass through a unit thickness of an aquifer. Hydraulic conductivity K and Transmissivity T are related by the expression. Thus,

$$K = T/b \quad \ldots\ldots 11$$

where b = saturated thickness of the aquifer, which is equivalent to total screen length (Tse & Amadi, 2010).

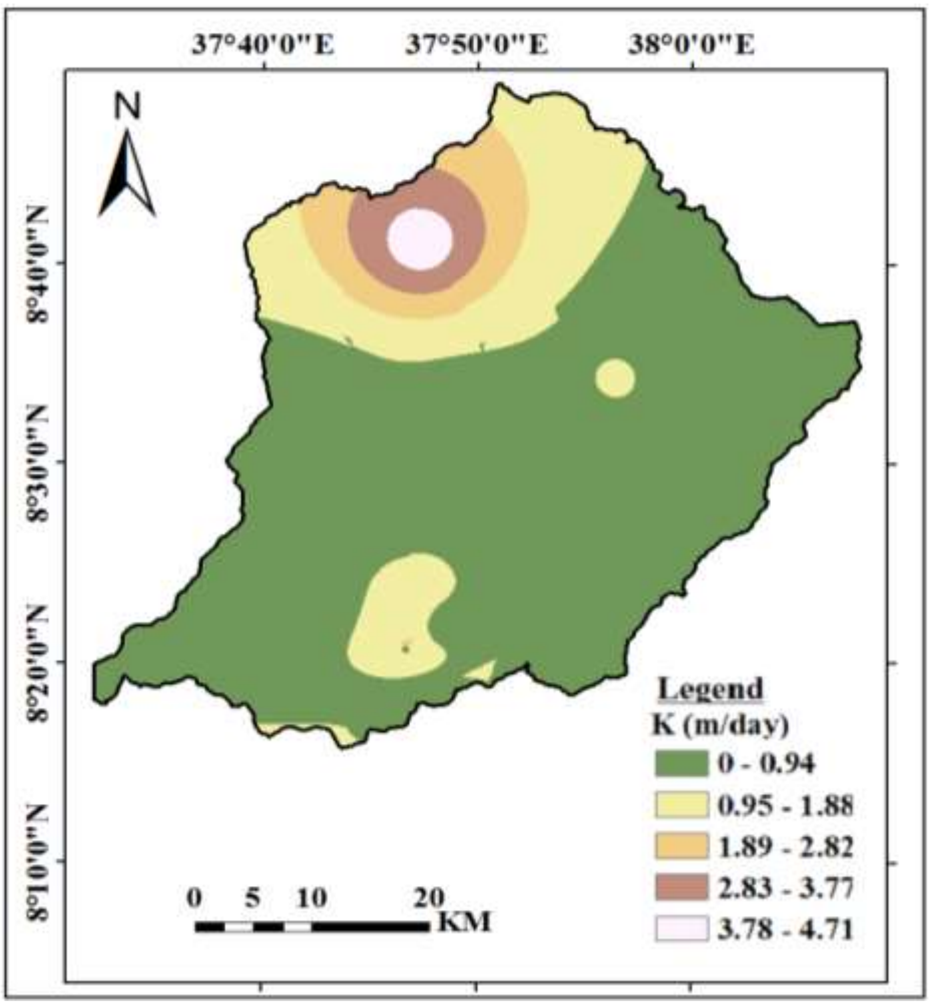

Figure 23. Spatial distribution of Hydraulic Conductivity of Study area

4.4. Groundwater potential evaluation

Groundwater potential evaluation is an essential for the proper utilization and management of this precious natural resource. Among techniques used to evaluate groundwater potential; GIS and remote sensing are efficient techniques in groundwater studies; in facilitate better data analysis and their interpretations of groundwater potential controlling parameters (Gintamo, 2015; Hussein et al., 2017; Oikonomidis et al., 2015; Solomon & Quiel, 2006; Yeh et al., 2016b).

All the thematic layers were then assigned weights according to their relative importance in groundwater occurrence and the corresponding normalized weights were obtained based on the Saaty's analytical hierarchy process (Saaty, 1984). Digital image processing of the satellite data were carried out for extraction of pertinent information about the potential groundwater. The groundwater potential assessment using multi-criteria evaluation involved thematic map generation and their integration through GIS.

Analytical Hierarchy Process (AHP) is one of the more popular methods of MCDA techniques and has many advantages. One of its advantages is its ease of use, its use of pairwise comparisons can allow decision makers to weight coefficients and compare alternatives with relative ease. It is scalable, and can easily adjust in size to accommodate decision making problems due to its hierarchical structure and although it requires enough data to properly perform pairwise comparisons (Velasquez & Hester, 2013).

Prior to integration of different information, individual class weights and map scores were assessed based on Satty's Analytic Hierarchy process where a pair – wise comparison matrix prepared for each map using a nine point important scale (Whitaker & Foundation, 2017, Wang et al., 2017). The main purpose of this study is to determine groundwater potential using Geographic Information System and Remote Sensing.

Table 5. Scale of Relative importance (Goepel, 2013)

Intensity of I	Definition	Explanation
1	Equal Importance	Two activities contribute equally to the objective
3	Weak importance of one over another	Experience and judgement slightly favor one activity over another
5	Essential or strong importance	Experience and judgement strongly favor one activity over another
7	Demonstrated importance	An activity is strongly favored and its dominance demonstrated in practice
9	Absolute Importance	The evidence favoring one activity over another is of the highest possible order of affirmation
2,4,6,8	Intermediate values between the two adjacent judgements	When compromise is needed
Reciprocals of above nonzero	J has reciprocal value with i	

4.4.1. Preparation of thematic maps using GIS and RS

The groundwater potential evaluation involved thematic map generation and their integration through GIS. Thematic maps were prepared in the proper scale with a spatial resolution of 30 meter pixel size from satellite imagery, topographical, and geological mapping and other hydrogeological field data.

All the thematic maps were converted into grid (raster format) and superimposed by weighted overly method (rank and weight wise thematic maps and integrated with one another through ArcGIS).The maps were developed in a GIS environment using eight input parameters for groundwater potential evaluation. Groundwater potential zonation means identifying and mapping the prospective ground water zones in an area by quantitative assessment of the controlling and indicative parameters.

The thematic layers considered in this study were lithology, drainage density, recharge, discharge, soil, slope, land use/ land cover and Groundwater depth. Thematic maps for each parameters were prepared as follows:

Precipitation

For hydrologic analyses it is important to know the areal distribution of precipitation. Several areal precipitation estimation techniques are currently used for averaging precipitation depths collected at ground stations.

The Inverse distance weight and Kriging spatial interpolation techniques are conventional techniques that are usually applied to estimate the areal precipitation . As stated under 4.2.1, data from eight meteorological station having 22 years record was used for this study.

The higher the amount of rainfall indicates as there is groundwater recharge and lower amount of rainfall indicates lower values of groundwater potential. But, the recharge from rainfall is influenced by slope, land use land cover, soil, lithology and drainage density.

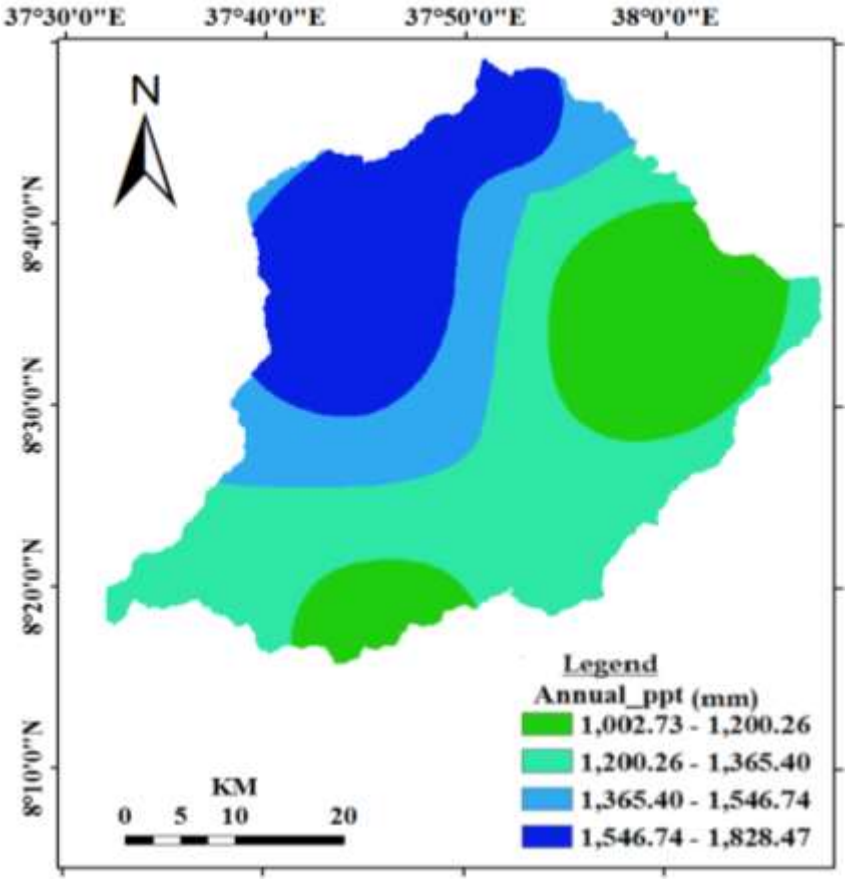

Figure 24. Reclassified annual precipitation of Walga catchment

Slope

Slope is one of the important terrain parameters, explained by horizontal spacing of the contours. The lower slope values indicate the flatter terrain (gentle slope), shown by sparse contours and higher slope values correspond to steeper slope of the terrain showing closely spaced contours (Waikar & Nilawar, 2014).

The slope gradient directly influences the infiltration of rainfall. Larger slopes produce a smaller recharge because water flows rapidly down a steep slope during rainfall, so it does not have sufficient time to infiltrate the surface and recharge the saturated zone (Yeh et al.,2016b). Steeper the slope, greater will be the runoff and thus lesser is the groundwater recharge. Digital Elevation model (DEM) is derived using contour information from the topographical map for estimation of slope in degree (Bose et al., 2010,).

In this study, slope map (figure 19) was reclassified into four classes like 0-6° (gentle), 6-15° (moderate), 15-27° (high), and 27-46° (more (steep).

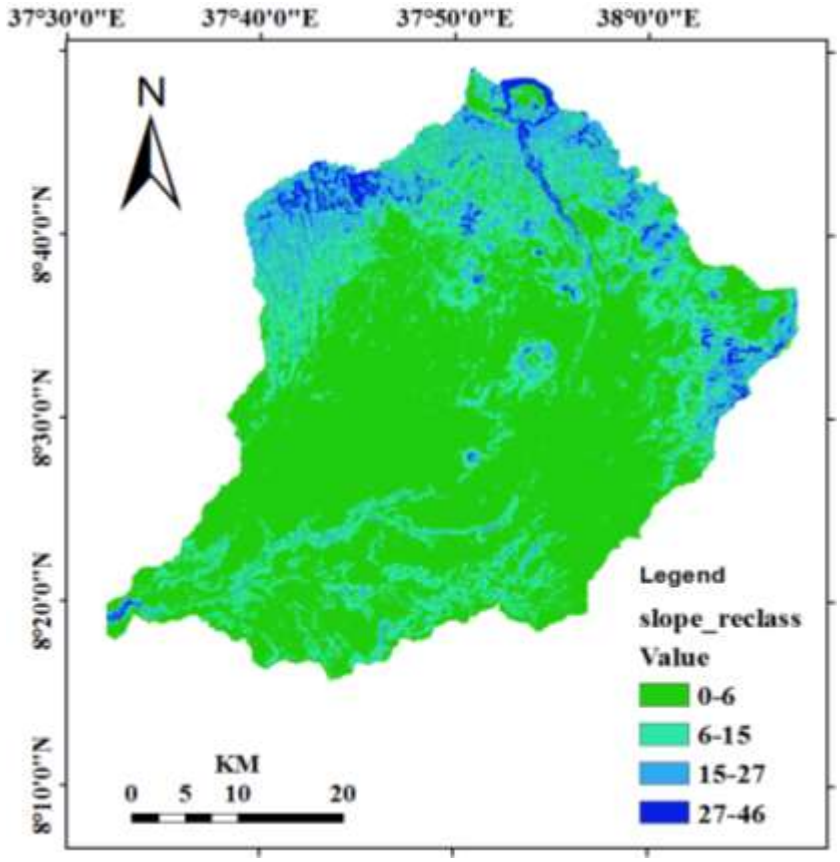

Figure 25. Reclassified slope

Drainage density map

Drainage density indicates rock permeability and infiltration capacity, and therefore recharges capacity. They are reflection of the rate that precipitation infiltrated compared to surface runoff. Where rocks are highly permeable, infiltration to groundwater is high, and less water is transported in rivers as surface water; but where rocks have low permeability there is little infiltration and more surface water runoff. Low drainage density is therefore related to higher recharge and higher groundwater potential (Rahmati et al., 2016, Nagarajan & Singh, 2009, Hussein et al., 2017).

Drainage density delineated using Digital Elevation Model hydro-processing module of SRTM data of the study area after consecutive processes such as importing of SRTM data, filled sinks for undefined values, created flow direction, created flow accumulation, created stream network, generated stream order and finally converted stream order to drainage density. The stream order values were regrouped to produce a drainage density map that was reclassified into four categories i.e., 0-0.33(high), 0.33-0.665 (medium) , 0.665-0.99 (low), and 0.99-1.33 (very low) density.

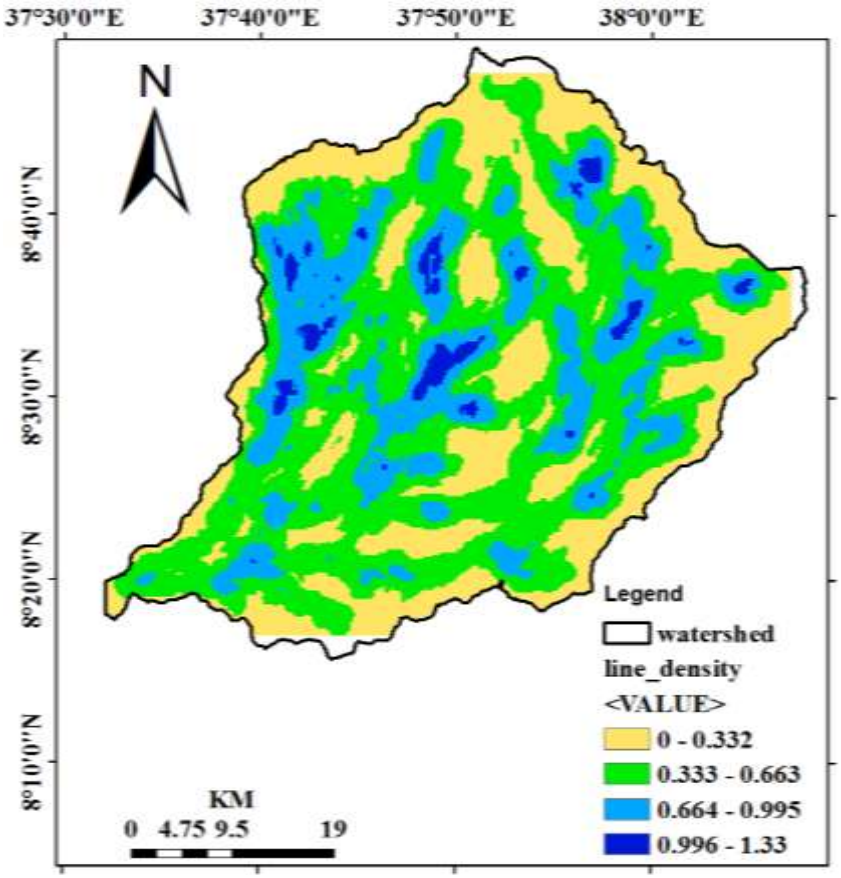

Figure 26. Reclassified Drainage Density map

Land use Land Cover

Land use plays a significant role in the development of groundwater resources. It controls many hydrogeological processes in the water cycle viz.,infiltration, evapotranspiration, surface runoff etc. Surface cover provides roughness to the surface, reduce discharge thereby increases the infiltration. In the forest areas, infiltration will be more and runoff will be less whereas in urban areas rate of infiltration may decrease. Land use map prepared for WetSpass can be used for groundwater potential evaluation (figure 16).

Soil map

Soil properties influence the relationship between runoff and infiltration rates which in turn control the degree of permeability, the principal factor in hydrogeology that determines the groundwater potential (Manikandan et al. 2014). Clay soil enhances surface runoff due to its low permeability while Sandy clay loam reduces surface runoff due to its high permeability. In general soil type influences the amount of groundwater recharge which has an influence on groundwater potential mapping. Soil map prepared for WetSpass data input was used after reclassification (figure 17).

Lithology/Geology

Lithology plays an important role in the occurrence and distribution of groundwater (Yeh, et al. 2016b). Higher porosity contributes to higher groundwater storage and higher permeability contributes to higher groundwater yields.

Manikandan et al., (2014) identified as the storage capacity of the rock formations depends on the porosity of the rock. In the rock formation the water moves from areas of recharge to areas of discharge under the influence of hydraulic gradients depending on the hydraulic conductivity or permeability. The same map (figure 6) was used.

Groundwater recharge

One of the outputs of WetSpass simulation was groundwater recharge (figure 42) was used in evaluating groundwater potential zoning of Walga catchment. Areas of good groundwater recharge was given higher value while the reverse is true.

Groundwater Depth

Shallow groundwater table was given higher rank while deep groundwater was given lower rank (figure 39).

4.4.2. Groundwater Potential Zone

After spatially analyzed weighted overlay analysis Walga catchment was classified into four groundwater potential zone. Very good groundwater potential of the area covers 46.6km^2 while 0.87km2 of bare impermeable rock area is very poor groundwater potential. High amount of rainfall, gentle slope, fractured rocks, low drainage density, good ground coverage and sand clay loam area is classified und eve good groundwater potential.

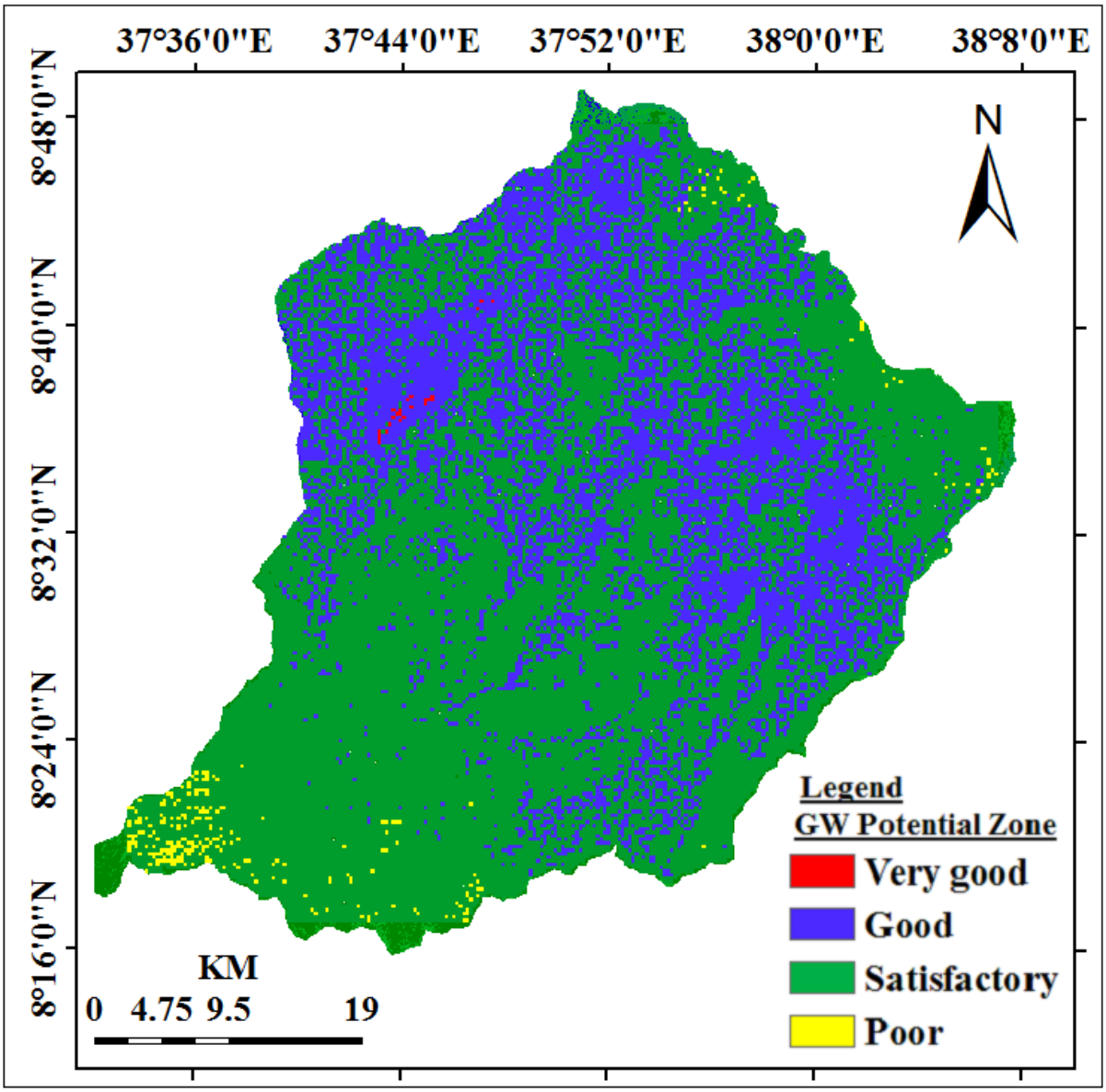

Figure 27. Groundwater potential zone

4.5.Groundwater quality/ Hydro-geochemistry

Water quality is a term used to describe the chemical, physical, and biological characteristics of water, usually in respect to its suitability for a particular purpose.

Groundwater of Walga catchment is mainly used for drinking and irrigation purposes. Therefore, quality criteria depend on the use of water for a particular purpose, and quality standards have to be maintained in water supply for different uses to avoid deleterious effects. In other words, whether a groundwater of a given quality is suitable for a particular purpose depends on the criteria or standards of acceptable quality for that use (Patil et al., 2012).

Ayenew, (2006), has been carried out a broad survey to study the spatial variation of the major ions composition of the surface and groundwater systems in the Ethiopian volcanic terrain and associated Plio-Quaternary sediments. The result revealed wide hydrochemical variations controlled by geological, geochemical, geomorphological and climatological factors

Hydro-geochemistry is the study of the chemical composition of natural waters (Canora et al., 2019; Rajesh et al., 2019). The chemical composition of natural waters results from both geogenic (natural) and anthropogenic sources. Once precipitation reaches the ground, it reacts with soil, rock, and organic debris, dissolving still more chemicals naturally aside from any pollution generated by human activities (Rahmanian et al., 2015). Among the factors determining the level of trace and major elements are the content of solute in the initial rain, the extent of reaction with rock and soil, loss of constituents by precipitation or absorption, and loss of water because of evaporation, transpiration or reaction with minerals.

According to Rahmanian et al., (2015), one of the most important natural changes in groundwater chemistry occurs in the soil. Soils contain high concentrations of carbon dioxide which dissolves in the groundwater, creating a weak acid capable of dissolving many silicate minerals. In its passage from recharge to discharge area (Nur et al., 2012), groundwater may dissolve substances it encounters or it may deposit some of its constituents along the way. The eventual quality of the groundwater depends on temperature and pressure conditions, on the kinds of rock and soil formations through which the groundwater flows, and possibly on the residence time.

The present study focused on the hydrochemistry of groundwater in Walga watershed to assess the quality of groundwater for determining its suitability for drinking and agricultural purposes using analysis of Laboratory result.

4.5.1. Laboratory result data Collection and Analysis

Chemical groundwater result data were collected from Woliso town water supply and sewerage authority, Southwest Shoa Zone water resource development and energy office and Ethiopian Construction Design and Supervision Works Corporation (ECDSWC). A total of 148 schemes (72 BH, 13 HDW, 17SHW and 46 spring) laboratory results data were collected and analyzed using piper diagram and chart. Data collected contains physical parameters such as pH, electrical conductivity (EC), total dissolved solids (TDS), salinity, temperature (T), and ions including Ca^{2+}, Na^{+}, K^{+}, Mg^{2+},Cl^{-}, $SO_4 2^{-}$, NO_3^{-} and HCO_3^{-}.

Table 6. Descriptive statics of water quality parameters with WHO standards (Kurniawan et al., 2019)

Parameter	Max	Min	Mean	STDE	WHO limits
Temp. ^{o}C	40. 5	7.08	23.63	12.53	
Ph	9.66	6.37	7.56	0.78	6.5-8. 5
Electrical Conductivity(µS/cm)	1172.1.00	185.9	535.03	317.54	-
T. Dissolved Solid 1050c	750.6	138.47	292.7	115.12	1000
Ammonia(mg/l NH3)	1.51	0.00	0.28	0.29	25
Sodium (mg/l Na)	300.00	4.50	80.27	69.06	200
Potassium (mg/l k)	23.50	0.09	7.23	4.93	200
Total Hardness(mg/l CaCo3)	421	40	114.49	58. 57	300
Calcium (mg/l Ca)	155.80	2.28	33.13	34.96	200
Magnesium (mg/l Mg)	66.70	0.55	9.62	11.71	150
Total Iron (mg/l Fe)	4.29	0.00	0.18	0.59	0.3
Manganese (mg/l Mn)	2.20	0.00	0.14	0.31	1
Fluoride (mg/l F)	16.40	0.00	1.40	2.90	1. 5
Chloride (mg/l Cl)	127.50	0.00	15.98	21.49	600
Nitrite (mg/l No2)	1.00	0.00	0.12	0.26	1
Nitrate (mg/l No3)	84.70	0.00	10.54	17.91	10
Alkalinity(mg/l CaCo3)	948.00	5.63	238.38	160.92	200
Carbonate (mg/l CO3)	90.00	0.00	22.79	16.48	-
Bicarbonate (mg/l HCO3)	1156.60	31.72	279.26	198.58	-
Sulphate (mg/l SO4)	169.80	0.10	14.76	32.18	250
Phosphate (mg/l PO4)	23.00	0.08	1.08	4.00	50

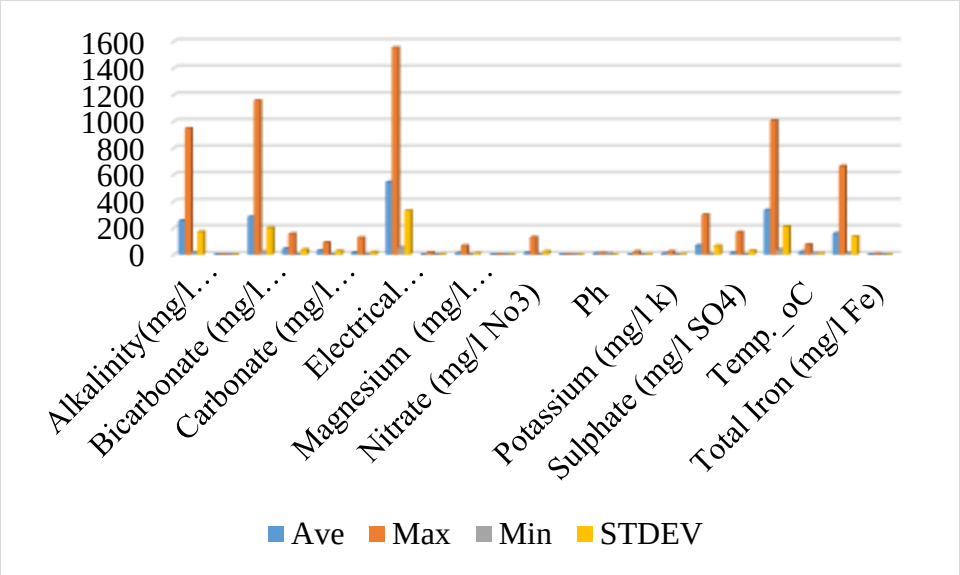

Figure 28. Bio-statistical representations of phsio-chemical parameters

4.5.2. Phsico-chemical Analysis

According to Patil et al., (2012), physico chemical parameter study is very important to get exact idea about the quality of water and we can compare results of different physico chemical parameter values with standard values. In specifying the quality characteristics of groundwater, physical (temperature, turbidity, color and tastes and odor) and chemical (total solids, total dissolved solids, total suspended solids, specific conductance, PH, dissolved oxygen, hardness and alkalinity) analysis were done from previously collected laboratory results as follows.

4.5.2.1.Classification and presentation of analytical results

Piper diagram outline certain fundamental principles in a graphic procedure which appears to be an effective tool in separating analytical data for critical study with respect to sources of the dissolved constituents in water(Tank & Chandel, 2010; Rajesh et al., 2019). Piper diagram consists of three parts: two trilinear diagrams along the bottom and one diamond-shaped diagram in the middle. The trilinear diagram illustrates the relative concentration of cations (left diagram) and anions (right diagram) in each sample. The concentration of 8 major ions (Na^+, K^+, Mg^{2+}, Ca^{2+}, Cl^-, CO_3^{2-}, HCO^-_3 and SO_4^{2-}) are represented on a trilinear diagram by grouping the K^+ with Na^+ and the CO_3^{2-} with HCO^-_3, thus reducing the number of parameters for plotting to 6 (Amadi et al., 2014). On the Piper diagram, the relative concentration of the cations and anions are plotted in the lower triangles, and the resulting two points are extended into the central field to represent the total

ion concentrations. The degree of mixing between freshwater and saltwater can also be shown on the Piper diagram.

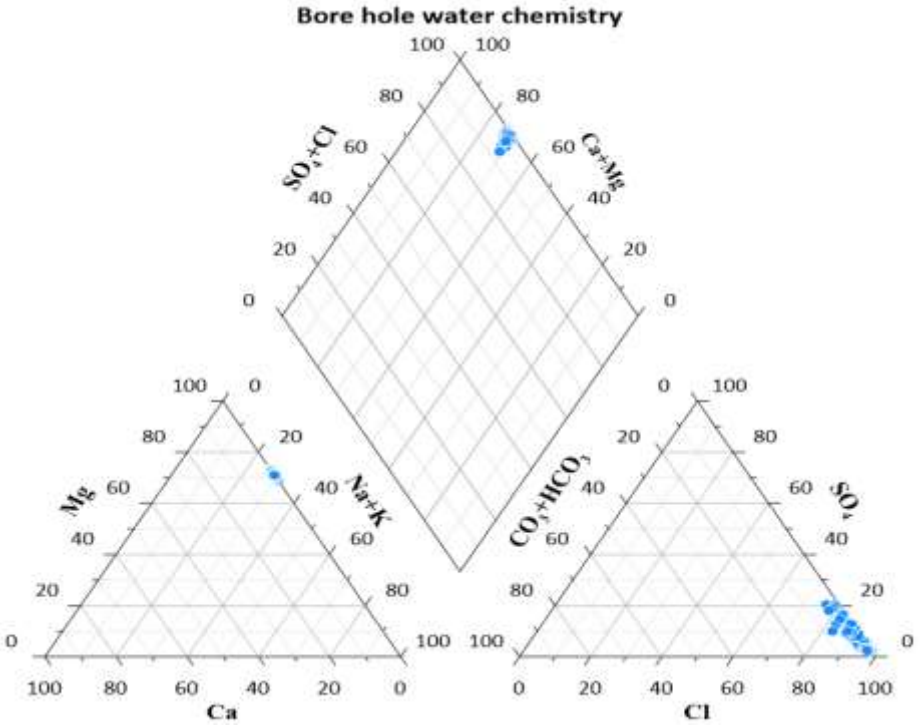

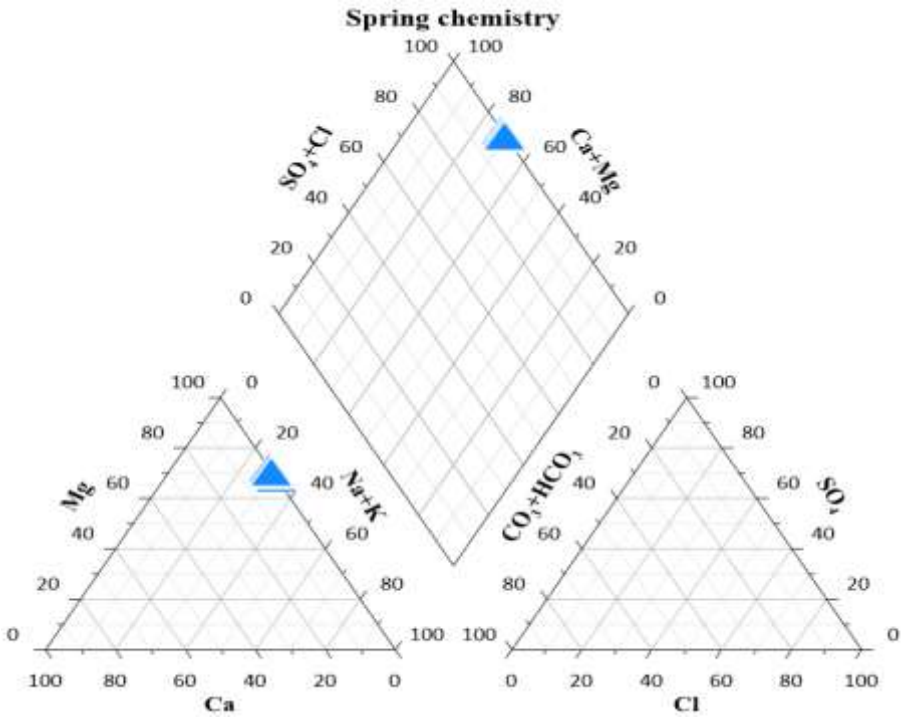

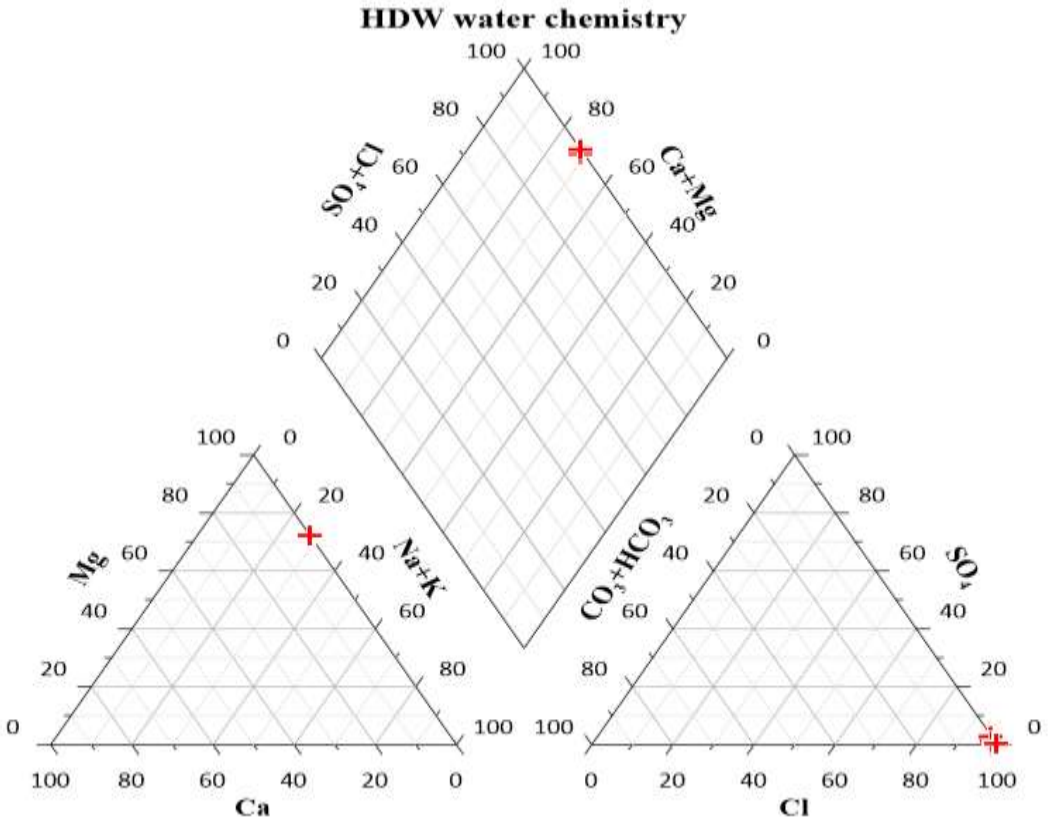

Figure 29. Piper diagram of different water sources

The Piper diagram can also be used to classify the hydro-chemical facies of the groundwater samples according to their dominant ions. The water in the area is majorly Na-Cl-facies, followed by Ca-Mg-HCO3-facies, Na-Ca-SO4-facies, Ca-Mg-Cl-facies, Na-K-Cl-facies and facies in their order of dominance respectively.

4.5.3. Drinking water Quality Variations

Fluoride

Fluoride is a naturally occurring element in water that is dissolved from some types of rocks or associated with geothermal waters. Rock-water interaction is the prime factor responsible for fluoride enrichment in water (Dinu et al., 2017; Tekle-Haimanot et al., 2006).

The concentration of fluoride in ground drinking water greater than the world health organization standard value imposes a serious health, social and economic problem in developing countries. In the Ethiopian Rift Valley where deep wells are the major source of drinking water, high fluoride level is expected (Halford et al., 2006; Demelash et al., 2019).

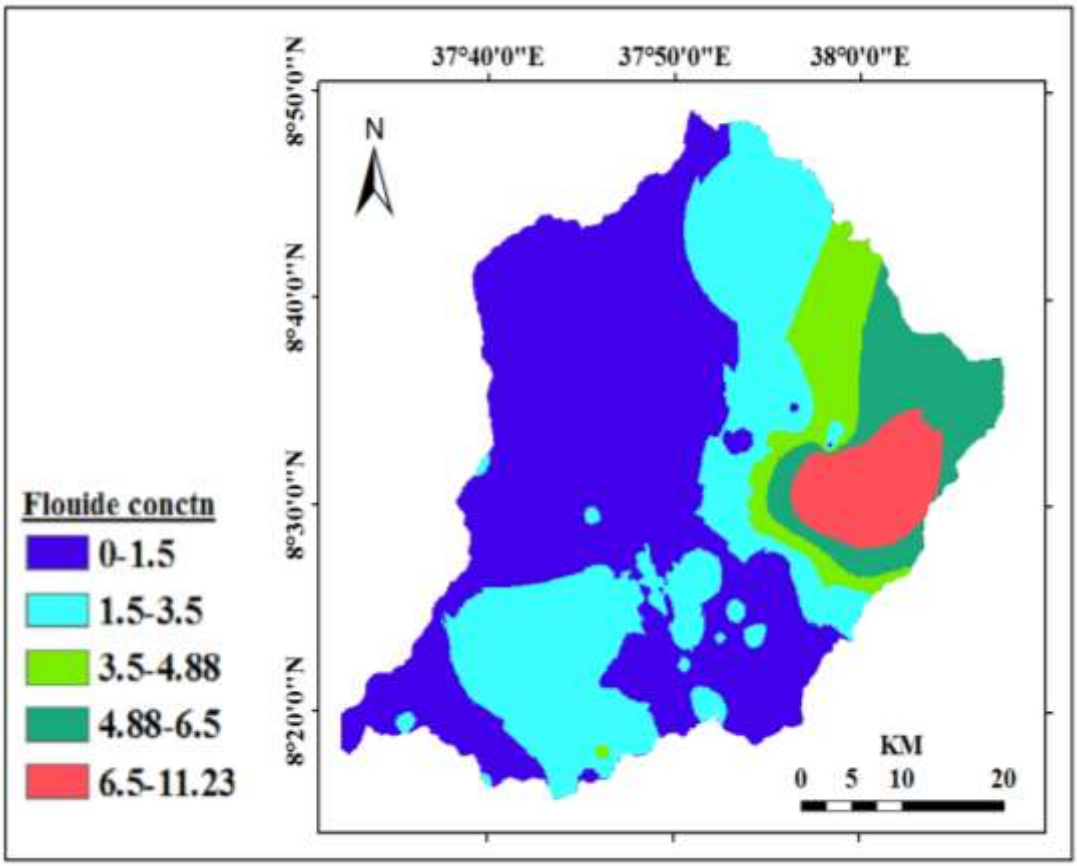

Figure 30. Spatial distribution of Fluoride concentration

Table 7. Areal coverage of Fluoride

No	Level of Fluoride	Area km^2	Percent(%)
1	0-1.5	1099.512	49.34
2	1.5-3.5	671.1984	30.12
3	3.5-4.88	149.976	6.73
4	4.88-6.5	182.088	8.17
5	6.5-11.23	125.4528	5.63

Fluoride is beneficial when present in small concentrations (0.8 to 1.0 mg/l) in drinking water for calcification of dental enamel but it causes dental and skeletal fluorosis if present in higher amounts. Higher concentrations of fluoride in drinking water are also linked with cancer. The permissible limit of Fluoride depends on temperature; a higher intake of fluoride can be permissible in colder climates (Fejerskov et al., 1994).

Hardness

Hardness of water is its content of metallic ions which reacts with sodium soaps to produce solid soaps or scummy residue and which react with negative ions, when the water is evaporated in boilers, to produce solid boiler scale (Camp, 1963). It is predominantly caused by divalent cations such as calcium, magnesium, alkaline earth metal such as iron, manganese, strontium, etc. It is a water quality indication of the concentration of alkaline salts in water, mainly calcium and magnesium.

Hardness is normally expressed as the total concentration of Ca^{2+} and Mg^{2+} as milligrams per liter equivalent $CaCO_3$. The total hardness is the sum of calcium and magnesium concentrations, both expressed as $CaCO_3$ in mg/l.

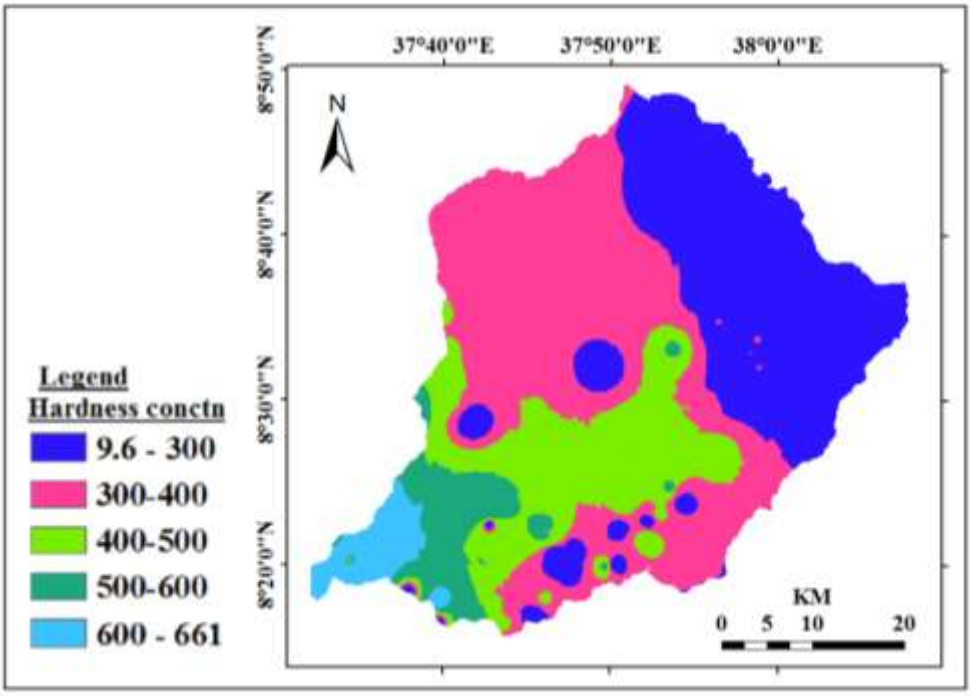

Figure 31. Spatial distribution of Total hardness of Walga catchment

Table 8. Areal coverage of Hardness

No	Hardness	Area	Percent (%)
1	9.6 - 300	725.9184	32.58
2	300-400	858.9888	38.55
3	400-500	419.3568	18.82
4	500-600	143.7552	6.45
5	600 - 6615	80.208	3.60

4.5.4. Irrigation water quality

The primary water quality in most irrigation situations is salinity levels, since salts can affect both the soil structure and crop yield. Irrigation water containing large amounts of sodium is of special concern due to sodium's effects on the soil and poses a sodium hazard (Tank & Chandel, 2010). Sodium hazard is usually expressed in terms of SAR or the sodium adsorption ratio. SAR is calculated from the ratio of sodium to calcium and magnesium (Fipps, 1995).

$$SAR = \frac{(Na^+)}{\sqrt{\frac{(Ca^{2+})+(Mg^{2+})}{2}}}, \quad \text{.....12}$$

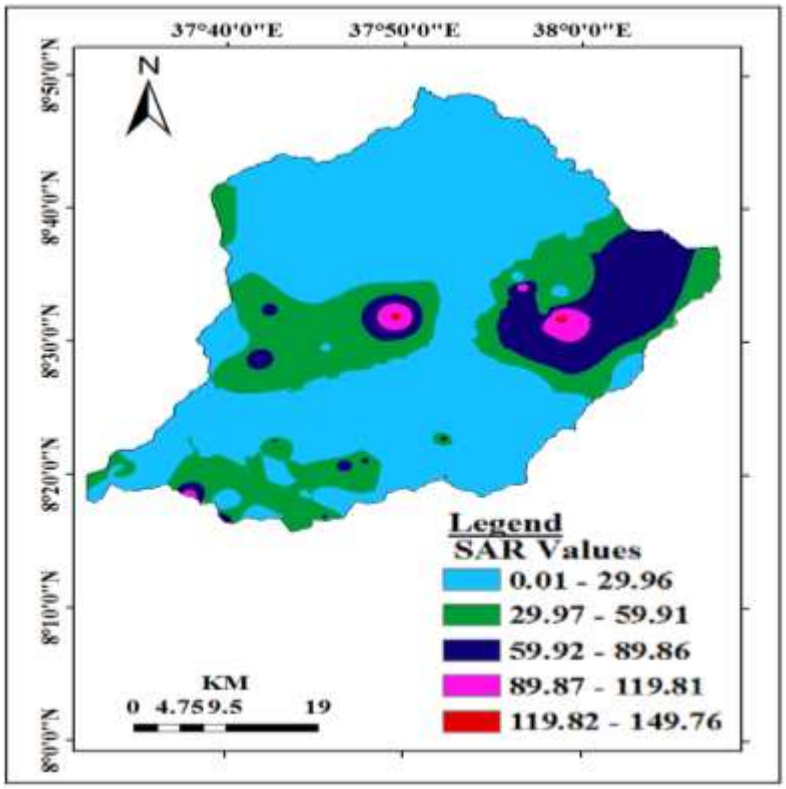

Figure 32. Spatial distribution of SAR values of the stud area

Salinity of water is usually measured by the TDS (total dissolved solids) or the EC (electric conductivity). TDS is sometimes referred to as the total salinity and is measured or expressed in parts per million (ppm) or in the equivalent units of milligrams per liter (mg/L) (Kumar, 2014). EC is a good measure of salinity hazard to crops. Excess salinity reduces the osmotic activity of plants and thus interferes with the absorption of water and nutrients from the soil (Tank & Chandel, 2010).

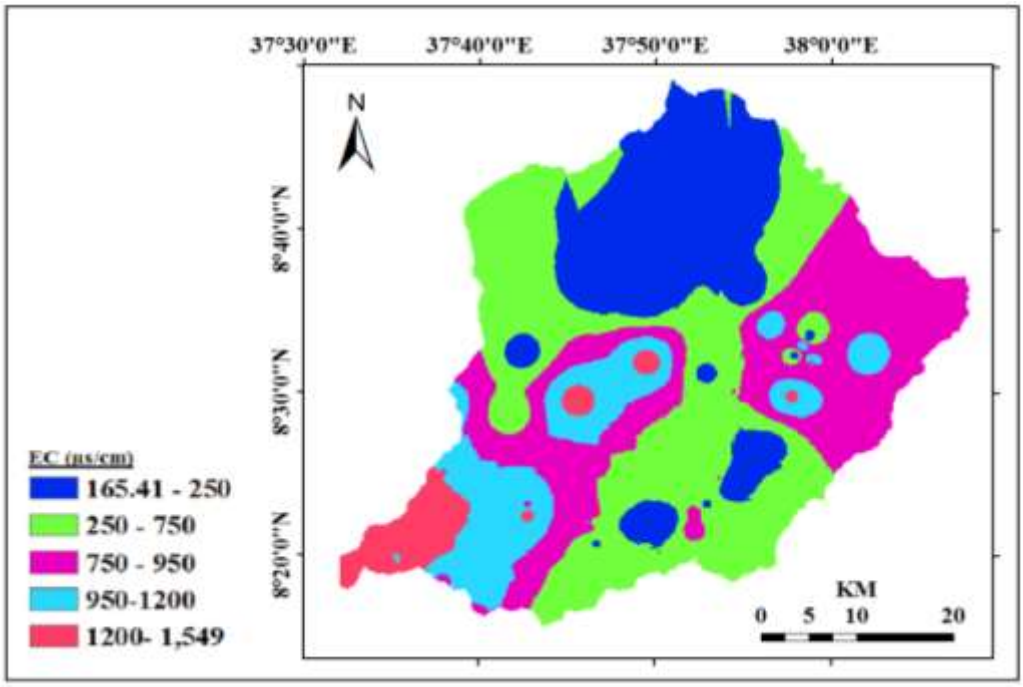

Figure 33.Spatial distribution of EC

The sodium in irrigation water is usually expressed in % Na. As per Indian standards maximum of 60% sodium is permissible for irrigation water. Tank and Chandel, (2010) formulated the following equation to determine % Na.

$$Na\% = (Na^+ + K^+)100/(Ca^{2+} + Mg^{2+} + Na^+ + K^+) \quad \ldots\ldots 13$$

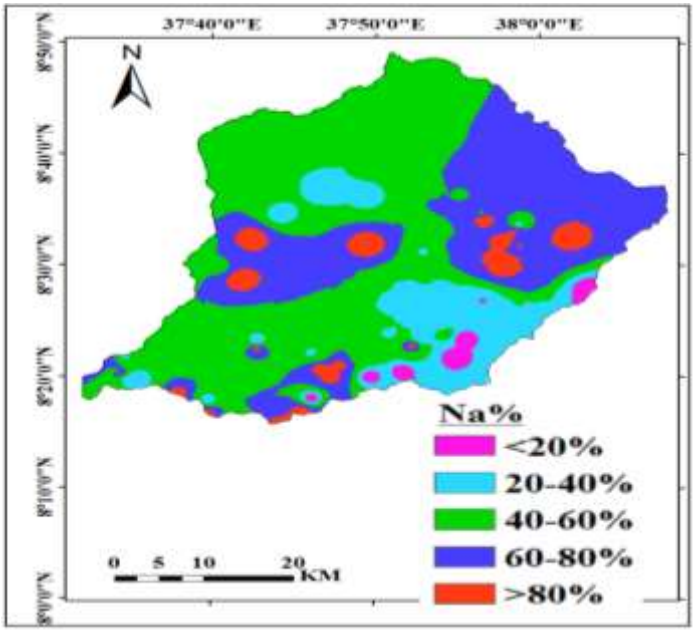

Figure 34. Spatial distribution of sodium %

Table 9. Areal distribution of EC

No	EC (µs/cm)	Area	Percent (%)
1	165.41 - 250	517.133	23.2
2	250 - 750	770.026	34.6
3	750 - 950	569.275	25.5
4	950-1200	268.978	12.1
5	1200- 1,549	102.816	4.6

Table 10. Irrigation water quality evaluation based on EC and SAR

(adapted from Tank and Chandel, 2010)

Water class	Excellent	Good	Permissible	Doubtful	Unsuitable
EC (µs/cm)	0-250	251-750	751-2250	2251-3000	3000
Na%	<20%	20-40%	40-60%	60-80%	>80%
Sodium hazard of water	Low	Medium	High	Very high	
SAR Values	1-10	10-18	18-26	>26	

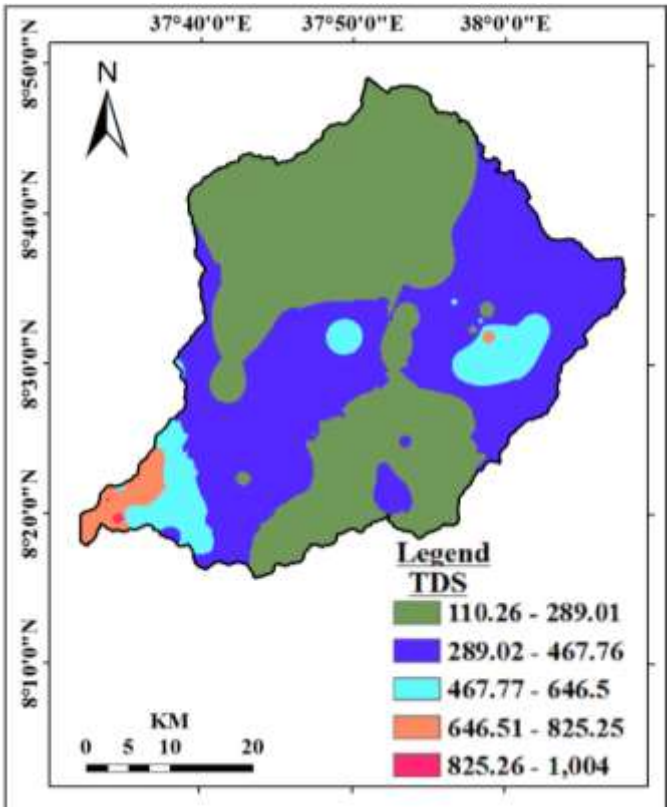

Figure 36. Spatial distribution of TDS

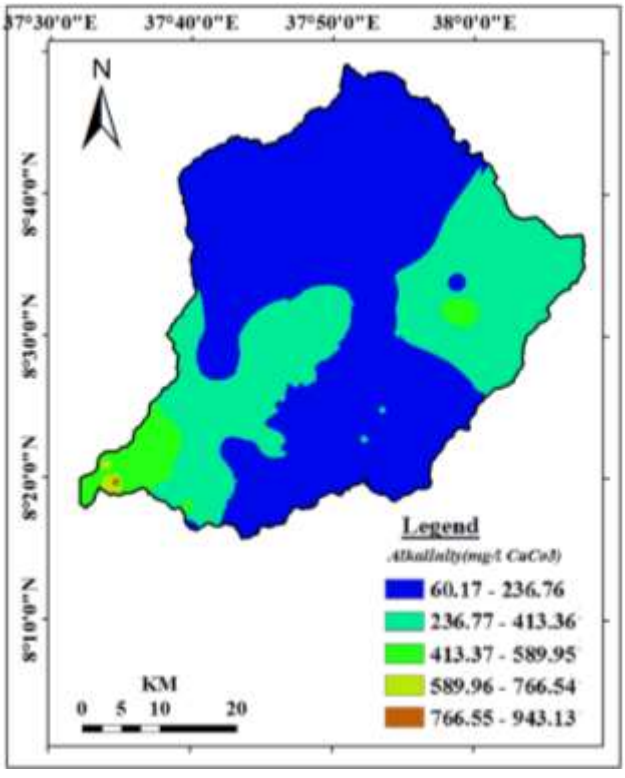

Figure 35. Spatial distribution of Alkalinity in mg/l of $CaCO_3$

CHAPTER FIVE

5. RESULTS AND DISCUSION

5.1. Hydro-meteorological data analysis

To estimate hydrological balance of a given basin, each of the hydro-meteorological elements has to be quantified. Those basic meteorological data are; rainfall, wind speed, temperature, humidity and sunshine hours. Accordingly groundwater recharge, actual evapotranspiration and surface runoff have been calculated.

5.1.1. Rainfall

Rainfall distribution analysis and its temporary variability which was done based on rainfall data obtained in and near the study area was characterized by unimodal (single peak) rainfall pattern. It is the major factor controlling the hydrologic cycle of a region. Since much of the ecology, geography, and land use of Walga catchment depend upon the function of the hydrological cycle, and therefore precipitation provides both constraints and opportunities in land and water management of the catchment. The relevant precipitation in the catchment is in the form of rainfall. Rainfall is one of the most important climatic variables, which shows the nature and climatic conditions of Walga Catchment. The catchment has four seasons, named as summer (which is June to August), autumn; (September to November), winter; (December to February) and spring; (March to May). The main rainy months are June, July, August and September which is considered as Summer season and the rest months are considered as dry months in the modeling.

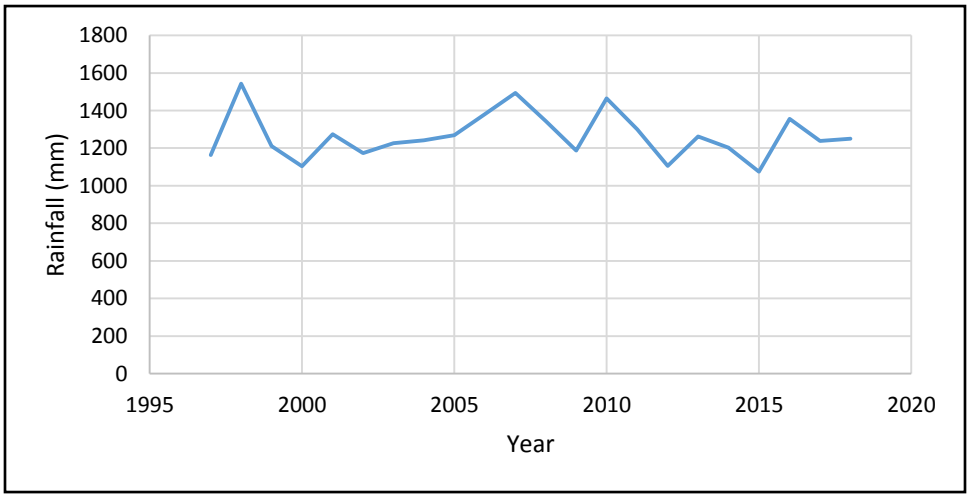

Figure 37. Annual average rainfall

Figure 37 shows that, the rain fall pattern over the years showed variation, the area received highest and lowest rainfall in the year of 1998 and 2015 respectively. The rainfall of the area also showed a decreasing trend from the year of 2010.

The distributed rainfall map is generated using interpolation tool by kriging in ArcGIS spatial analyst module using the point rainfall data from the meteorological stations. Accordingly, the area receives an average annual rain fall of 1357.43 mm per year. The summer average rainfall is 794.08mm while winter average rainfall is 541.19mm (figure 11).

5.1.2. Temperature

The average temperature values of each season are converted to spatially distributed grid maps using ordinary kriging. The monthly temperature results were subdivided into two seasons; four months of summer and eight months of winter. The grid maps of temperature for both seasons were converted to ASCII file format and used with other input parameter in WetSpass model.

Mean, minimum & maximum temperature data were collected from National Meteorological Service of Ethiopia which has been measured at Woliso, Wolkite, Ameyya and Ambo meteorological stations for 22 years (1987-2018). Based on the data it could be observed that Walga catchment is experiencing high temperature in the months February, March & April and low temperature in October. The following graph shows the monthly average, maximum and minimum temperature recorded at Woliso weather station over the years.

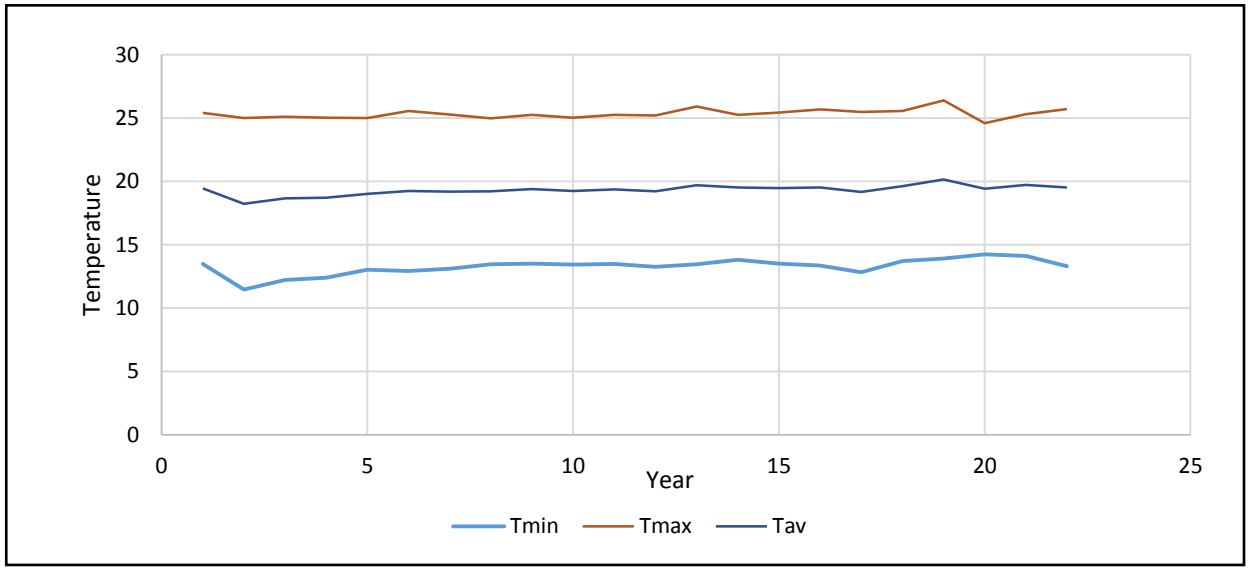

Figure 38. Monthly min, max and Average Temperature

The summer season average temperature is 18.18 ^{0}c while the winter is 19.98^{0}c. The annual minimum and maximum average temperature is 17.4^{0}c and 19^{0}c respectively (figure 13).

5.1.3. Wind Speed

Wind speed data are available for few meteorological stations. These data were used uniformly over the watershed. Similar to the other seasonal parameters, wind speed results are also subdivided into two seasons i.e. 4 months of summer (June to September) and 8 months of winter (October to May). Then, the average wind speed values of each season, were interpolated and converted to grid maps using ordinary kriging interpolation method. These grid maps of wind speed for both seasons were converted to ASCII file format and used as input parameters in WetSpass model. The average wind speed of summer and winter is 1.12m/s and 5.37m/s respectively (figure 14).

5.1.4. Potential evapotranspiration

According to Dereje & Nedaw (2019), evapotranspiration is an important parameter in water budget which abstracts water from the system and controls the soil moisture content, groundwater recharge and stream flow components of a certain basin.

Penman-Montieth based FAO CROPWAT software was used to estimate potential evapotranspiration of Walga watershed using two meteorological stations having recorded minimum and maximum temperature, wind speed, sunshine hours and relative humidity. As other meteorological data, PET calculated monthly results are subdivided into two main seasons i.e. 4 months of summer (rainy season) and 8 months of winter (Dray season). Finally, those PET values of each season, were converted to spatially distributed grid maps by means of kriging interpolation.

As listed under (figure 15), summer average potential evapotranspiration is 354.3 mm, where the winter is 982 mm, and the average annual potential evapotranspiration is 1336.5 mm with 1311 mm and 1387 mm as the minimum and maximum annual PET respectively.

5.1.5. Groundwater depth

A total of 175 water schemes static water level was collected for groundwater depth mapping. Ground water level elevation was calculated by subtracting water depth (SWL) from elevation

above sea level. The minimum and maximum groundwater level is 1484m and 2592m while 1865m is the average depth of groundwater level.

Static water level (depth to groundwater table) of Walga catchment ranges from free flowing (artesian) to 98m, with average depth is 16m to groundwater (figure 39). The distributed groundwater depth map is generated using interpolation tool by kriging in ArcGIS spatial analyst module using collected groundwater data as shown on (figure 18).

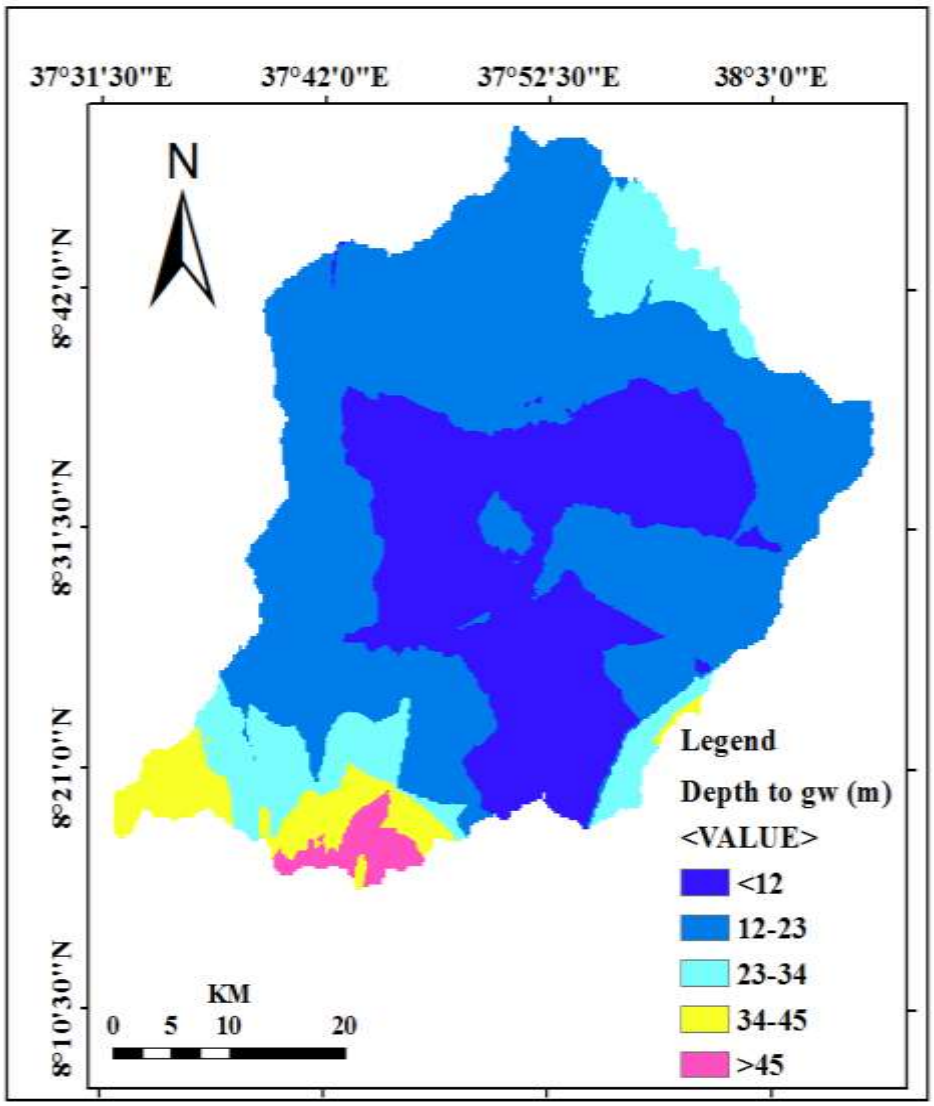

Figure 39. Depth to groundwater table

5.2. Output of the WetSpass model

The main outputs of the WetSpass model are raster maps of seasonal groundwater recharge, surface runoff and actual evaporation for the period of 1997 to 2018. In this maps every pixel represents the magnitude of the water budget components.

5.2.1. Actual evapotranspiration

It is difficult to directly measure actual evapotranspiration, hence it is estimated from potential evapotranspiration. A WetSpass model calculates a total actual evapotranspiration per pixel as a sum of evaporation from open water, impervious surface area, bare soil, interception of vegetated area and the transpiration of the vegetated cover (Salem et al., 2019).

Evapotranspiration is the process which returns water to the atmosphere and therefore completes the hydrologic cycle and, it includes evaporation from open water, vegetation and ground surface. Also transpiration, which is the removal of water from the soil by plant roots, transport of the water through the plant into the leaf as well as evaporation of the water from the leaf's interior into the atmosphere. Actual evapotranspiration is one components of water balance to determine groundwater recharge of Walga watershed using WetSpass model.

The model simulated the annual evapotranspiration of the watershed to be 282.39 mm and 1336.4 mm as minimum and maximum values respectively while 736 is the mean AET which accounts for about 54.22% of the total annual rainfall lost by evapotranspiration. About 58.2% of the total annual evapotranspiration is lost during winter season while the rest 41.8% is released in the summer season. This variation occurs due to low cloud cover, minimum relative humidity and longer time range in winter than summer season. As a result the winter evapotranspiration is higher than the summer.

The output annual evapotranspiration grid map (figure 40) shows that high annual evapotranspiration is observed in northern, middle parts and north eastern parts of the catchment, because these areas covered by cultivated crop, woodland, and also the presence of high annual rainfall. Lower annual actual evapotranspiration is observed at southern and southeastern part of the catchment due low coverage of forest, woodland and low annual rainfall. Generally, the value of annual evapotranspiration of Walga river catchment varies with land-use/land-cover. Hence, land-use/land-cover are the main controlling factors of evapotranspiration in the catchment.

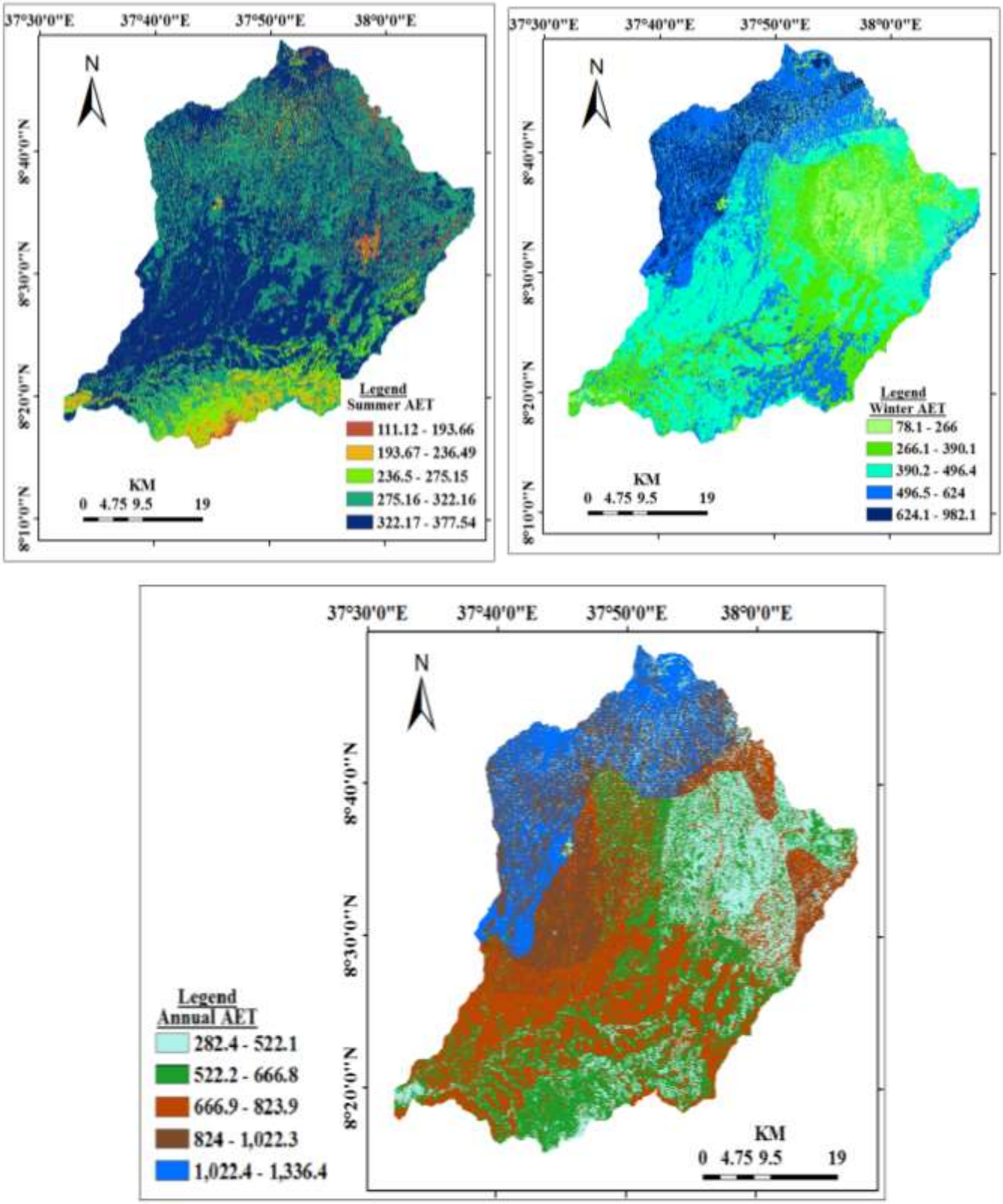

Figure 40. Summer, Winter and Annual AET of Walga catchment

5.2.2. Surface runoff

To estimate the surface runoff of Walga catchment WetSpass uses runoff coefficient which varies its value with vegetation type, soil type and slope. The surface runoff of Walga catchment shows variation with land-use, soil type, slope, topography, precipitation and the other meteorological parameters.

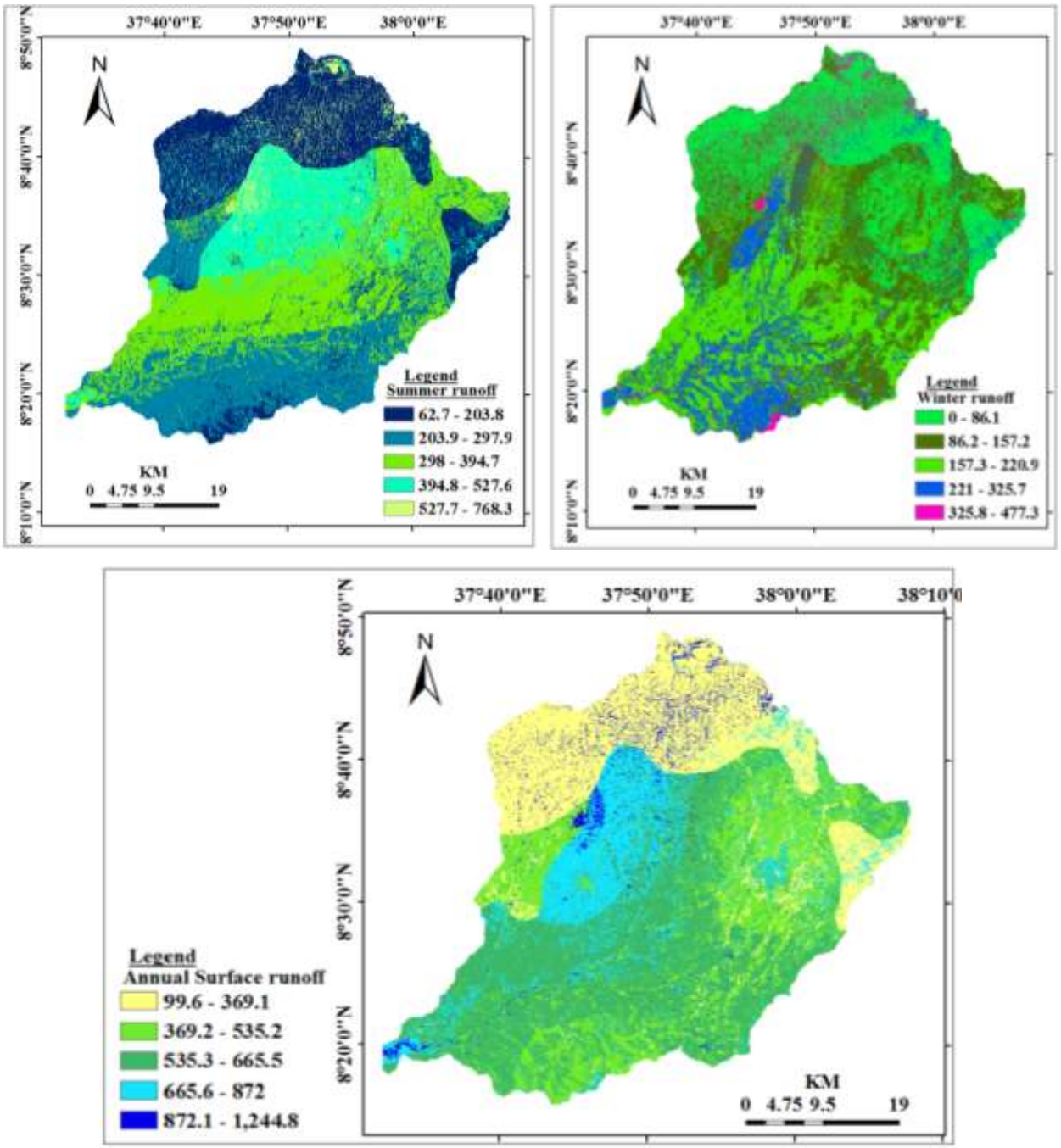

Figure 41. Summer, Winter and Annual Surface runoff

The simulated annual surface runoff varies from a minimum of 99.6mm to a maximum of 1244.76mm with a mean of 519.16mm that accounts about 38.25% from the mean annual rainfall (1357.43). The amount of surface runoff also shows variation in summer and winter season. The mean surface runoff (Sv) of the watershed in rainy season is 301. 5 mm, while the mean surface runoff (Sv) in dry season is approximately 148.7 mm. About 66.97% of Sv occurs during the rainy seasons (June to September), while the remaining 33.03% occurs in dry months (October to may). This variation comes from rainfall changes in the two seasons.

Higher surface runoff occurs partially at north, middle pat, and south western parts of the catchment due to cliff topography, steep slope, clay soil and poor vegetation cover (figure 4.1). Vegetation enhances rainfall reception and evapotranspiration increasing infiltration of water into soil and recharging groundwater. Northern, eastern and southern part of Walga catchment is dominantly areas of low surface runoff due to forest, grass land with shrub with high ground cover, agriculture, clay loam, sandy clay loam, sandy loam and gentle topography. Surface runoff of Walga catchment is strongly influenced by landscapes and land use land cover

5.2.3. Groundwater recharge

Recharge is an important factor in evaluating groundwater resources but is difficult to quantify. The WetSpass model estimates seasonal and annual long term spatial distribution amounts of groundwater recharge of Walga catchment as a spatial variable dependent on the soil texture, land-use, slope, meteorological conditions by subtracting the seasonal and annual surface runoff and evapotranspiration from the seasonal and annual precipitation respectively. The annual groundwater recharge of Walga catchment varies from 0 mm to 564.17mm with 102.2 mm mean value. The average annual groundwater recharge is 7.5% of the annual average precipitation.. Based on this the average groundwater recharge is estimated to be 227.7 MCM. This amount of infiltration into the groundwater depends on vegetation cover, slope, soil composition, depth to the water table, the presence or absence of confining beds and other factors. Recharge is promoted by natural vegetation cover, flat topography, permeable soils, a deep water table and the absence of confining beds (Graf & Przybyłek, 2018).

Usually the recharge areas are in topographic high places; discharge areas are located in topographic low. Using only topographic setup of the area could not be enough to classify the area as recharge and discharge zones. Land use/land cover, soil types and morphology of land are

equally important in classification of the area into recharge and discharge zones. The highland area gets relatively higher precipitation than the lowland.

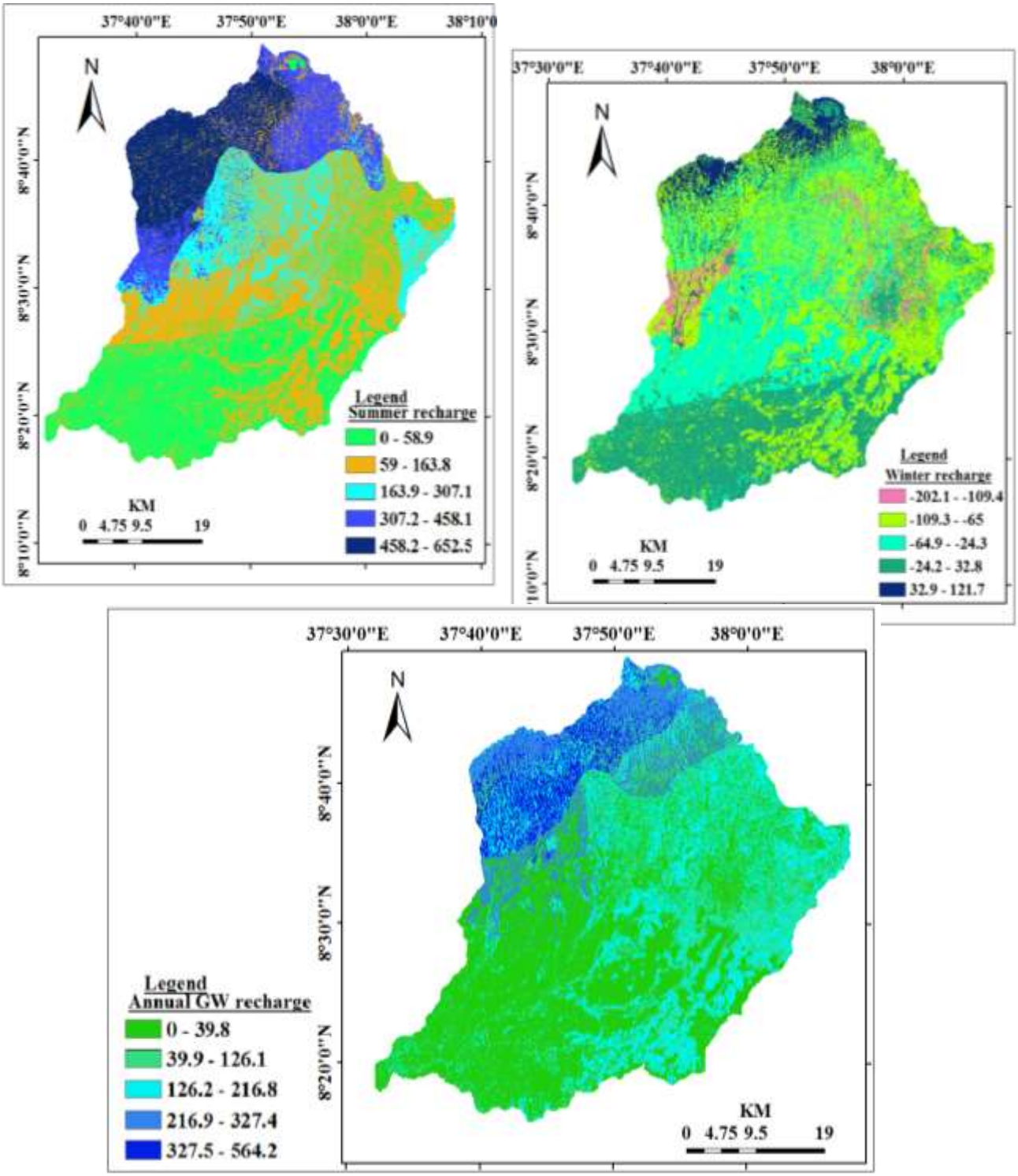

Figure 42. Summer, Winter and Annual Walga recharge

Figure 42 above shows that Northern and north western part is areas of high groundwater recharge due to sand clay loam soil texture (relative proportion of clay, silt and sand), dense forest, vegetation and high rainfall. Eastern and south eastern part of study area also classified under high groundwater recharge enhanced by soil surface roughness (ploughed land), cultivated crop land and irrigation area, gentle to moderate slope and lower drainage density. South and south western part is areas of low groundwater recharge due to high drainage density, steep slope, impermeable clay soil and poor ground cover. Summer and annual groundwater recharge map shows that Wonchi lake is classified under low groundwater recharge and during dry season the lake and groundwater recharges surface water. Kasahun Beyene (2005) has conducted his study entitled " groundwater resources evaluation of Walga river basin" over area of about 1786.75 km^2 and estimated groundwater recharge was 174.42mm using water balance method. Abera Gonfa (2018), has estimated the spatial variability of ground water recharge of Walga catchment using SWAT model based on precipitation distribution, soil type, land cover, topography (slope class) of the study area. According to his study, total groundwater recharge to shallow aquifer, as estimated using SWAT model was 315mm/yr, which is 24.4% of the annual rainfall amount of the study area.

Table 11.Summary of annual water balance components

Water balance component	Annual (mm)		
	Min	Max	Mean
Precipitation (P)	1003	1827	1357.43
Evapotranspiration (AET)	282.39	1336.4	736
Runoff (RO)	99.6	1244.76	519.16
Recharge (GR)	0	564.17	102.2
Difference	P-AET-RO-GR=0.07		

The mean annual water balance components (0.07mm) shown on table 12 above shows that groundwater recharge estimation using WetSpass is the best method, since it is a dynamic state spatially distributed water balance model for simulating groundwater recharge. The simulated groundwater recharge is minimum due to high actual evapotranspiration and high surface runoff. Simulated annual and seasonal water balance components ae shown under annex 6

5.3. Aquifer Characterization

In the study area (Walga catchment), pumping test is one of the ways to determine the performance and efficiency of a well and also to characterize and parameterize the hydraulic properties of an aquifer for a lot of bore holes located in this catchment. Step drawdown, Constant discharge and Recovery tests was done on single well to provide estimation of hydraulic parameters. The aquifer hydraulic properties were estimated from the pumping test by fitting mathematical models (type curves) to response data (water level changes) through computer software known as AQUIFER TEST. The Cooper Jacob's Straight-line was used to analyze the pumping test results of drawdown with respect to time. This method was chosen because it is built upon the most simplified assumptions.

Borehole properties in terms of depth, screen intervals (assumed aquifer thickness), static and dynamic water levels, drawdown and yield together with the aquifer constants T, K and Sc obtained from the Cooper- Jacob methods are presented in Table 6 below.

Table 12. Summary of aquifer properties

Properties	Max	Min	Ave
Well Depth (m)	473.58	12	105.35
SWL (m)	98	0	17.66
Q (l/s)	60.7	0.15	4.09
Sc (l/s/m)	75.79	0.0167	9.39
DD(m)	147.8	3.72	45.66
T (m^2/day)	290	0.00045	50.94
K (m/sec)	16.04	0	1.2

Well depth ranges from 12m (hand dug well) to 474m (bore holes) with average depth of 105m is drilled in the Walga catchment by government, private, NGOs and cooperation. Yield or discharge (Q) values range from 0.15 l/sec. to 61 l/sec (figure 20). The mean discharge value for the 72 boreholes is 4.09 l/s. The maximum discharge in Walga catchment is extracted from fractured basalt and ignimbrite aquifer lithologies while lowest discharge is from pyroclastic fall.

Transmissivity (figure 22) ranges from 3.5 $x10^{-4}$ m^2/day to 290 m^2/day with an average of 50.94 m^2/day. The lowest transmissivity values $3.5x10^{-4}$ m^2/day is indicative of the poor permeability in

the pyroclastic lithologic formations, the same to low discharge to wells. The low T values also imply that it will take a considerable time for the aquifers to replace water into wells removed during pumping. Hydraulic conductivity values ranges from 0 to 16.04 m/se with mean values of 1.2 m/s (figure 23) . The sum of the yield from 72 boreholes is 430 l/s (119.4 m^3/hr), this gives a total of 37152000 liters per day. Drawdown of cover between 3.72 and 147.8m were recorded in most boreholes and this gives an indication of the relative inefficiency of the aquifer materials as hydraulic structures.

5.4. Groundwater potential evaluation

To evaluate the different ground water potential zones, essential parameters were considered, and the maps were prepared for each layer. These maps were converted to raster data sets having the same pixel size and different weightage were assigned as per their groundwater potential controlling capacity within the study area and reclassification of each map was done based on the weight values produced.

Accordingly, the value 1 was given for highly controlling units, 2 for moderately controlling units, 3 for low controlling units and 4 for poor controlling reclassified units. Finally the maps integrated using GIS software with the purpose intended to delineate the groundwater potential areas for the study region.

5.4.1. Criteria weights and map scores

Thematic map with another paired-comparison 8x8 matrix was prepared by 28 pair wise comparison on Satty's importance scale to determine the relative importance or weights of each. These matrices have the property of consistency known as consistency ratios (CR). Satty indicates that the matrices with CR ratings greater than 0.1 should be re-evaluated. This way it helps to analyses the matrix to determine the inconsistency in defining the interrelationships. In this case the consistency value was 7% which was accepted (Figure 43). The weights were normalized by multiplying with 100 to avoid complexities of computation (table 14). These weights were applied in linear summation equation to obtain a unified weight map containing due weights of all input variables, which was further reclassified to arrive at groundwater potential map.

A total of eight thematic map were used for analyzing groundwater potential of Walga catchment. The contribution of rainfall in recharging groundwater is very high and has taken 26.1% while the

role of drainage density in the area is very low (2.2%). High scale value (4) was assigned for lower annual rainfall, while lowest value (1) for highest annual rainfall. To account for varying geology; Fractured mokonnin basalt and lower jimma basalt have given 1 scale values while wochecha trachyte and wonchi dendi pyroclastic fall contribution in evaluating groundwater potential is giver lowest (4) scale value.

The slope degree between 0-6° (high value), 6-15° (moderate value), 15-27° (low value), and 27-46° (least value) was assigned on account of increasing run off and decreasing infiltration respectively. The resulting weights for the criteria based on pairwise comparison of the following criteria is as follows. In the contrary to lineament density, higher drainage density value were assigned the lowest and the lowest drainage density values assigned highest values for decreasing runoff in the area.

For clayey Soil least value was assigned because of the presence of clay-horizons in the area considerably restricts percolation whereas highest value was assigned for fine sandy clay loam for their low water holding capacity and high permeability allow fast percolation. Shallow groundwater table area (discharge area) assigned highest values and deep groundwater table (areas of recharge) assigned least values.

Table 13. Relative weight and ranks of criteria

No	Categories	Weight(%)	Rank
1	Recharge	26.1	1
2	LULC	18.0	2
3	Discharge	15.4	3
4	Groundwater depth	14.1	4
5	Slope	10.4	5
6	Soil	9.2	6
7	Lithology	4.5	7
8	Drainage density	2.2	8

Table 14. Paired comparison matrix

Matrix		Recharge 1	Discharge 2	GW_depth 3	Soil 4	LULC 5	Slope 6	Lithology 7	DD 8	0 9	0 10	normalized principal Eigenvector
Recharge	1	1	3	3	3	1	3	5	7	-	-	26.10%
Discharge	2	1/3	1	1	3	1/2	3	3	7	-	-	15.38%
GW_depth	3	1/3	1	1	3	1	1	5	3	-	-	14.05%
Soil	4	1/3	1/3	1/3	1	1	1	3	5	-	-	9.20%
LULC	5	1	2	1	1	1	3	3	7	-	-	18.04%
Slope	6	1/3	1/3	1	1	1/3	1	5	7	-	-	10.44%
Lithology	7	1/5	1/3	1/5	1/3	1/3	1/5	1	5	-	-	4.55%
DD	8	1/7	1/7	1/3	1/5	1/7	1/7	1/5	1	-	-	2.23%
0	9	-	-	-	-	-	-	-	-	1	-	0.00%
0	10	-	-	-	-	-	-	-	-	-	1	0.00%

AHP Analytic Hierarchy Process n= 8 Input 1

Objective: Determining groundwater potential zone

Only input data in the light green fields!

Please compare the importance of the elements in relation to the objective and fill in the table: Which element of each pair is more important, A or B, and how much more on a scale 1-9 as given below.

Once completed, you might adjust highlighted comparisons 1 to 3 to improve consistency.

n	Criteria	Comment	RGMM	+/-
1	Recharge		26.1%	9.4%
2	Discharge		15.3%	6.5%
3	GW_depth		14.1%	6.3%
4	Soil		9.2%	3.9%
5	LULC		18.1%	7.5%
6	Slope		10.4%	4.7%
7	Lithology		4.5%	2.2%
8	DD		2.3%	1.1%
9		for 9&10 unprotect the input sheets and expand the		
10		question section ("+" in row 66)		

Participant 1 | 1 | α: 0.1 | CR: 7%

I	J	Criteria A	Criteria B	more important ? A or B	Scale (1-9)
1	2	Recharge	Discharge	A	3
1	3		GW_depth	A	3
1	4		Soil	A	3
1	5		LULC	B	1
1	6		Slope	A	3
1	7		Lithology	A	5
1	8		DD	A	7
2	3	Discharge	GW_depth	A	1
2	4		Soil	A	3
2	5		LULC	B	2
2	6		Slope	A	3
2	7		Lithology	A	3
2	8		DD	A	7
3	4	GW_depth	Soil	A	3
3	5		LULC	A	1
3	6		Slope	A	1
3	7		Lithology	A	5
3	8		DD	A	3
4	5	Soil	LULC	A	1
4	6		Slope	A	1
4	7		Lithology	A	3
4	8		DD	A	5
5	6	LULC	Slope	A	3
5	7		Lithology	A	3
5	8		DD	A	7
6	7	Slope	Lithology	A	5
6	8		DD	A	7
7	8	Lithology	DD	A	5

Figure 43. Principal Eigen value and CR

From the table 14, recharge map and LULC holds the first and second ranks while drainage density contribution is very low in groundwater potential evaluation when compared with other criteria's.

5.4.2. Groundwater potential zoning map

By integration of all the thematic maps, groundwater potential zones were delineated and classified as: very good (most important, high groundwater potential), good (important), Satisfactory (less important) and poor (not much important) potential zones (figure 27). The very good potential zones correspond to alluvial plains, lacustrine sediments, the fracture valleys, and valley fills, which coincide with the low slope and high lineaments density areas. The good zones mainly comprise structural hills and escarpments which contributes high run-off. Poor groundwater potential zones are present in the mountain peaks, plateaus and escarpments with steep cliff, where consolidated pyroclastic fall and less fractured acidic rocks exists.

Table 16 specifies that, 65.8% of Walga catchment coverage is under Satisfactory ground water potential while 0.72% is classified under very good groundwater potential, as well as 1.53% is areas here there is Poor groundwater table, gentle slope and very low drainage density is covered by good groundwater potential.

Table 15. Area coverage of groundwater potential zone

No	Groundwater potential zone	Area Coverage (km^2)	Percentage
1	Very good	16	0.72
2	Good	712	31.96
3	Satisfactory	1466	65.80
4	Poor	34	1.53

5.5.Groundwater Quality

5.5.1. Dinking water

PH value

The statistical summary of ground water data is shown in table 6. Majority groundwater pH ranges from 6.37 to 9.66 with mean of 7. 6. Measurement of pH relates to the acidity or alkalinity of the water, meanwhile majority of the water sample of Walga catchment is classified under alkaline water shows as there is disinfection in water and above WHO maximum limit. The maximum pH value 9.66 was collected from Galeyi rogda deep bore hole of 459m depth extracted from fractured basalt aquifer and minimum pH value 6 measured at Goru kersa site of Goro woreda.

Electrical Conductivity

It is the ability of water to carry out electric current. The presence of dissolved solids such as calcium, chloride, and magnesium in water samples carries the electric current through water. The maximum electrical conductivity is 1172.1 µS/cm measured at Kulit/shola ber shallow bore hole site at downstream of Walga catchment while the minimum EC value is 185.93 µS/cm. According to Rahmanian et al., (2015), it is expected to find high mineral contents in mineral water, which resulted in higher conductivity value. They also stated that, conductivity does not have direct impact on human health. It is determined for several purposes such as determination of mineralization rate (existence of minerals such as potassium, calcium, and sodium) and estimating the amount of chemical reagents used to treat this water.

High conductivity may lead to lowering the aesthetic value of the water by giving mineral taste to the water. For the industrial and agricultural activity, conductivity of water is critical to monitor. Spatial distribution map (figure 33) of EC (µS/cm) of Walga catchment shows; the Northern part is classified under low EC while the Southern part is under high EC (figure 33). Water with high conductivity may cause corrosion of metal surface of equipment such as boiler, home appliances such as water heater system and faucets.

Total Dissolved Solids

The maximum inorganic matters and minimum amounts of organic matter (TDS), which are present as solution in water sample of the area is 750.6mg/l, 138.47mg/l while the mean is 292.7 mg/l (figure 35). The standard allowable value set by WHO is 1000mg/l. But, all water sample of Walga catchment are below maximum allowable limits.

Fluoride

Statistical data (table 7) shows, the maximum fluoride concentration 16.4 mg/l is recode at Negash logde site medium bore hole of 297m depth meanwhile 0, 1.4 and 2.9 is the minimum, mean and standard deviation of fluoride concentration in Walga catchment. A lot of bore holes for Woliso town water supply and Private(mercy, lions club, and Negash lodge) bore holes were closed due to high fluoride concentration above maximum allowable limit set by WHO.

Spatial distribution of Fluoride concentration Walga catchment (figure 30) shows dominantly the area exceeds permissible WHO limit. Since the area is classified under intense agriculture, F^- concentration results from soil contamination as a result of the use of phosphate fertilizers and pesticides leached in to the aquifer.

According to guidelines for drinking water-quality set by WHO (2017), the chemicals of greatest health concern in some natural waters are usually excess natural fluoride, nitrate/nitrite and arsenic. Some commercial water treatment technologies are available for small applications for the removal of chemical contaminants. For example, anion exchange using activated alumina or iron-containing products will effectively reduce excess fluoride concentrations. Bone char has also been used to reduce fluoride concentrations.

Total Hardness

The maximum, minimum, average and standard deviation of hardness in Walga catchment is 421, 40,114.5 and 58.47espectively. WHO has not established guideline value for hardness because of not of health concern at levels found in drinking-water. Depending on the interaction of other factors, such as pH and alkalinity, water with a hardness above approximately 200 mg/l may cause scale deposition in the treatment works, distribution system and pipework and tanks within buildings. It will also result in high soap consumption and subsequent "scum" formation (WHO, 2017) .

5.5.2. Irrigation water quality

Spatial distribution of electrical conductivity (figure 33) shows dominantly the study area is suitable for irrigation in terms of EC. Spatial distribution of EC ranges from 165 to 1549 with mean of 507.26 and std dev of 174.36.

SAR is important parameters for determining the suitability of groundwater for irrigation because it is a measure of sodium hazard to crops. Spatial distribution of SAR value in the study area (figure 32) ranges from 0.01 to 149.76 with mean of 30.22 and std dev of 20.68. Irrigation water quality index based on SAR values adapted from Kuma (2014), Walga catchment lies from low to high salinity area.

Spatial distribution of Na^+ (figue 34), percentage of sodium ranges from 0.004 to 95.9, while 53 and 14.2 is the mean and standard deviation of Na%. It shows, majority of the study area is in between 40-60% which is permissible quality of water for irrigation (table 8)

Classification of groundwater

Piper diagram (figure 28) and (table 6) shows, existing works and data on physico- chemical parameters of groundwater quality in Walga ccatchment shows that, the category of water type is bicarbonate, Na-HCO3 type as a leading followed by Ca-Na-HCO3 type and Mg-HCO3 type.

CHAPTE SIX

6. CONCLUSION AND ECOMMENDATION

6.1.Conclusion

Being water is life, proper planning and management for utilization of this resource is very important. In order to have successful groundwater management, identifying the amount of spatial and temporal recharge and characterizing aquifer properties is very essential. WetSpass was applied to estimate long-term seasonal/annual average spatial and temporal groundwater recharge, actual evapotranspiration and surface runoff of the basin as a function of land-cover, soil type, topography and hydro-meteorological factors in Walga catchment. The mean value of surface runoff accounts 38.75% of the total annual precipitation, 54.22% of the total annual rainfall is lost by evapotranspiration while 7.5% of annual rainfall is recharged the groundwater of Walga catchment. The total water balance of this catchment is 0.07mm that shows that WeSpass gives good estimation of groundwater recharge. Less groundwater recharge is simulated due to high evapotranspiration and surface runoff which leads to drop in water table. It has also a negative impact in fulfilling increasing demand of water in Walga catchment.

Recharge is the primary method through which water enters an aquifer. In order to characterize the aquifer properties hydrogeological data was collected and aquifer hydraulic properties were estimated from the pumping test by fitting mathematical models to response data through computer software known as AQUIFER TEST. The Cooper Jacob's Straight-line was used to analyze the pumping test results of drawdown with respect to time. The maximum discharge in Walga catchment is extracted from fractured basalt and ignimbrite aquifer lithologies while lowest discharge is from pyroclastic fall. The low T values of the catchment implies poor permeability in the pyroclastic lithologic formations, the same to low discharge to wells and that it will take a considerable time for the aquifers to replace water into wells removed during pumping.

The source of groundwater recharge in Walga catchment is mainly rainfall. Rainfall has contributed highest weightage in evaluating groundwater potential of Walga catchment. To account for varying geology; Fractured mokonnin basalt and lower jimma basalt have given highest scale values while wochecha trachyte and wonchi dendi pyroclastic fall contribution in evaluating groundwater potential is given lowest scale value. By integration of all the thematic maps (Rainfall, Lithology, Slope, Groundwater depth, Soil, LULC and Drainage density),

groundwater potential zones were delineated and classified as: very good (most important, high groundwater potential), good (important), poor (not much important) and very poor (least important) potential zones. From classified groundwater potential delineation 66.4% of Walga catchment is classified as good groundwater potential. Integrated GIS and remote sensing techniques are very efficient and useful, time and cost effective tool for the identification/delineation of groundwater potential zones. Paired Comparison matrix analysis indicates that all parameters are significant but the most effective parameters in the area are: litho logy, geomorphology, lineament density, drainage density and slope.

Understanding only the amount of groundwater recharge, aquifer properties and delineating groundwater potential is not enough unless its quality is not known. Descriptive statics of water quality parameters shows that the average water quality parameters are within the limited WHO standards. Irrigation water quality was studied based on EC, SAR and Na%. Spatial distribution of electrical conductivity shows dominantly the study area is suitable for irrigation in terms of EC. Irrigation water quality index based on SAR values Walga catchment lies from low to high salinity area while Na% shows majority of the study area is permissible quality of water for irrigation.

6.2.Recommendations

WetSpass input data was prepared from meteorological data with a lot of missing values filled by linear regression; the result can be changed based on accurate input of hydro meteorological data, soil and land use land cover. Water chemistry used in this research is based on laboratory data collected from different office, since quality varies spatially and temporally recent water sample data can change what is presented in this work. Based on this

- Proper recorded hydrogeological and hydrogeochimcal data is very important for management and scientists interested to study Walga catchment.
- Groundwater monitoring is very fundamental step towards evaluating and managing shallow and deep groundwater resources since there is less groundwater recharge.
- Further study on groundwater chemistry is needed to have clear information of groundwater for drinking and irrigation water supply.
- In general, proper well inventory with full necessary data is needed to have good water planning and management and also make life easy for further study.

Bibliography

Amadi, A. N., Olasehinde, P. I., Dan-Hassan, Okoye, N. O., & Ezeagu, G. G. (2014). Hydrochemical Facies Classification and Groundwater Quality Studies in Eastern Niger Delta, Nigeria. *International Journal of Engineering Research and Development*, *10*(3), 2278–67.

Amatya, D. M., Harrison, C. A., & Trettin, C. C. (2014). *Comparison of Potential Evapotranspiration (PET) using Three Methods for a Grass Reference and a Natural Forest in Coastal Plain of South Carolina*. (2011).

Aquifer, C., Flow, G., Conductivity, H., Table, W., & Hydrogeology, A. (2015). *Unconfined Aquifer Unconfined Aquifers The Subsurface Environment Groundwater Hydrology*.

Area, M., Africa, S., & Kurniawan, T. A. (2019). *Hydrogeochemical Assessment of Groundwater Using Statistical Approach*.

Aslan, S., Yozgatligil, C., Iyigun, C., & Batmaz, I. (2013). Comparison of Missing Value Imputation Methods for Turkish Monthly Total Precipitation Data. *Theor Appl Climatol*, 143–167. https://doi.org/10.1007/s00704-012-0723-x

Ayenew, T. (2006). Major ions composition of the groundwater and surface water systems and their geological and geochemical controls in the Ethiopian volcanic terrain. *SINET: Ethiopian Journal of Science*, *28*(2), 171–188. https://doi.org/10.4314/sinet.v28i2.18253

Ayenew, T., Demlie, M., & Wohnlich, S. (2008). Hydrogeological framework and occurrence of groundwater in the Ethiopian aquifers. *Journal of African Earth Sciences*, *52*(3), 97–113. https://doi.org/10.1016/j.jafrearsci.2008.06.006

Bashe, B. B. (2017). Groundwater Potential Mapping using Remote Sensing and GIS in Rift Valley Lakes Basin, Weito Sub Basin, Ethiopia. *International Journal of Scientific & Engineering Research*, *8*(2), 43–50. Retrieved from http://www.ijser.org

Batelaan, O., & De Smedt, F. (2001). WetSpass: A flexible, GIS based, distributed recharge methodology for regional groundwater modelling. *IAHS-AISH Publication*, (269), 11–18.

Batelaan, O., & De Smedt, F. (2007). GIS-based recharge estimation by coupling surface-subsurface water balances. *Journal of Hydrology*, *337*(3–4), 337–355. https://doi.org/10.1016/j.jhydrol.2007.02.001

Baxter, C. (2016). *Gradient Effects on Measured Hydraulic Conductivity Submitted to the Faculty of Christopher David Price Baxter In Partial Fulfillment of the Requirements for the Degree of Master of Science in Civil Engineering August 1994*. (January 1994). https://doi.org/10.13140/RG.2.2.24655.07845

Canora, F., Rizzo, G., Panariello, S., & Sdao, F. (2019). Hydrogeology and hydrogeochemistry of the lauria mountains northern sector groundwater resources (basilicata, italy). *Geofluids*, *2019*, 1–16. https://doi.org/10.1155/2019/7039165

Chandra Bose, A. S., Giridhar, M. V. S. S., & Viswanadh, G. K. (2010). Identification of groundwater potential zones using RS and GIS. *31st Asian Conference on Remote Sensing 2010, ACRS 2010*, *1*, 327–333.

CSA, MOWIE, World Bank, UNICEF, W. and J. (2017). *Drinking Water Quality in Ethiopia. Results from the 2016 Ethiopia Socioeconomic Survey*. (December), 22.

Demelash, H., Beyene, A., Abebe, Z., & Melese, A. (2019). Fluoride concentration in ground water and prevalence of dental fluorosis in Ethiopian Rift Valley: Systematic review and meta-analysis. *BMC Public Health*, *19*(1). https://doi.org/10.1186/s12889-019-7646-8

Dereje, B., & Nedaw, D. (2019). Groundwater Recharge Estimation Using WetSpass Modeling in Upper Bilate Catchment, Southern Ethiopia. *Momona Ethiopian Journal of Science*, *11*(1), 37. https://doi.org/10.4314/mejs.v11i1.3

Dhar, A., Sahoo, S., Dey, S., & Sahoo, M. (2014). Evaluation of Recharge and Groundwater Dynamics of a Shallow Alluvial Aquifer in Central Ganga Basin, Kanpur (India). *Natural Resources Research*, *23*(4), 409–422. https://doi.org/10.1007/s11053-014-9251-y

Dinu, C., Drobot, R., Pricop, C., & Blidaru, T. V. (2017). Flash-Flood Modelling With Artificial Neural. *Mathematical Modelling in Civil Engineering*, *13*(3), 10–20. https://doi.org/10.1515/mmce

Editor, S., Carlos, J., & Cerezal, S. (n.d.). *Springer Hydrogeology*.

Edmond Moeletsi, M., Phumlani Shabalala, Z., De Nysschen, G., & Walker, S. (2016). Evaluation of an inverse distance weighting method for patching daily and dekadal rainfall over the free state province, South Africa. *Water SA*, *42*(3), 466–474. https://doi.org/10.4314/wsa.v42i3.12

Eilers, A., Miller, J., Watson, A., & Sigidi, N. (2017). Groundwater Recharge Quantification from Historical Rainfall Records and Salinity Profiling in the RAMSAR Listed Verlorenvlei Catchment, South Africa. *Procedia Earth and Planetary Science*, *17*, 586–589. https://doi.org/10.1016/j.proeps.2016.12.150

Erickson, T. O., & Stefan, H. G. (2008). Baseflow analysis of the Upper Vermillion River, Dakota County, Minnesota. *University of Minnesota St. Anthony Falls Laboratory Project Report*, (507), 55.

Ewusi, A., & Kuma, J. S. Y. (2014). Groundwater Assessment for Current and Future Water Demand in the Daka Catchment, Northern Region, Ghana. *Natural Resources Research*, *23*(4), 355–365. https://doi.org/10.1007/s11053-014-9227-y

Fejerskov, O., Larsen, M. J., Richards, A., & Baelum, V. (1994). Dental tissue effects of fluoride. *Advances in Dental Research*, *8*(1), 15–31. https://doi.org/10.1177/08959374940080010601

Fipps, G. (1995). Standards and Salinity Management and Salinity Management Water Analysis : *Agrilife Extension*, *4*(3), 1–17.

Gintamo, T. T. (2015). Ground Water Potential Evaluation Based on Integrated GIS and Remote Sensing Techniques, in Bilate River Catchment: South Rift Valley of Ethiopia. *American Scientific Research Journal for Engineering, Technology, and Sciences (ASRJETS) ISSN (Print)*, (January), 2313–4410. Retrieved from http://asrjetsjournal.org/

Goulburn-Murray Water (GMW). (2010). Groundwater Terms and definitions. *Goulbourn-Muray Water*, (February), 1–22.

Graf, R., & Przybyłek, J. (2018). Application of the WetSpass simulation model for determining conditions governing the recharge of shallow groundwater in the Poznań Upland, Poland. *Geologos*, *24*(3), 189–205. https://doi.org/10.2478/logos-2018-0020

Haile, M. Z., & Mohammed, E. T. (2019). *Analysis of Physico-chemical Characteristics of Water Collected from Different Sampling Sites of Lake Hawassa* ,. *9*(2), 38–45. https://doi.org/10.5923/j.env.20190902.02

Halford, K. J., Weight, W. D., & Schreiber, R. P. (2006). Interpretation of transmissivity estimates from single-well pumping aquifer tests. *Ground Water*, *44*(3), 467–471. https://doi.org/10.1111/j.1745-6584.2005.00151.x

Hamerlynck, O. (2013). Water conflict. In *New Scientist* (Vol. 218). https://doi.org/10.1016/S0262-4079(13)60875-1

Hammouri, N., El-Naqa, A., & Barakat, M. (2012). An Integrated Approach to Groundwater Exploration Using Remote Sensing and Geographic Information System. *Journal of Water Resource and Protection*, *04*(09), 717–724. https://doi.org/10.4236/jwarp.2012.49081

Hasanuzzaman, M., Song, X., Han, D., Zhang, Y., & Hussain, S. (2017). Prediction of groundwater dynamics for sustainable water resource management in bogra district, northwest bangladesh. *Water (Switzerland)*, *9*(4). https://doi.org/10.3390/w9040238

Hoque, M. A., & Burgess, W. G. (2012). 14C dating of deep groundwater in the Bengal Aquifer System, Bangladesh: Implications for aquifer anisotropy, recharge sources and sustainability. *Journal of Hydrology*, *444–445*, 209–220. https://doi.org/10.1016/j.jhydrol.2012.04.022

Hussein, A.-A., Govindu, V., & Nigusse, A. G. M. (2017). Evaluation of groundwater potential using geospatial techniques. *Applied Water Science*, *7*(5), 2447–2461. https://doi.org/10.1007/s13201-016-0433-0

I, A. E., P, F. I., Resources, W., & State, C. R. (2018). *Determination of Aquifer Hydraulic Parameters Using Single Well Pumping Test Borehole Data within Boki Local Government Area , Cross River State , South Eastern Nigeria*. *8*(3), 26–36.

I, Yu, C., Chen, R., Li, J. J., Li, J. J., Drahansky, M., … Reading, F. (2012). We are IntechOpen , the world ’ s leading publisher of Open Access books Built by scientists , for scientists TOP 1 %. *Intech*,

i(tourism), 13. https://doi.org/10.1016/j.colsurfa.2011.12.014

In, S., Africa, S., Lorentz, S., & Hughes, G. O. (2003). *TECHNIQUES FOR ESTIMATING GROUNDWATER RECHARGE AT DIFFERENT Groundwater Recharge Estimation in Southern Africa Edited by Published by UNESCO Paris Printed in Cape Town*.

Jhariya, D. C., Kumar, T., Gobinath, M., Diwan, P., & Kishore, N. (2016). Assessment of groundwater potential zone using remote sensing, GIS and multi criteria decision analysis techniques. *Journal of the Geological Society of India*, *88*(4), 481–492. https://doi.org/10.1007/s12594-016-0511-9

Kawo, N. S., & Karuppannan, S. (2018). Groundwater quality assessment using water quality index and GIS technique in Modjo River Basin, central Ethiopia. *Journal of African Earth Sciences*, *147*(June), 300–311. https://doi.org/10.1016/j.jafrearsci.2018.06.034

Khadri, S. F. R., & Moharir, K. (2016). Characterization of aquifer parameter in basaltic hard rock region through pumping test methods: a case study of Man River basin in Akola and Buldhana Districts Maharashtra India. *Modeling Earth Systems and Environment*, *2*(1), 1–18. https://doi.org/10.1007/s40808-015-0047-9

Kumar, P. J. S. (2014). *Interpretation of groundwater chemistry using piperand chadha ´ s diagrams : a comparative study from perambalur taluk Geoscience Interpretation of groundwater chemistry using piper and chadha ´ s diagrams : a comparative study from perambalur taluk*. (January 2013).

Lapworth, D. J., Krishan, G., MacDonald, A. M., & Rao, M. S. (2017). Groundwater quality in the alluvial aquifer system of northwest India: New evidence of the extent of anthropogenic and geogenic contamination. *Science of the Total Environment*, *599–600*(May), 1433–1444. https://doi.org/10.1016/j.scitotenv.2017.04.223

Manikandan, J., Kiruthika, A. M., & Sureshbabu, S. (2014). Evaluation of groundwater potential zones in Krishnagiri District , Tamil Nadu using MIF Technique. *International Journal of Innovative Research in Science, Engineering and Technology*, *3*(3), 10524–10534.

Meier, P. M., Carrera, J., & Sánchez-Vila, X. (1998). An evaluation of Jacob's method for the interpretation of pumping tests in heterogeneous formations. *Water Resources Research*, *34*(5), 1011–1025. https://doi.org/10.1029/98WR00008

Meresa, E., & Taye, G. (2018). Estimation of groundwater recharge using GIS-based WetSpass model for Birki watershed, the eastern zone of Tigray, Northern Ethiopia. *Sustainable Water Resources Management*, *0*(0), 0. https://doi.org/10.1007/s40899-018-0282-0

Meybeck, M., Kuusisto, E., Mäkelä, A., & Mälkki, E. (1996). Quality Water. *Water Quality Monitoring - A Practical Guide to the Design and Implementation of Freshwater Quality Studies and Monitoring Programmes*, 1–22.

Modelling, M., Engineering, C., Mawlood, D. K., Region, K., Mustafa, J. S., Directorate, G., & Region, K. (2016). *COOPER-JACOB ' S METHOD FOR ESTIMATING OF THE AQUIFER PARAMETERS*. *12*(1), 9–20. https://doi.org/10.1515/mmce

Murthy, K. S. R., Amminedu, E., & Venkateswara Rao, V. (2003). Integration of thematic maps through GIS for identification of groundwater potential zones. *Journal of the Indian Society of Remote Sensing*, *31*(3), 197–210. https://doi.org/10.1007/BF03030826

Nag, S. K. (2008). Application of remote sensing and GIS in groundwater exploration. *Groundwater Dynamics in Hard Rock Aquifers: Sustainable Management and Optimal Monitoring Network Design*, *3*(10), 87–92. https://doi.org/10.1007/978-1-4020-6540-8_5

Nagarajan, M., & Singh, S. (2009). Assessment of groundwater potential zones using GIS technique. *Journal of the Indian Society of Remote Sensing*, *37*(1), 69–77. https://doi.org/10.1007/s12524-009-0012-z

Naranjo, G., Cruz-Fuentes, T., Cabrera, M. del C., & Custodio, E. (2015). Estimating natural recharge by means of chloride mass balance in a volcanic aquifer: Northeastern Gran Canaria (Canary Islands, Spain). *Water (Switzerland)*, *7*(6), 2555–2574. https://doi.org/10.3390/w7062555

Nur, A., Ishaku, J. M., & Yusuf, S. N. (2012). Groundwater Flow Patterns and Hydrochemical Facies Distribution Using Geographical Information System (GIS) in Damaturu, Northeast Nigeria. *International Journal of Geosciences*, *03*(05), 1096–1106. https://doi.org/10.4236/ijg.2012.35111

Oikonomidis, D., Dimogianni, S., Kazakis, N., & Voudouris, K. (2015). A GIS/Remote Sensing-based methodology for groundwater potentiality assessment in Tirnavos area, Greece. *Journal of Hydrology*, *525*, 197–208. https://doi.org/10.1016/j.jhydrol.2015.03.056

Patil, P. N., Sawant, D. V, & Deshmukh, R. N. (2012). *Physico-chemical parameters for testing of water – A review*. *3*(3), 1194–1207.

Pollution, G., & Recharge, A. (2015). *MIEA & Erasmus Mundus GroundwatCH · Groundwater Pollution and Protection · (M. Teresa Condesso de Melo)*. Retrieved from https://fenix.tecnico.ulisboa.pt/downloadFile/1970943312278793/GROUNDWATER RECHARGE.pdf

Rahmanian, N., Hajar, S., Ali, B., Homayoonfard, M., Ali, N. J., Rehan, M., … Nizami, A. S. (2015). *Analysis of Physiochemical Parameters to Evaluate the Drinking Water Quality in the State of Perak , Malaysia*. *2015*(Cd).

Rahmati, O., Pourghasemi, H. R., & Melesse, A. M. (2016). Application of GIS-based data driven random forest and maximum entropy models for groundwater potential mapping: A case study at Mehran Region, Iran. *Catena*, *137*, 360–372. https://doi.org/10.1016/j.catena.2015.10.010

Rajesh, R., Brindha, K., & Techniques, G. (2019). *Hydrogeochemistry Methods for Assessing the Groundwa- ter Quality*.

Romman, Z. A., Al-bakri, J., & Kuisi, M. Al. (2019). *Estimation of Rainfall Missing Data in an Arid Area using Spatial and EM Estimation of Rainfall Missing Data in an Arid Area using Spatial and EM Methods*. (March). https://doi.org/10.9790/9622-

Rukundo, E., & Doğan, A. (2019). Dominant influencing factors of groundwater recharge spatial patterns in Ergene river catchment, Turkey. *Water (Switzerland)*, *11*(4). https://doi.org/10.3390/w11040653

Rushton, K. R. (1991). *Groundwater support of stream flows in the Cambridge area , UK*. (202), 367–376.

Salem, A. (n.d.). *Assessment of Groundwater Recharge , Evaporation , and Runoff in the Drava Basin in Hungary with the WetSpass Model*. 1–11. https://doi.org/10.3390/hydrology6010023

Sattari, M., Rezazadeh-joudi, A., & Kusiak, A. (2016). *Uncorrected Proof missing data in precipitation studies Uncorrected Proof*. 1–13. https://doi.org/10.2166/nh.2016.364

Scanlon, B. R., Healy, R. W., & Cook, P. G. (2002). Choosing appropriate techniques for quantifying groundwater recharge. *Hydrogeology Journal*, *10*(1), 18–39. https://doi.org/10.1007/s10040-001-0176-2

Sener, E., Davraz, A., & Ozcelik, M. (2005). An integration of GIS and remote sensing in groundwater investigations: A case study in Burdur, Turkey. *Hydrogeology Journal*, *13*(5–6), 826–834. https://doi.org/10.1007/s10040-004-0378-5

Solomon, S., & Quiel, F. (2006). Groundwater study using remote sensing and geographic information systems (GIS) in the central highlands of Eritrea. *Hydrogeology Journal*, *14*(5), 729–741. https://doi.org/10.1007/s10040-005-0477-y

Tank, D. K., & Chandel, C. P. S. (2010). *Analysis Of The Major Ion Constituents In Groundwater Of Jaipur City*. *2*(5), 1–7.

Tekle-Haimanot, R., Melaku, Z., Kloos, H., Reimann, C., Fantaye, W., Zerihun, L., & Bjorvatn, K. (2006). The geographic distribution of fluoride in surface and groundwater in Ethiopia with an emphasis on the Rift Valley. *Science of the Total Environment*, *367*(1), 182–190. https://doi.org/10.1016/j.scitotenv.2005.11.003

Teklebirhan, A., Dessie, N., & Tesfamichael, G. (2012). Groundwater Recharge, Evapotranspiration and Surface Runoff Estimation Using WetSpass Modeling Method in Illala Catchment, Northern Ethiopia. *Momona Ethiopian Journal of Science*, *4*(2), 96. https://doi.org/10.4314/mejs.v4i2.80119

Tilahun, K., & Merkel, B. J. (2009). *Estimation of groundwater recharge using a GIS-based distributed water balance model in Dire Dawa , Ethiopia*. 1443–1457. https://doi.org/10.1007/s10040-009-0455-x

Tse, A., & Amadi, P. (2010). Hydraulic properties from pumping tests data of aquifers in Azare area, North Eastern Nigeria. *Journal of Applied Sciences and Environmental Management*, *11*(4). https://doi.org/10.4314/jasem.v11i4.55198

Velasquez, M., & Hester, P. T. (2013). *An Analysis of Multi-Criteria Decision Making Methods*. *10*(2), 56–66.

Waikar, M. L., & Nilawar, A. P. (2014). *Identification of Groundwater Potential Zone using Remote Sensing and GIS Technique*. *3*(5), 12163–12174.

Wang, S., Sheng, Z., Xi, Y., Ma, X., Zhang, H., Kang, M., … Han, Z. (n.d.). *The Application of the Analytic Hierarchy Process and a New Correlation Algorithm to Urban Construction and Supervision Using Multi-Source Government Data in Tianjin*. https://doi.org/10.3390/ijgi7020050

Whitaker, R., & Foundation, C. D. (2017). *The Analytic Hierarchy Process – What It Is and How It Is Used*. *0255*(December 1987). https://doi.org/10.1016/0270-0255(87)90473-8

Xia, Y., Fabian, P., Stohl, A., & Winterhalter, M. (1999). Forest climatology: Estimation of missing values for Bavaria, Germany. *Agricultural and Forest Meteorology*, *96*(1–3), 131–144. https://doi.org/10.1016/S0168-1923(99)00056-8

Yair, A., & Kossovsky, A. (2002). Climate and surface properties: Hydrological response of small arid and semi-arid watersheds. *Geomorphology*, *42*(1–2), 43–57. https://doi.org/10.1016/S0169-555X(01)00072-1

Yeh, H. F., Cheng, Y. S., Lin, H. I., & Lee, C. H. (2016a). Mapping groundwater recharge potential zone using a GIS approach in Hualian River, Taiwan. *Sustainable Environment Research*, *26*(1), 33–43. https://doi.org/10.1016/j.serj.2015.09.005

Yeh, H. F., Cheng, Y. S., Lin, H. I., & Lee, C. H. (2016b). Mapping groundwater recharge potential zone using a GIS approach in Hualian River, Taiwan. *Sustainable Environment Research*, *26*(1), 33–43. https://doi.org/10.1016/j.serj.2015.09.005

Yenehun, A., Walraevens, K., & Batelaan, O. (2017). Spatial and temporal variability of groundwater recharge in Geba basin, Northern Ethiopia. *Journal of African Earth Sciences*, *134*, 198–212. https://doi.org/10.1016/j.jafrearsci.2017.06.006

Zeinolabedini, M., & Esmaeily, A. (2015). Groundwater potential assessment using geographic information systems and AHP method (case study: Baft city, Kerman, Iran). *International Archives of the Photogrammetry, Remote Sensing and Spatial Information Sciences - ISPRS Archives*, *40*(1W5), 769–774. https://doi.org/10.5194/isprsarchives-XL-1-W5-769-2015

Appendices

Annex 1: Mean monthly annual rainfall of Walga catchment

Years	Jan	Feb	Mar	Apr	May	Jun	Jul	Aug	Sep	Oct	Nov	Dec
1997	40.37857	0.1	66.54286	107.5557	74.31429	179.9714	271.4571	178.9129	102.4143	88.79286	51.91429	0.4
1998	53.18571	35.45714	72.58571	76.4	158.2214	274.0686	330.0929	318.2743	153.43	66.93857	4.008571	0
1999	8.785714	3.485714	27.45714	20.91429	104.4143	183.3714	281.0714	272.8286	151.8957	153.0429	0.185714	3.301429
2000	1.575714	2.628571	10.61429	78.91143	90.45714	142.5271	250.5714	235.3057	187.1286	59.81429	30.48571	13.57143
2001	5.528571	10.08571	90.2	60.88571	148.6857	190.4	322.4143	256.2	117.8	55.15714	13.74286	2.357143
2002	54.98571	40.02857	129.5286	46.74286	77.3	213.2286	247.3757	234.7343	85.82857	2.998571	0	40.52857
2003	31.11429	37.82857	73.11429	115.0571	18.94286	191.8714	290.5143	275.9429	153.7114	15.51429	6.914286	15.35714
2004	61.7	19.37143	43.97	111.5857	54.67143	220.2429	261.7271	247.2857	163.0429	46.95714	5.228571	6.457143
2005	49.32083	1.997917	92.03542	110.6604	89.65833	181.575	257.55	221.3625	175.9875	61.2	27.475	0.55
2006	6.5125	27.8875	104.7375	86.86125	115.875	183.5625	296.5175	312.8313	140.2875	60.5375	23.50292	22.0875
2007	40.875	56.7	54.7375	84.125	175.5125	248.9	322.7875	270.5	205.4625	33.85	0	0
2008	0.277083	3.7	8.160417	49.00417	200.4125	206.25	326.875	276.7375	140	63.25417	67.5	1.60625
2009	31.1325	25.2275	47.11875	68.52125	82.76125	122.1125	253.1875	300.475	117.2625	106.8563	0.78125	31.2625
2010	19.95	69.7	76.325	87.4125	186.2125	188.6688	315.4813	312.4792	144.8125	9.479167	17.18958	36.375
2011	19.7625	8.39875	44.3625	91.3	154.7958	187.46	264.0517	290.4038	183.8917	14.64458	39.15625	1.23375
2012	6.271875	7.198333	23.55292	87.10313	75.44396	170.1354	271.0425	216.385	201.9531	34.62813	6.708333	4.998958
2013	2.538958	6.163333	62.21583	121.8713	134.7938	171.7646	261.0736	247.3625	152.5538	87.8125	12.53125	1.873958
2014	13.00688	37.79125	64.2125	47.17708	193.1613	143.3646	281.0958	183.8854	187.9146	40.59438	9.187292	1.417708
2015	15.73875	18.2375	55.87	42.49	143.6613	166.5963	265.6083	202.3625	122.9	7.445625	20.59104	13.90271
2016	27.91458	7.1375	54.21875	165.3	224.3338	189.1031	196.105	243.72	183.41	30.24	20.48083	13.62271
2017	2.48875	24.13875	39.57375	68.79875	138.0388	157.445	230.5263	270.9094	155.7313	112.2125	33.22688	4.585
2018	9.91875	13.85	73.6675	163.4813	189.1588	154.8013	167.8925	200.3775	107.4888	61.49875	100.0238	7.0775

Annex 2: Chemical parameters of DBH, SBH, HDW and MBH

SN	X	Y	Z,(m)	Depth, (m)	SWL,m	Aquifer_Lith.	T ºC	Ph	EC(µS/cm)	TDS	NH3 (mg/l)	Na (mg/l)	K (mg/l)	TH (mg/l)	Ca (mg/l Ca)
1	358290	926080	1699	459	82.0	Fractured Basalt	28	9.660	994	209	0.260	72	0.500	20.000	4.800
2	370781	943250	1867	470.52	29.3	Bsaltic	24.7	7.66	974	595	0.55	230	7.85	40	11.5
3	385801	939409	1953	473.58	65	Basalt and ignimbrite	30	7	920	598	1.35	200	19	69.7	18.4
4	389562	922209	1931	450	98	pyroclastic		7.05	515	340	0.340	118	9.100	42.840	14.690
5	375734	926348	1787	360	8.9	Fractured Basalt		7.930	565	360	1.510	115	3.400	32.000	8.000
6	357700	944225	1822	360	25	Basaltic		8.28	287	168	0.05	72	2	108	4
7	383826	947387	2058	265	0	Fractured Basalt		7.790	835	476	0.340	166	12.500	26.600	6.080
8	408282	939498	2311	360	22	Pyroclastic		7.35	413	236	0.17	76	9	32.3	8
9	363415	915588	1788	280	98	Pyroclastic		9.46	414	216	0.17	89	1	28.8	4
10	376617	902505	1941	347	57	Pyroclastic		6.90	425	278	0.20	64	10	78.3	26.4
11	386183	943986	2023	108	0	Basaltic / Ash	29	9.000	303	190	0.25	61	3.000	22.000	5.000
12	387549	945858	2067	93	0.0	Basaltic /Ash		8.51	303	190	0.25	61	3.2	21.7	5.2
13	393191	944399	2153	47	0	Pyroclastic	40.5	7.000	741	488	0.13	147	9.000	33.000	11.000
14	342165	903933	1654	45	0	Basaltic	24.1	7.51	490	320	0.19	20	7.6	209	67.6
15	339077	902523	1685	60	20	Basaltic	20.7	6.92	360	232	0.17	16	3.3	142.5	45.6
17	342000	903672	1669	60		Basaltic									
18	342369	903357	1655	8	1	Basaltic	18.7	6.98	465	304	0.22	31	6.3	186.2	60.8
19	337131	931265	1525	39	10		20.7	7.34	652	420	0.2	82	7.5	190	50.16
20	337246	929566	1538	52	33			7.29	617	404	0.39	45	6.1	247	76
21	337688	927934	1548	54	11			7.87	1316	852	0.11	282	7.1	30.4	6.84
22	338664	924779	1527	51	23	Basaltic		7.34	1193	770	0.2	190	19	210.9	63.1
23	340300	924367	1551			Basaltic		7.18	1080	700	0.48	124	14	269.8	73.7
24	340966	924430	1558	130		Basaltic		7.28	1246	810	0.28	158	14.5	323	85.1
25	339029	924979	1519			Basaltic	20.8	7.29	1116	720	0.65	194	15.5	191.9	53.2
26	341088	924567	1557	81	35	Basaltic	20.9	8.01	726	466	0.73	125	11	89.3	19
27	340662	924050	1547	54		Basaltic	21.9	7.05	890	570	0.36	84	10.7	285	79.04
28	342102	923134	1526	58	42	Basaltic	22.7	7.18	1301	842	0.71	198	13.8	307.8	55.5
29	343453	924775	1587	61	41	Basaltic	23.1	7.08	939	604	0.59	50	9.1	418	102.6
30	342266	922432	1533	54		Basaltic	22.2	7.05	1275	826	0.65	126	9.2	446.5	129.2
31	343035	921923	1547	92	48	Basaltic	23.1	7.55	1166	754	0.29	220	11.6	152	34.2
32	343578	920886	1540	70		Basaltic	23	6.64	1555	1008	0.73	102	15	665	155.8
33	344574	921296	1549			Basaltic	21	7.08	782	510	0.43	28	5.3	351.5	123.9

34	344752	920691	1535	69	36	Basaltic	19.5	7.31	855	556	0.65	33	7.6	389.5	98.04
35	349391	918430	1632			Basaltic	21.8	9.23	575	374	0.08	134	3.4	19	3.8
36	347338	916729	1582	78	42	Basaltic	20.7	7.14	954	620	0.12	45	9.2	427.5	126.9
37	352791	917485	1668	10		Basaltic	19.5	7.12	820	536	0.12	46	6.5	361	98.8
38	352585	915007	1691	80		Basaltic	22.4	8.32	566	370	0.06	113	2.1	19	4.56
40	360489	912322	1747	82		Basaltic	20.9	7.99	442	282	0.12	87	2.7	47.5	14.44
41	387659	946376	2065	93	0	Basaltic		7.78	337	222	0.12	32	6.6	108.3	30.4
44	387835	943260	2037	297	5	Basaltic		7.84	1185	770	0.47	300	11	11.4	2.3
45	387802	943130	2034	300	5	Basaltic	16.9	8.000	180	680		236	12.000	23.000	6.000
46	386986	945147	2050	133	0	Basaltic		7.39	845	510	0.1888	130	23.5	86.8	27.8
47	383586	933863	1925	15	8	Basaltic	18.4	6.82	314	206	0.13	9	2.7	155.8	39.5
48	381713	933854	1896	100	7.46	Basaltic		7.28	339	222	0.16	18	6	136.8	35.7
49	379119	929764	1869	12	2.20	Pyroclastic	17	6.51	222	146	0.13	8	7.1	85.5	28.12
51	378206	930111	1858	50	5	Pyroclastic	21.4	7.09	517	338	0.23	22	4	237.5	76
52	376875	927146	1803			Pyroclastic	22.8	7.02	358	230	0.79	18	10	152	45.6
53	375476	924377	1812	9	8.2	Pyroclastic	19.1	6.74	573	374	0.17	27	20	178.6	57
54	372612	925524	1814	20	14	Basaltic	18.8	6.89	165	110	0.21	15	7.6	45.6	15.2
55	369056	924670	1812	10		Pyroclastic	19.2	6.63	286	190	0.09	16	8.3	106.4	34.2
56	367619	923308	1730			Pyroclastic	20.6	8.72	395	252	0.03	82	2.8	19	3.8
57	365029	924648	1743	60	28	Pyroclastic	20.5	7.41	506	290	0.12	39	16	172.9	57
58	364581	925183	1753	23	12.60	Pyroclastic	20.4	7.04	677	448	0.23	30	7.9	304	92.7
59	365125	925132	1763	14	7.60	Pyroclastic	20.1	7.43	448	286	0.13	33	8.8	157.7	53.96
60	358314	927117	1671	7	3	Basaltic	20	7.31	623	406	0.98	36	6.4	266	87.4
62	357207	927172	1647	8	3	Basaltic	22.4	7.27	685	448	0.49	58	6.5	258.4	73.7
63	365447	922747	1713	152	53.68	Basaltic	24.4	9.16	360	240	0.12	75	0.6	9.5	2.28
64	366637	921104	1746	146	29.38	Basaltic		8.39	439	286	0.23	90	5	28.5	7.6
65	367564	915793	1864			Pyroclastic		7.92	319	204	0.12	32	11.2	95	30.4

66	365168	908852	1845	105		Basaltic	16.9	8.2	493	320	0.11	86	7.1	57	15.2
67	398319	885302	2881	175			14	6.64	107	72	0.05	9	5.8	32.3	7.6
69	406040	939023	2071			Pyroclastic	24.7	7.08	412	272	0.13	24	6	171	45.6
71	349638	939008	1781	54	10	Basaltic	20.9	7.14	807	532	0.17	72	11	307.8	100.3
72	351822	949233	1906	60	18	Trachy basalt	23.8	6.71	449	298	0.18	22	5.5	176.7	55.5
74	366001	952270	2065			Basaltic	17.6	6.45	241	166	0.12	10	3.3	95	24.3
75	370635	950938	2003			Basaltic			209	140	0	12	2	87	24
76	373172	928362	1782	66	17	Basaltic		8.000	431	282	0.18	30	5.000	181.000	55.000
77	352087	943847	1816	57	12.5	Trachy basalt		8.000	511	344	0.2	59	5.000	179.000	55.000
79	376015	902512	1928	66	25	Pyroclastic		7.000	222	66	0.08	11	4.000	29.000	6.000
80	377799	900288	1975			Pyroclastic		6.37	99	68	0.07	5	0.09	28.5	8
82	377401	897193	1989	25		Pyroclastic		6.000	158	64	0.1	7	6.000	30.000	7.000
83	377414	897350	1969	30		Pyroclastic		7	270	192	0.11	25	7.2	98.8	31.9
84	374345	933340	1839	61	5	Basaltic		7.000	425	270	0.12	24	5.000	186.000	54.000
85	381267	951278	2093	53		Basaltic		7	235	174	0.12	23	9.2	76	16.7
86	378626	961413	2572	173		Pyroclastic	82	7.000	235	154	0.12	23	9.000	76.000	17.000
87	377000	942000	1952	174	14.7	Basaltic	7.08		338	222		25	4	136.5	40.32
88	363500	939000	1779	53	15	Basaltic	7.55	7.55	978	642		186	12	128.1	40.32
89	363500	939000	1783	56	15	Basaltic	7.48		702	442		109	9.1	157.5	42
90	356500	937500	1721	56	16	Basaltic	9.15		382	228		88	0.9	14.7	4.2
91	378500	945500	2156	56	21	Basaltic		7	393	258		12	5.000	206.000	
127	355538	900934	1858	147				7.000		320	0.324				
128	355920	899064	1854	57				7.000	418	199					72.000
129	357237	898799	1829	63				7.000	345	164	0.051				
130	358405	896016	1882	56				7.000	411	198					
131	358975	892500	1918	149				8.000	393	276	0.347		3.000		
132	359617	895285	1882	149				9.000	526	252	0.0017		9.000	239.000	14.000

133	367270	905131	1902	172				7.000	408							30.000
134	368709	891744	1906	62				7.000	285	135	0.049					
135	374419	908195	1876	226				8.000	468	325						
136	381524	915483	1877	134				7.000	444	298	0.375		7.000	48.000		39.000
137	367147	916532	1859	200	41.7	pyroclastic		7.220	431	248	0.120	53	9.700	116.000		28.000
138	366872	916448	1863	200	76	pyroclastic		7.240	389	235	0.000	83	5.900	95.000		26.400
139	368739	906671	1901	215	65.05	pyroclastic		6.790	142	96	0.160	23	4.500	42.000		8.000
140	367928	905831	1887	226	157.6			6.950	243	146	0.470	20	4.700	91.080		25.340

	Mg (mg/l)	Fe(mg/l)	Mn (mg/l)	F (mg/l)	Cl (mg/l)	NO2 (mg/l)	NO3 (mg/l)	Alkalinity (mg/l CaCo3)	Carbonate (mg/l CO3)	Bicarbonate (mg/l HCO3)	Sulphate (mg/l SO4)	Phosphate (mg/l PO4)	Date of Analysis	Water Point Type	Remark
1		0.080	Trace	1.300	38.720	0.001	1.090	110.000	Nil	31.720	20.880	0.860		DBH	
2	2.5	0.01	Trace	0.25	127.5	0.005		335	Nil	409	11.5	0.25		DBH	
3	5.9	0.07	Trace	6.12	29.54	0.01		247	Nil	301.44	3.12	0.08		DBH	
4	1.470	0.130	Trace	0.870	23.030	0.010	0.200	234.300	Nil	285.850	22.490	0.330	15/12/2017	DBH	
5	2.880	4.290	Trace	0.780	28.210	Trace	0.110	260.300	Nil	317.570	15.110	1.470		DBH	
6	0.55	0.00	Trace	0.60	10.60	0	0.10	124.00	90	34	3	18.000		DBH	
7	2.740	0.020	-	1.140	27.30	Trace	6.710	370.500	NIL	452.010	0.190	0.310	22/2/2012	DBH	Artesian
8	3.19	0.19	0	1.03	11.83	Trace	0.23	189.00	Nil	231	12	0.400		DBH	
9	4.75	0.07	Trace	0.70	23.45	1	3.64	140.80	69	32	37	0.130		DBH	
10	2.88	0.13	Trace	0.76	13.23	Trace	1.20	190.00	Nil	232	20	0.180		DBH	
11	2.000	0	0	6.000	6.000		8.000		9.6	155.000	0.28	0.08	01-24-06	DBH	
12	2.1	0	0	1.6	5.8		8		0	154.7	0.28	0.08	01-24-06	MBH	Artesian
13	1.000	0	0	6.000	11.28		0.000		0	438.000	7.15	0.164	04-18-06	SBH	
14	9.66	Trace	trace	0.64	7.6		66.2	210	Nil	256.2	0.29	0.2		SBH	
15	6.9	0.02	0.05	0.63	5.7		30.2	160	Nil	195.2	1.1	0.46		MBH	
17														MBH	
18	8.28	0.01	0.05	0.82	14.25		26.7	222	Nil	270.8	0.3	0.43		HDW	

19	15.64	0.02	trace	0.73	3.8		25.6	370	Nil	451.4	0.29	0.38		SBH	
20	13.8	0.02	0.02	0.8	3.8		5	336	Nil	409.9	0.38	0.36		SBH	
21	3.22	0.11	0.02	0.55	36.1		8.11	580	Nil	707.6	76.8	0.26		SBH	
22	12.9	0.08	0.02	0.62	62.7		6.9	460	Nil	561.2	116.3	0.41		SBH	
23	20.7	0.02	trace	0.28	43.7		18.9	388	Nil	473.36	136	0.33		MBH	
24	26.7	0.11	0.02	0.15	48.5		15.2	422	Nil	514.8	169.8	0.5		DBH	
25	14.26	0.28	0.02	0.69	52.3		46.3	410	Nil	500.2	76.16	0.33		MBH	
26	10.12	0.31	0.02	0.51	44.7		1.8	316	Nil	385.5	28.6	0.17		MBH	
27	21.2	0.44	0.05	0.8	24.7		18.6	394	Nil	480.68	68.9	0.5		SBH	
28	40.9	0.38	0.02	1.11	15.2		1.7	710	Nil	866.2	18.7	0.25		SBH	
29	39.1	0.25	0.02	0.68	5.7		10.4	530	Nil	646.6	9	0.31		MBH	
30	29.9	0.06	trace	0.58	62.7		47.9	576	Nil	702.7	65.2	0.32		SBH	
31	16.5	0.31	0.02	0.74	16.15		1.4	570	Nil	695.7	9.6	0.41		MBH	
32	66.7	Trace	trace	0.82	20.9		1.3	948	Nil	1156.6	0.48	0.55		MBH	
33	10.12	0.02	trace	0.68	9.5		31.8	400	Nil	488	1.05	0.28		MBH	
34	34.96	0.02	trace	0.83	10.45		41.3	460	Nil	561.2	0.28	0.3		MBH	
35	2.3	Trace	trace	1.07	24.7		0.9	240	26.4	239.12	29.6	0.13		MBH	
36	26.7	0.2	trace	0.7	15.2		84.7	490	Nil	597	0.57	0.3		MBH	
37	27.6	Trace	0.07	0.65	9.5		7.5	450	Nil	549	0.19	0.44		HDW	
38	1.84	0.03	0.03	0.74	60.8		28.4	138	9.6	148.8	40.3	0.29		MBH	
40	2.76	0.02	trace	0.5	10.45		1.8	210	Nil	256.2	0.5	0.25		MBH	
41	7.82	0.01	trace	0.97	8.55		9.1	168	Nil	204.96	0.19	0.37		MBH	
44	1.38	0.02	trace	16.4	37.05		1.3	536	Nil	653.9	0.28	0.35		MBH	
45	2.000	0.06	2.2	14.000	14.00		10.000	504		615.000	0.83			DBH	
46	4.2	0.1	0.05	2	69.1		14.25		0	336	46.8	0.246	01-24-06	DBH	
47	13.8	0.02	trace	0.39	19.95		58	86	Nil	104.9	0.57	0.13		HDW	
48	11.5	0.02	trace	0.97	5.7		8.5	184	Nil	224	0.19	0.25		DBH	

49	3.68	0.24	0.03	0.22	10.45		32	88	Nil	97.6	1.4	0.25		HDW	
51	11.5	Trace	0.02	1.45	3.8		29.1	264	Nil	322.1	0.28	0.19		HDW	
52	9.2	0.12	0.03	1.2	5.7		1.39	184	Nil	224.5	1.4	0.76		HDW	
53	7.8	0.32	0.03	0.18	2.85		129.9	76	Nil	92.72	47.6	0.41		HDW	
54	1.84	0.13	trace	0.65	8.55		13.2	60	Nil	73.2	2.38	0.28		HDW	
55	5.06	0.35	trace	0.9	10.5		14.1	130	Nil	158.6	0.48	0.33		HDW	
56	2.3	0.02	trace	0.76	11.4		0.69	180	12	195.2	0.19	0.21		MBH	
57	7.36	0.03	trace	0.65	3.8		2.67	260	Nil	317.2	0.19	0.13		MBH	
58	17.5	0.02	trace	0.37	26.6		75.7	314	Nil	383.1	4	0.61		HDW	
59	5.52	0.02	0.02	1.64	11.4		9.8	202	Nil	246.4	0.38	0.41		HDW	
60	11.5	0.04	0.03	0.68	7.6		46.9	330	Nil	402.6	0.48	0.4		HDW	
62	17.9	0.05	0.02	1.4	5.7		18.7	374	Nil	456.3	0.28	0.54		HDW	
63	0.92	0.02	trace	1.3	24.7		0.4	124	19.2	112.24	26.4	0.11		DBH	
64	2.3	0.03	0.02	0.93	11.4		1.5	212	9.6	239.1	9.9	0.09		DBH	
65	4.6	0.22	0.02	1.46	3.8		0.84	154	Nil	187.9	0.19	0.16		MBH	
66	4.6	0.02	trace	0.5	2.85		1.14	232	12	263.5	0.19	0.11		DBH	
67	3.22	0.09	0.02	0.39	4.75		4.8	52	Nil	63.44	0.19	0.25		DBH	
69	13.6	0.04	trace	0.66	6.65		8.7	210	Nil	256.2	0.47	0.26		MBH	
71	13.8	0.03	trace	0.7	5.7		9.3	464	Nil	566.1	0.19	0.17		SBH	
72	9.2	0.18	trace	0.8	23.8		78.2	150	Nil	183	2	0.26		MBH	
74	9.18	0.11	trace	0.22	7.6		51.3	80	Nil	97.6	3.7	0.23		MBH	
75	6	0	Trace	0.3	3.8		9.1	110	Nil	134.2	0.2	0.53		MBH	
76	11.000	0.03	trace	0.000	11.33		25.000	228.9	Nil	279.000	1.43	0.15		MBH	
77	10.000	0.03	trace	1.000	7.21		6.000	319.2	Nil	389.000	0.95	0.35		SBH	
79	3.000	Trace	0.02	0.000	1		4.000	56	Nil	68.000	0.57	0.138		MBH	
80		0.03	trace	0.46	1.90		6.70	50	Nil	61	0.19	0.09		MBH	
82	3.000	0.09	0.03	0.000	1		1.000	48	Nil	59.000	0.19	0.49		SBH	
83	4.6	0.23	0.02	1.03	1.9		1.3	140	Nil	170.8	0.19	0.27		SBH	
84	12.000	0.03	0.02	0.5	2.85		3.000	230	Nil	281.000	0.1	0.24		MBH	
85	8.28	0.23	trace	1.02	3.8		12.4	120	Nil	146.4	0.5	0.33		SBH	

86	8.000	0.23	trace	1.02	3.8		12.000	120	Nil	146.000	0.5	0.33		DBH	
87	8.67	0.1		1.3	5.96		0.16	180		219.6		0.25	11-06-08	DBH	
88	6.63	0.03		0.97	47.66		0.2	398		485.56	46.1	0.26	24/06/2008	SBH	
89	12.75	0.01		0.93	3.97		0.22	364		444.08	22.4	0.19	24/06/2008	SBH	
90	1.02	0.03		0.9	26.81	0.005	0.03	148	24	131.76	15.26	0.07	24/06/2008	SBH	
91	17.000	0.05		0.000	0.000		0.000	216		264.000	3.31	0.17		MBH	
127					0.000		1.000	249.6		305.000				DBH	
128					1.000		2.000	166		166.000				MBH	
129					1.000		1.000	140		140.000				MBH	
130					1.000			146		146.000				MBH	
131					1.000		4.000	201.6	19.2	207.000				DBH	
132					0.000			154	16	138.000				DBH	
133					1.000		0.000	218.96		267.000				DBH	
134					0.000		1.000	106		106.000				MBH	
135					1.000		0.000	5.63		254.000				DBH	
136					1.000		4.000	220		269.000				DBH	
137	11.040	0.600	0.320	0.584	5.840	0.020	0.660	195.700	Nil	238.750			25/02/2016	DBH	
138		0.030	0.028	1.200	8.000	0.100	`1.5	165.000	26.400	198.400	5.000	23.000		DBH	
139		0.040	Trace	0.620	2.770	0.020	0.220	82.000	Nil	100.040	0.300	0.280		DBH	
140		0.200	0.020	0.650	3.580	0.010	0.210	132.670	Nil	161.850	0.590	0.350		DBH	

Annex 3: Hydrogeological parameters

SN	X	Y	Z	Depth,m	SWL,m	Aquifer_Lith.	Q,l/s	Sc, l/s/m	DD,m	T, m^2/day	EC (µS/Cm)	Temp._° C	Water Point Type	Remark
1	358290	926080	1699	459	82.0	Fractured Basalt	11	0.1970	53	20	994	28	DBH	
2	364751	906029	1910	307	173.1	basalt	0.75		47.15				DBH	
3	370781	943250	1867	470.5	29.3	Bsaltic	16.37	0.3	53.7	43.1	974	24.7	DBH	
4	385801	939409	1953	473.6	65	Basalt and ignimbrite	60.7	2.76	22.02	6.66	920	30	DBH	
5	389562	922209	1931	450	98	pyroclastic	20.3	0.41	49.13	36	488		DBH	
6	375734	926348	1787	360	8.9	Fractured Basalt	3	0.0169	148				DBH	
7	357700	944225	1822	360	25	Basaltic	5.3	0.043	124	24	287		DBH	
8	383826	947387	2058	265	0	Fractured Basalt	22	0.2861	77	125			DBH	Artesian
9	408282	939498	2311	360	22	Pyroclastic	24	1	43	43	413		DBH	
10	363415	915588	1788	280	98	Pyroclastic	3	0	23	3	414		DBH	
11	337295	929032	1526	354	114	Fractured trachy Basalt & scoriacious basalt							DBH	
12	376617	902505	1941	347	57	Pyroclastic	25	4	7	604	425		DBH	
13	386183	943986	2023	108	0	Basaltic overlaid by Ash	5.00	76	75.79		303	29	DBH	
14	387305	945410	2052	100	0	Pyroclastic			54.66				MBH	
15	387549	945858	2067	93	0.0	Basaltic overlaid by Ash	11.10		12.68				MBH	Artesian
16	389339	940715	1992	50	28.5	Pyroclastic							SBH	
17	408475	952876	2276	50	10	Basaltic							SBH	
18	407460	953526	2277	36	9	Trachy basalt							SBH	
19	381158	951315	2099	60		Basaltic							SBH	
20	383469	948467	2071	60	0	Basaltic					150	18.4	SBH	
21	415254	939047	2378	47									SBH	
22	412826	949736	2260	50	0	Pyroclastic							SBH	
23	402350	951544	2426	60	26.73	Pyroclastic	0.18	18	16.37				MBH	
24	393964	957477	2489	61	39.12	Basaltic	0.14	6	8.58				MBH	
25	397276	954511	2394	61	17.45	Basaltic	0.55	6	36.55				MBH	
26	397540	953574	2376	60	17.93	Pyroclastic	0.15	6	34.87				MBH	

27	396861	952816	2388	36	20.48	Trachy basalt	2.17	6	4.17				SBH	
28	398182	951093	2377	62	14.13	Pyroclastic	1.30	6	32.92				MBH	
29	400409	954207	2376	48	21.58	Pyroclastic	4.00	6	4.65				SBH	
30	398901	951499	2400	60	24.43	Basaltic	1.30	12	21.03				MBH	
31	400317	931223	2150	66	38.35	Pyroclastic	0.12	23	14.75				MBH	
32	394200	944338	2214	62	36.5	Pyroclastic	0.16		18.39				MBH	
33	381500	933000	1928	100	7.33	Pyroclastic	5.60	42	3.72				MBH	
34	393191	944399	2153	47	0	Pyroclastic	20.00	12			741	40.5	SBH	
35	342165	903933	1654	45	0	Basaltic					300	24.1	SBH	
36	339077	902523	1685	60	20	Basaltic					250	20.7	MBH	
37	342000	903672	1669	60		Basaltic							MBH	
38	342369	903357	1655	8	1	Basaltic					320	18.7	HDW	
39	337131	931265	1525	39	10						320	20.7	SBH	
40	337249	931410	1538	41	15		3.00				320		SBH	
41	337246	929566	1538	52	33		3.50				480		SBH	
42	337688	927934	1548	54	11		1.50				970		SBH	
43	338664	924779	1527	51	23	Basaltic	1.75				560		SBH	
44	340300	924367	1551			Basaltic					470		MBH	
45	340966	924430	1558	130		Basaltic					500		DBH	
46	339029	924979	1519			Basaltic					520	20.8	MBH	
47	341088	924567	1557	81	35	Basaltic	2.00				400	20.9	MBH	
48	340662	924050	1547	54		Basaltic	2.50				410	21.9	SBH	
49	342102	923134	1526	58	42	Basaltic	2.50				530	22.7	SBH	
50	343453	924775	1587	61	41	Basaltic	3.50				430	23.1	MBH	
51	342266	922432	1533	54		Basaltic					500	22.2	SBH	
52	343035	921923	1547	92	48	Basaltic	3.5				500	23.1	MBH	
53	343578	920886	1540	70		Basaltic					580	23	MBH	
54	344574	921296	1549			Basaltic					390	21	MBH	
55	344752	920691	1535	69	36	Basaltic	0.50				410	19.5	MBH	
56	344600	920184	1532	81	24	Basaltic	3.00				430	20.5	MBH	

57	345006	920268	1521	82	27	Basaltic	1.75				360	21.8	MBH	
58	345108	920062	1545	74	50	Basaltic	0.50				380	21.8	MBH	
59	346814	919983	1582	74	50	Basaltic	0.50				380	22.1	MBH	
60	346819	920574	1562			Basaltic					370	21.3	MBH	
61	349391	918430	1632			Basaltic					330	21.8	MBH	
62	347338	916729	1582	78	42	Basaltic					420	20.7	MBH	
63	348795	916923	1624	115		Basaltic							DBH	
64	348571	919246	1612			Basaltic					370	24.4	MBH	
65	350867	918698	1615	52	16	Basaltic	1.00				370	20.7	SBH	
66	352791	917485	1668	10		Basaltic					390	19.5	HDW	
67	352585	915007	1691	80		Basaltic					330	22.4	MBH	
68	353117	915342	1719	39		Basaltic							SBH	
69	352065	916658	1683	90		Basaltic							MBH	
70	355341	916638	1732	204		Basaltic							DBH	
71	354023	915772	1716	84		Basaltic					320	22.3	MBH	
72	355882	914531	1541	84		Basaltic					310	22	MBH	
73	356903	915385	1761	85		Basaltic							MBH	
74	356884	914283	1716			Basaltic					350	21.5	MBH	
75	357443	913873	1722	64		Basaltic					350	20.2	MBH	
76	360489	912322	1747	82		Basaltic					280	20.9	MBH	
77	387659	946376	2065	93	0	Basaltic	11.1		12.68				MBH	
78	388820	947604	2085	148	5	Basaltic							DBH	
79	375409	928322	1846	80	7.46	Basaltic	5.6				200	23.2	MBH	
80	375733	928451	1846	14	2	Basaltic					230	21.6	HDW	
81	377246	929075	1861	12	2	Basaltic					260	17.7	HDW	
82	387025	943705	2052		9	Basaltic							HDW	
83	387835	943260	2037	297	5	Basaltic	7.50				1185		MBH	
84	387802	943130	2034	300	5	Basaltic	7.50		44.04		180	16.9	DBH	
85	386986	945147	2050	133	0	Basaltic	11.10				845		DBH	
86	383711	933823	1926	15	9	Basaltic							HDW	
87	383586	933863	1925	15	8	Basaltic					150	18.4	HDW	
88	383538	933892	1926	15	10	Basaltic					200	17.6	HDW	
89	382633	934291	1913	15	8	Basaltic					180	21.1	HDW	

90	382560	934038	1924	16	11	Basaltic					150	18	HDW	
91	381713	933854	1896	100	7.46	Basaltic	5.6				339		DBH	
92	381304	933280	1896	16		Basaltic					200	19.3	HDW	
93	379119	929764	1869	12	2.20	Pyroclastic					180	17	HDW	
94	379015	929886	1856	10		Pyroclastic					140	18.5	HDW	
95	379757	929087	1905	12		Pyroclastic	3.00				210	22.6	HDW	
96	379726	928664	1879	15		Pyroclastic					250	20.1	HDW	
97	378805	929216	1870	15		Pyroclastic					150	19	HDW	
98	378206	930111	1858	50	5	Pyroclastic					270	21.4	HDW	
99	379297	930413	1864	22		Pyroclastic					250	19.1	HDW	
100	379714	930273	1872			Pyroclastic					210	22	HDW	
101	374091	926846	1829	17		Basaltic					200	20.6	HDW	
102	376875	927146	1803			Pyroclastic					230	22.8	HDW	
103	375881	926048	1788	12	10	Pyroclastic					200	20	HDW	
104	375476	924377	1812	9	8.2	Pyroclastic					310	19.1	HDW	
105	372612	925524	1814	20	14	Basaltic					140	18.8	HDW	
106	372198	924591	1761	15	11	Pyroclastic					180	19.7	HDW	
107	372148	924659	1780	14	13	Pyroclastic					158	20.5	HDW	
108	372178	924570	1783	10	9	Pyroclastic					190	19.7	HDW	
109	371819	924542	1773	60		Pyroclastic					260	25.6	MBH	
110	373129	924713	1781			Pyroclastic					310	23.8	MBH	
111	371319	925254	1793	9	8	Pyroclastic					140	16.6	HDW	
112	369812	924396	1828	19	14.70	Pyroclastic					190	19	HDW	
113	369056	924670	1812	10		Pyroclastic					200	19.2	HDW	
114	369578	924736	1829	17	13.40	Pyroclastic					180	18.8	HDW	
115	369399	923494	1807	12		Pyroclastic							HDW	
116	369057	923489	1812	18	5.20	Pyroclastic					430	19.8	HDW	
117	369100	923299	1801	9	1.80	Pyroclastic					200	19.2	HDW	
118	369141	923357	1808	8	3.00	Pyroclastic					300	20.1	HDW	
119	369254	923373	1804	9	1.60	Pyroclastic					310	18.8	HDW	
120	369317	923493	1818	10	5.70	Pyroclastic					230	20.5	HDW	
121	369255	923511	1831	19	10.60	Pyroclastic					170	20.6	HDW	
122	367619	923308	1730			Pyroclastic					260	20.6	MBH	
123	365029	924648	1743	60	28	Pyroclastic	0.40				300	20.5	MBH	
124	363868	925587	1748	75		Basaltic							MBH	
125	364581	925183	1753	23	12.60	Pyroclastic					340	20.4	HDW	

126	365125	925132	1763	14	7.60	Pyroclastic					260	20.1	HDW	
127	358314	927117	1671	7	3	Basaltic					330	20	HDW	
128	357207	927172	1647	8	3	Basaltic					330	22.4	HDW	
129	358319	926963	1676	195		Basaltic							DBH	
130	364905	923161	1690	152	11.74	Basaltic	7.20		44.83	56.92			DBH	
131	365433	923338	1693	200	34.55	Basaltic	2.40		104	0.616			DBH	
132	365427	923242	1688	103	2.96	Basaltic	8.40		6.63	221.4			DBH	
133	365447	922747	1713	152	53.68	Basaltic	4.68		83.13	1.76	240	24.4	DBH	
134	366319	921583	1738	160		Basaltic	5.50						DBH	
135	366637	921104	1746	146	29.38	Basaltic	10.0		51.92		439		DBH	
136	369148	915960	1831	105		Pyroclastic							DBH	
137	369104	915815	1828	81	21.83	Pyroclastic	2.00		15.32	4.83			MBH	
138	372001	916722	1843	68.5	11.95	Pyroclastic	2.50		39.39	13.73	348	25.1	MBH	
139	369592	915660	1838			Pyroclastic					200	20	HDW	
140	369739	915686	1849	14	8	Pyroclastic					210	20.1	HDW	
141	367564	915793	1864			Pyroclastic					323		MBH	
142	365168	908852	1845	105		Basaltic					300	16.9	DBH	
143	365732	908980	1825			Basaltic					280	14.8	MBH	
144	364468	907392	1894	78		Basaltic					131.5	18.7	MBH	
145	358908	904545	1857			Pyroclastic					241	21.6	MBH	
146	355924	903192	1809	73		Basaltic							MBH	
147	352242	903636	1744	75		Basaltic					310		MBH	
148	393894	886062	2764	175	92.95		5.95	25.32	14.1	39.2			DBH	
149	398319	885302	2881	175							92.4	14	DBH	
150	397933	884153	2869	188									DBH	
151	399310	885059	2905	48									SBH	
152	406040	939023	2071			Pyroclastic					237	24.7	MBH	
153	403037	937939	2256	10		Pyroclastic					225	17.5	HDW	
154	387202	944167	2043		2	Basaltic							HDW	
155	347532	943211	1815	175		Basaltic							DBH	
156	349638	939008	1781	54	10	Basaltic	0.40				360	20.9	SBH	

Annex 4.. Summer Land Use parameters

NUMBEA1: N27R	LUSE_TYPE	RUNOFF_VEG	NUM_VEG_RO	NUM_IMP_RO	VEG_ AREA	BARE_ AREA	IMP_ AREA	OPENW_ AREA	ROOT_ DEPTH	LAI	MIN_ STOM	INTERC_ PER	VEG_ HEIGHT
1	city	center	build	up	grass	2	1	0.2	0	0.8	0	0.3	2
21	agriculture	crop	1	0	0	1	0	0	0.35	0	180	0	0.6
33	mixed	forest	forest	3	0	0.5	0.5	0	0	2	4.5	500	38
36	shrub	grass	2	0	0.2	0.8	0	0	0.6	0	110	5	2
37	beach/dune	bare	soil	4	0	0.3	0.7	0	0	0.5	2	110	15
51	navigable	river	open	water	5	0	0	0	0	1	0.05	0	110

Annex 5. Winter Land Use parameters

NUMBER	LUSE_ TYPE	RUNOFF_ VEG	NUM_VEG _RO	NUM_ IMP_RO	VEG_ AREA	BARE_ AREA	IMP_ AREA	OPENW_ AREA	ROOT_ DEPTH	LAI	MIN_ STOM	INTERC _PER	VEG_ HEIGHT
1	city	center	build	up	grass	2	1	0.2	0	0.8	0	0.3	2
21	agriculture	crop	1	0	0.8	0.2	0	0	0.4	4	180	15	0.6
33	mixed	forest	forest	3	0	1	0	0	0	2	5	375	35
36	shrub	grass	2	0	1	0	0	0	0.6	6	110	15	2
37	beach/dune	bare	soil	4	0	0.3	0.7	0	0	0.5	2	110	15
51	navigable	river	open	water	5	0	0	0	0	1	0.05	0	110

Annex 6. Annual and Seasonal Water balance components

	Annual				Rainy Season				Dray Season			
Components	Min	Max	Ave	Stdev	Min	Max	Ave	Stdev	Min	Max	Ave	Stdev
Precipitation	1003	1827	1357.38	193.74	394.42	1122	794.08	166.36	240.1	707.67	541.19	118.79
Evapotranspiration (AET)	282.39	1336.29	736	214.3	111.12	377. 54	312.68	68.08	78.08	982.09	434.95	135.03
Runoff (RO)	99.6	1244.76	519.16	188.8	62.7	768.3	301. 5	119.2	0	477.3	148.7	86
Recharge (GR)	0	564.17	102.2	118.19	0	652. 5	179.8	175.2	-202.1	121.7	-41.98	44.93